Maturation of Stem Cell-Derived Cardiomyocytes via Coculture for Cellular Manufacturing

By

Kaitlin Kelly Dunn

A dissertation submitted in partial fulfillment of

the requirements for the degree of

Doctor of Philosophy

(Chemical and Biological Engineering)

at the

UNIVERSITY OF WISCONSIN-MADISON

2019

Date of final oral examination: 03/04/2019

The dissertation is approved by the following members of the Final Oral Committee:

Sean P. Palecek, Professor, Chemical and Biological Engineering
Eric V. Shusta, Professor, Chemical and Biological Engineering
Brian F. Pfleger, Professor, Chemical and Biological Engineering
John Yin, Professor, Chemical and Biological Engineering
Kristyn S. Masters, Professor, Biomedical Engineering

Maturation of Stem Cell-Derived Cardiomyocytes via Coculture for Cellular Manufacturing

Kaitlin Kelly Dunn

Under the supervision of Professor Sean P. Palecek
at the University of Wisconsin-Madison

Abstract

Heart disease is a burgeoning epidemic in the world today, resulting in an alarming increase of heart attacks each year. Myocardial infarctions cause irreversible damage to the heart, motivating the development of innovative therapies. Millions of heart muscle cells, called cardiomyocytes (CMs), are killed during a heart attack which decreases the functionality of the tissue. As adult CMs cannot regenerate, the only current treatment to restore contractile function is whole heart transplant. Human pluripotent stem cell-derived (hPSC-) CMs provide an abundant source of CMs to replenish those lost during a heart attack. While chemically-defined methods to produce virtually pure hPSC-CMs have been established, one drawback to these cells is their lack of maturity. hPSC-CMs are more fetal-like in physiology and functionality compared to their adult counterparts, resulting in arrhythmias when implanted into primate myocardial infarction models.

Many methods to induce hPSC-CM maturation have been tested, including mechanical stimulation, electrical stimulation, and coculture with other cell types, yet no method has produced an adult-like hPSC-CM. Intercellular interactions have proven essential for proper heart formation. Presently, the cell-cell interactions necessary for CM maturation are unknown. The following work investigated the interaction of CMs and their progenitors (CPCs) with endothelial cells (ECs) and epicardial cells (EpiCs), two support cell types found within the heart, to determine if they provide maturation-inducing interactions. We discovered that EC-induced maturation of hPSC-CMs is dependent on the stage of differentiation of the CMs; hPSC-CPCs cocultured with ECs induced heightened maturation compared to cocultured hPSC-CMs. Additionally, we modeled the interactions of CMs with EpiCs during heart development using two different coculture systems. One maintained the identity of hPSC-EpiCs throughout the coculture and the second allowed the EpiCs to undergo an epithelial to mesenchymal transition into other stromal cells while in coculture with the CPCs. We found that EpiC and EpiC-derived cell cocultures affected CM maturation, each inducing different phenotypic changes associated with CM maturation. Overall these studies motivate the inclusion of intercellular interactions during hPSC-CM manufacturing and demonstrate the importance of integrating these interactions at earlier stages of differentiation to create mature hPSC-CMs for use in cardiac patches.

Acknowledgements

The pursuit of my Ph.D. in Chemical and Biological Engineering has truly been a life-changing journey, complete with many personal and professional trails along the way. I would like to thank all my friends, family, co-workers, and countless others who have encouraged me to persevere throughout my years at the University of Wisconsin-Madison.

I would like to first give my deepest thanks to Prof. Sean P. Palecek. As my Ph.D. advisor, he has provided guidance and support through my Ph.D, in addition to helping me develop my skills as an independent researcher. His patience and understanding of the trials of graduate life has been greatly appreciated. I also thank Prof. Eric V. Shusta who has also provided great advice and feedback on my research. I would like to thank my other Ph.D. committee members for their guidance on my project including Prof. Brian F. Pfleger, Prof. John Yin, and Prof. Kristyn S. Masters. I would also like to thank all the members of the Palecek lab for their technical and emotional support through the years, especially: Dr. Scott Canfield and Dr. Xiaoping Bao, who both mentored and trained me when I first joined the lab; Dr. Matthew Stebbins, Dr. Amritava Das, and Dr. Moriah Katt who provided me much needed advice for my research and career aspirations; Dr. Vijesh Bhute, Gyuhyung Jin, Martha Floy, Koji Foreman, and Aaron Simmons who have put up with my antics in the lab and made it a fun environment to work in. Finally, I also greatly appreciate the two undergraduate students Isabella Reichardt and Kelsey Hoon who I have had the pleasure to train and mentor. Both of them have been exceptional collaborators and have made many valuable contributions to this body of work.

Finally, I wish to give a heartfelt thank you to all my friends and family who have provided much needed support, especially my parents George Harvey Dunn III and Sandra Dunn, my siblings and their spouses, and all my friends whom I have made in Madison. Your encouragement, patience, and support has helped me through the many challenges I have faced along this journey.

Table of Contents

List of Figures

List of Tables

Chapter 1: Engineering Scalable Manufacturing of High-Quality Stem Cell-Derived Cardiomyocytes for Cardiac Tissue Repair

1.0 Summary

This chapter summarizes the field's current understanding in the differentiation of human pluripotent stem cell (hPSC)-derived cardiomyocytes (CMs) and the current limitations in manufacturing these cells as a potential therapeutic. Recent advances in the differentiation and production of hPSC-derived CMs have stimulated development of strategies to use these cells in human cardiac regenerative therapies. A prerequisite for clinical trials and translational implementation of hPSC-derived CMs is the ability to manufacture safe and potent cells on the scale needed to replace cells lost during heart disease. Current differentiation protocols generate fetal-like CMs that exhibit proarrhythmogenic potential. Sufficient maturation of these hPSC-derived CMs has yet to be achieved to allow these cells to be used as a regenerative medicine therapy. Insights into the native cardiac environment during heart development may enable engineering of strategies that guide hPSC-derived CMs to mature. Specifically, considerations must be made in regards to developing methods to incorporate the native intercellular interactions and biomechanical cues into hPSC-derived CM production that are conducive to scale-up.

This section was published as "Engineering Scalable Manufacturing of High-Quality Stem Cell-Derived Cardiomyocytes for Cardiac Tissue Repair" in journal, Frontiers of Medicine, on April 24th 2018.

1.1 Structural and functional considerations for cardiac tissue regeneration

The heart is a complex organ composed of three layers: the epicardium, myocardium, and endocardium. Within these layers reside many different cell types including cardiomyocytes, endothelial cells, smooth muscle cells, epicardial cells, fibroblasts, neurons, and immune cells (1). Cardiomyocytes (CMs) are the cardiac muscle cells, which provide the mechanical contractile function in the heart and reside specifically in the myocardium. They make up only 25-35% of the cells found in the heart (2). There are distinct CM subtypes, including nodal, ventricular, and atrial CMs, which differentially express over 6,274 genes (3). These CM subtypes originate from different mesodermal subtype populations and reside in different locations -- ventricular CMs in the ventricles, nodal CMs in the sinoatrial node, and atrial CMs in the atria (4). Additionally, the left ventricle pumps blood throughout the body whereas the right ventricle to the lungs. Thus, the left ventricular CMs must produce higher forces of contraction and require greater oxygen and nutrient uptake. Conversely, atrial CMs require less force generation to pump blood from the atria into the ventricles. The contraction of the heart is controlled by the cardiac pacemaker, which is comprised of sinoatrial-node CMs. These nodal CMs exhibit distinct electrophysiological and Ca^{2+} handling properties relating to their primarily stimulatory role (5). Thus, the unique functions of these CM subtypes are not interchangeable.

Throughout development and for normal function, CMs interact with other cell types in the heart. The epicardial cells, cells that comprise the outer layer of the heart, undergo epithelial-to-mesenchymal transition both during heart development and repair to produce smooth muscle cells (SMCs), fibroblasts, and possibly endothelial cells (ECs) (6, 7). These SMCs, fibroblasts, and ECs interact with CMs in the myocardium to influence their survival and function. The fibroblasts compromise approximately 20% of the nonmyocytes found in the heart and are primarily

responsible for the extracellular matrix (ECM) deposition in the heart (2, 8). SMCs aid in the regulation of blood flow in the heart. ECs are the most abundant nonmyocyte cell in the heart, comprising 60% of the nonmyocytes (2). They line the vasculature and aid in the delivery of nutrients and removal of waste. Endocardial ECs specifically line the heart chambers and myocardial ECs comprise the capillaries that directly interact with CMs. Interactions between these cardiac cell types are necessary to support the contractile function of the heart.

Cardiovascular disease is the leading cause of death globally. In 2015, it contributed to the death of about 17.7 million people, which accounts for 31% of the total deaths that year (9). This high mortality rate is caused by the death of millions of CMs, a cell type that has a very low ability to regenerate to replace damaged areas with healthy cells (10). Valvular heart disease and cardiac hypertension slowly kill CMs over time (11). In comparison, myocardial infarctions can cause 25% of the CMs in the left ventricle to undergo cell death in just a few hours (11). During an acute myocardial infarction, a blockage occurs in the blood flow of a coronary artery preventing the delivery of oxygen and nutrients to the cardiac tissue. The CMs in the left ventricle are most impacted by heart attacks due to their high demand of oxygen and nutrients. During the heart's chronic response to a myocardial infarction, fibroblasts proliferate and form scar tissue, stiffening the heart wall and disrupting the native conduction system, thereby contributing to the likelihood of cardiac failure.

Currently, the only method to completely restore cardiac function for extended duration in patients with advanced cardiac disease is a heart transplant. Alternatively, left ventricular assist devices can temporarily aid the ability of the heart to function but these devices pose significant risks for infection and thrombosis (12). Many efforts are being investigated to repair the damaged cardiac tissue, including creating new heart tissue from stem or progenitor cells or from

reprogrammed somatic cells. Some of the most promising stem cell sources for cardiac tissue include both human embryonic stem cells (hESCs) and induced pluripotent stem cells (iPSCs). Other potential cell types that could be used to repair cardiac tissue include the proliferation of a very rare population of adult cardiac progenitor cells (CPCs) or epicardial cells (10). The potential of epicardial cells to form CMs *in vitro* or *in vivo* remains controversial, but they contribute to nonmyocyte cell populations in the heart. Also further investigation will be required into methods to stimulate differentiation of adult CPCs, which have very low rates of CM formation, to realize their cardiac regenerative potential (10). The main advantage of using stem cells is that they can be expanded prior to differentiation. Estimates of one billion CMs are required for repair of the ventricle after a myocardial infarction (13). Unfortunately, human pluripotent stem cell (hPSC)-derived CMs are immature, exhibiting the structure and function of developing CMs found in a fetus instead of those in an adult heart (14). On the other hand, reprogramming fibroblasts is a relatively new and still inefficient method, requiring further characterization of the resulting CMs to determine their subtype and maturity (15). For these reasons, most research has focused on using hPSC-derived CMs to replace native CMs cells lost in cardiac diseases.

1.2 Differentiation of hPSCs to CMs

1.2.1 Generation of immature hPSC-derived CMs

Methods have greatly improved to manufacture sufficient quantities of essentially pure CMs from hPSCs under defined conditions to enable development of cardiac translational therapies. The original differentiation methods relied on isolating small populations of CMs, typically 1-5% of cells, which spontaneously formed in embryoid bodies (16, 17). While these initial demonstrations of CM differentiation generated cells for research purposes, advances in yield and purity were

necessary to generate enough CMs for investigation of their therapeutic potential. Over the past decade, CM differentiation processes have evolved and become more efficient. Major advances to this method have allowed the differentiation to be optimized, including the determination of pathways that are modulated during CM formation in the embryo, the timing at which to induce these pathway changes, and the ability to activate these pathways in the cells with growth factors and small molecules as seen in **Figure 1.1**. In 2007, Laflamme et al. cultured hESCs in a tissue culture plate coated with Matrigel (18). They obtained purities of ~30% CMs through modulation of TGFβ superfamily signaling using Activin A and BMP4 to induce cardiac mesoderm formation (18). In a suspension culture, addition of BMP4, bFGF, Activin A, Dkk1, and VEGF at different stages of differentiation yielded >50% CMs (19). This method was further improved by the inclusion of dorsomorphin and SC43152 (20). In another 2D differentiation approach, Lian *et al.* generated 80-98% pure populations of CMs solely by modulating the Wnt pathway with the small molecules CHIR99021 and IWP2 (21, 22). Combinations of these strategies incorporated activation of the BMP pathway along with the Wnt pathway modulation to yield ~90% CMs (23). Xeno-free differentiation platforms have been developed by adding ascorbic acid and replacing the B27 supplement with human recombinant albumin or removing the B27 supplement altogether (24, 25). These fully-defined, xeno-free methods reduce the variability in media components and eliminate possible patient immune reactions to animal components in the CM product. These protocols can serve as templates to enable the production of CMs at a scale required for regenerative medicines.

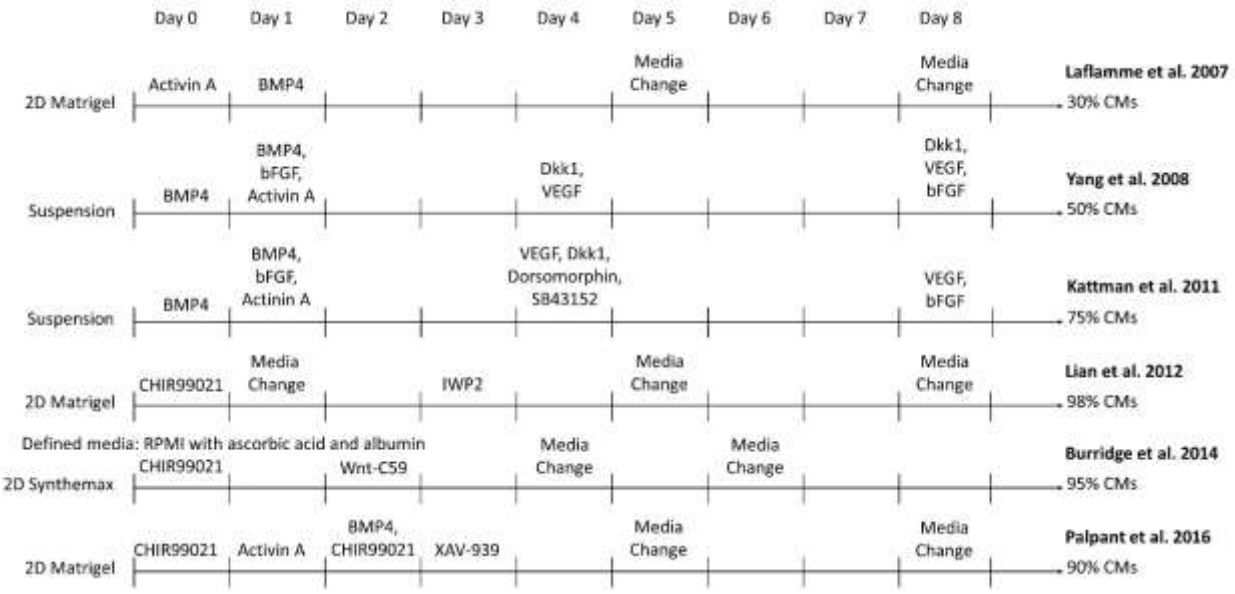

Figure 1.1: Comparison of select directed differentiation protocols for differentiating hPSCs to CMs.

1.2.2 Immature phenotypes of hPSC-derived CMs

The lack of mature, adult-like phenotypes in hPSC-derived CMs is a crucial limitation in advancing these cells toward clinical therapies. Their fetal-like state has been linked to arrhythmias after transplantation in large animal models (13). Chong *et al.* implanted hESC-derived CMs into infarcted macaque hearts through an intramyocardial injection. The immune-suppressed macaques that received the injection experienced irregular heart rates, with premature beating and tachycardia in the ventricle, with one monkey experiencing as many as a thousand non-sustained ventricular tachycardia episodes in a day. Shiba *et al.* injected CMs differentiated from MHC-matched, allogeneic, monkey induced pluripotent stem cells into infarcted hearts of Filipino cynomolgus monkeys (26). Though the grafts were not rejected and the CMs were able to integrate into the myocardial tissue partially restoring the heart, all the monkeys receiving CMs also experienced ventricular tachycardia episodes for up to 24 hours per day. In both studies, the arrhythmias decreased in frequency over time, perhaps due to a degree of *in vivo* maturation. For cell safety and efficacy, these hPSC-derived CMs must be matured enough to significantly reduce the potential to induce arrhythmias upon transplantation.

The hPSC-derived CM immature phenotype is characterized by a difference in marker expression, electrical and mechanical functionality, metabolism, calcium handling, and morphology in comparison to adult CMs, as summarized in **Table 1.1**. Structurally, hPSC-derived CMs are smaller, rounded cells, which more closely resemble embryonic CMs (27). In comparison, adult CMs have a much more elongated, rod-like shape as seen in **Figure 1.2** (28). Around 30% of adult CMs are multinucleated (29). Additionally, major changes affecting CM contractility occur in the organization of the CM sarcomeres and myofibrils during maturation (30). The anisotropic alignment of adult CMs is important to allow efficient propagation of electrical signals

(31, 32). These are aided by the formation of connexin-43 (Cx43)-containing gap junctions between the cells (33).

Many CM genes are more highly expressed in adult CMs than in hPSC-derived CMs. These genes encode ion channels, calcium regulators, sarcoplasmic reticulum transporters, and sarcomeric proteins including, but not limited to: *CACNA1C*, *HCN4*, *SCN5A*, *ATP2A2*, *MYL2*, *TNNI3*, *ACTN2*, *MYH7*, *MYL3*, *TNNC1*, *TNNT2*, *KCND3*, and *KCNH2* (34). Expression of different isoforms of sarcomeric proteins switch during CM maturation. Immature CMs express the slow skeletal isoform of troponin I (*TNNI1*) while more mature cells express the cardiac isoform (*TNNI3*) (35). Ventricular CMs primarily express MLC-2a and β-MHC early in development but upregulate MLC-2v and β-MHC as they mature (36). hPSC-derived CMs spontaneously beat while adult ventricular CMs are quiescent, requiring pacing by the nodal CMs (37). Also, the primary mode of carbon metabolism of CMs changes from glucose oxidation to fatty acid β-oxidation during development (38). The force of the adult CM contraction is on the order of μN, much larger than the reported hPSC-derived CM force of ~30 nN (39, 40).

hPSC-derived CMs have very immature, irregular electrophysiological responses. Their upstroke velocity ranges from 2 to greater than 200 V/s in comparison to 300 V/s in adult CMs (41). The immature CMs have reduced excitation-contraction coupling and a higher resting membrane potential of -58 mV, compared to the adult CM resting membrane potential of -80 mV (37). hPSC-derived CMs lack T-tubules, which aid in rapid signal transmission between cells through the sarcoplasmic reticulum (28). Instead, hPSC-derived CMs rely on trans-sarcolemmal calcium influx (28), which results in a reduced conduction velocity of 2.1-20 cm/s compared to 41-84 cm/s in adult CMs (42-44).

Table 1.1: Comparison of hPSC-derived CMs and adult CMs to demonstrate the changes during maturation.

Differences between hPSC-derived CMs and Adult CMs		
	hPSC-derived CMs	**Adult CMs**
Cell Structure and Organization		
Cell Shape	Round	Rod-like
	Mono-nucleated	30% Multinucleated
Cell Alignment	Disordered	Anisotropic alignment
Sarcomere Structure	Disordered sarcomere	I bands, M lines, A bands, Z bands, and Intercalated Discs
Sarcomeric Gene and Protein Expression	Low expression	High expression of *MYL2, TNNI3, ACTN2, MYH7, MYL3, TNNC1, TNNT2*
	MLC-2a	MLC-2v (ventricular CMs)
	α-MHC	β-MHC
	ssTnI	cTnI
Electrophysiology		
Upstroke velocity	2 to >200 V/s	300 V/s
Resting-Membrane Potential	-58 mV	-80 mV
Ion channel Gene Expression	Low expression	High expression of *CACNA1C, HCN4, SCN5A, ATP2A2, KCND3, and KCNH2*
Contractility		
Excitation-Contraction Coupling	Low coupling, spontaneous beating	High coupling, quiescent
Contraction force	~30 nN	on the order of μN
Gap Junctions	Low expression	High expression, including connexin-43
Ca2+ Handling		
T-tubules	Not present	Present
Conduction Velocity	2.1-20 cm/s	41-84 cm/s
Metabolism	Glucose oxidation	Fatty acid β-oxidation

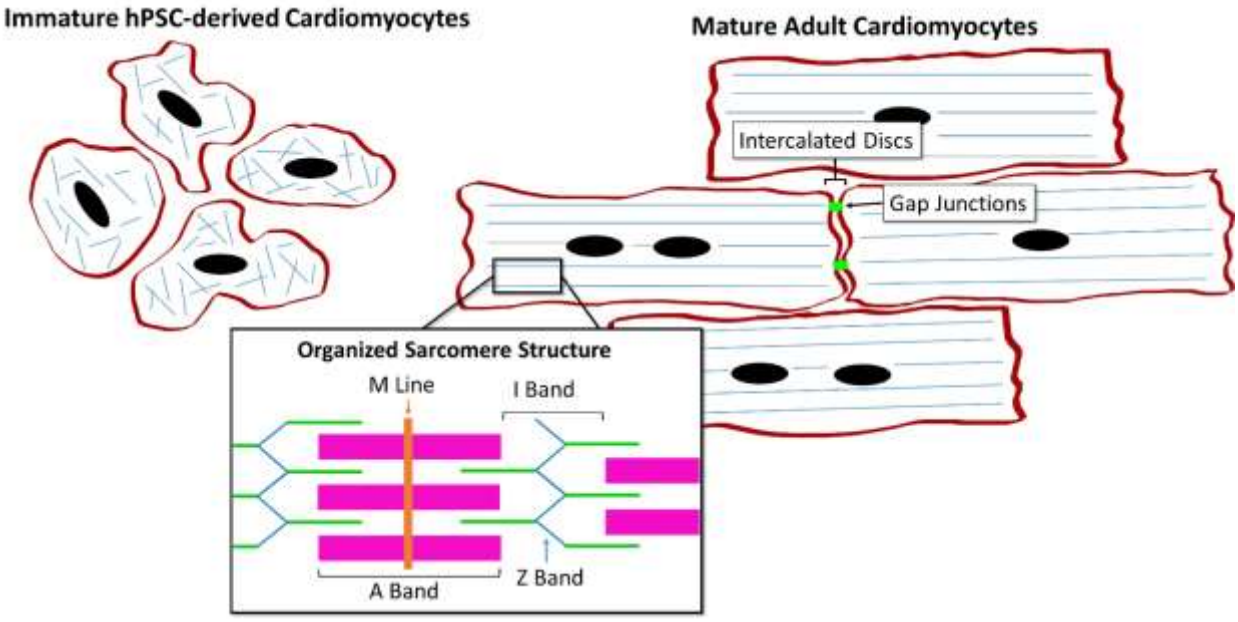

Figure 1.2: Comparison of hPSC-derived CMs and adult CMs demonstrating the structural and organizational changes during maturation.

One strategy to induce maturation of hPSC-derived cells involves implanting immature cells *in vivo*. This method has proved effective in maturing other hPSC-derived cell types including neural stem cells and pancreatic beta cell progenitors. For example, hESC-derived neural stem cells were implanted into C5 spinal cord lesion sites and increasing numbers of cells producing NeuN, a mature neural marker, were found throughout the following year (45). In addition, hESC-derived pancreatic progenitors differentiated into mature insulin-producing β-cells that expressed prohormone convertase enzymes upon implantation below the left kidney of immune-deficient mice (46, 47). Indeed, there is evidence that hPSC-CMs undergo a degree of maturation after implantation to the heart. For example, Kadota *et al.* demonstrated that implantation of CPCs and CMs into adult rat hearts exhibited maturation over time, as assessed by CM cell size, sarcomere length, and cTnI expression (48). However, after three months these cells had not yet reached the size of the rat CMs, suggesting they were still relatively immature. Some maturation was also seen over time in hESC-derived CMs grafts that were implanted in the macaques after they underwent an induced myocardial infarction, though many of the cells in the center of the grafts remained immature (13). The transplanted CMs in the graft core were not fully aligned, displayed low α-actinin expression and were much smaller than the hESC-derived CMs at the edge of the graft. Even if it were effective, implantation of hESC-CMs in an animal does not represent a realistic approach to scaling manufacturing of cells for human therapeutics. Therefore other methods must be pursued to mature hPSC-derived CMs in order to improve their safety and efficacy.

1.2.3 Design considerations to induce hPSC-derived CM maturation

A tradeoff between functional maturity and engraftment efficiency complicates selection of an ideal maturation state for transplanting hPSC-CMs. Funakoshi *et al.* reported that immature

day 20 iPSC-derived CMs injected intramyocardially into mouse hearts engrafted to a greater extent than more mature day 30 CMs, based on the number of human CMs found throughout the heart two months after transplantation (49). Testing on large animal models with a more similar physiology to human hearts will need to be done to determine the level of maturation that would be optimal for both integration and functional improvements in developing human cell-based therapies. Towards the goal of developing transplantable human iPSC-derived organs, Wu et al. are developing human-pig chimeras by incorporating human iPSCs into the inner cell mass of a pig blastocyst (50). Additionally, standardized maturity metrics are needed to compare how different signals and environments affect hPSC-CM maturation. Bedada *et al.* profiled the switch in expression of ssTnI to the cardiac isoform cTnI through cardiac development (35). Mouse stem cell-derived and rodent neonatal CMs exhibit significant levels of cTnI but human iPSC-derived CMs predominantly expressed ssTnI even after 9.5 months in culture. They suggested that the ratio of cTnI:ssTnI may serve as a useful marker for later stages of hPSC-derived CM maturation (35). However, the relationship between cardiac gene isoform switching and electromechanical and metabolic phenotypes has not yet been established. While determining the extent of maturation that leads to optimal regenerative performance and setting benchmarks to define when this level has been reached will be important steps toward creating cardiac cell-based therapies, a significant number of studies have been performed to attempt to accelerate maturation of hPSC-derived CMs through both biochemical and biophysical methods.

Several strategies to enhance maturation of hPSC-derived CMs have been described in recent years, with limited success in terms of rate and extent of maturation achieved. Both Ivashchenko *et al.* and Lundy *et al.* characterized the temporal changes in iPSC-derived CM maturation throughout time in culture, up to 80 days and 120 days respectively (51, 37). Though

the cells increased in size, organization, sarcomere length, expression of key cardiac genes, responsiveness to ion channel activators and inhibitors, and electrophysiology, they were still immature compared to adult CMs. Even though extended culture can be an effective strategy to mature hPSC-derived CMs, the amount of time required is generally not compatible with manufacturing timelines. Strategies to accelerate the rate of maturation include mechanical stimulation, electrical stimulation, altering ECM composition and substrate stiffness, directing cellular alignment, and coculture of the CMs with the other cell types prominent in the heart. These strategies provide differentiating CMs with cues found in the developing heart environment and their ability to induce maturation will be discussed in detail in Section 6.

1.2.4 The impact of nonmyocytes on hPSC-derived CM maturation

In a developing heart the CMs are in direct contact with and receive soluble cues from a variety of other cell types including fibroblasts, SMCs, ECs, and epicardial cells. In fact, when these interactions are eliminated in mouse embryos, the heart is unable to form correctly. For example, when Luxán *et al.* specifically inactivated Delta-Notch pathway components *Mib1* or *Jag1* in mouse myocardium or *Notch1* in the endocardium, the resulting hearts demonstrated left ventricular non-compaction cardiomyopathy (52). Similarly, Lavine *et al.* found *Fgf9* upregulation in both mouse endocardium and epicardium (53). *Fgf9* knockout resulted in decreased CM proliferation and dilated cardiomyopathy, a result that was also achieved by knocking out myocardium-specific expression of the receptors *Fgfr1* and *Fgfr2*.

As *in vitro* CM differentiation processes have evolved to become more efficient, signals from other cell types in a more heterogeneous population have been lost, perhaps altering the ability of the CMs to achieve mature phenotypes. For example, Kim *et al.* purified hESC-derived

CMs from embryoid bodies (EBs) at different time points and further cultured the cells to 60 days (54). The CMs maintained in culture with non-cardiomyocytes for longer time displayed enhanced maturation, including elevated expression of cardiac ion channels, electrophysiological maturity, and responsiveness to HCN, Na^+, and Ca^{2+} ion channel blockers, compared to CMs purified earlier. It is not clear why CMs cultured with non-cardiomyocytes for longer time achieved greater maturation than the CMs in monoculture. EBs are known to contain many cells types in addition to CMs, including endodermal, ECs, neural crest, and epicardial cells (53). With <7% of the EB composition being CMs, this study suggests that nonmyocytes may play an important role in phenotypic maturation of hPSC-derived CMs.

In tissue development and maintenance, cells interact in a variety of manners including autocrine and paracrine signaling, juxtacrine and biomechanical cues, and through remodeling of ECM components as shown in **Figure 1.3**. Identifying how various cardiac cell types impact CM phenotypes will be important for designing appropriate coculture systems that stimulate maturation of hPSC-derived CMs in a manufacturing setting. Some cues, such as soluble factors, are amenable to scale-up, while others like electrical and mechanical signals are more complicated to integrate into a bioreactor. The remainder of this review will focus on our current understanding of the role of both intercellular interactions and acellular methods to induce maturation in hPSC-derived CMs and cardiac tissues and discuss the logistics of incorporating these interactions into scalable CM manufacturing processes.

1.3 Mimicking intercellular interactions via soluble factors and ECM

The simplest method to incorporate intercellular signals into the production of CMs would be through the addition of soluble factors into the differentiation platform. If the pathways or

molecules through which various cardiac cells interact with CMs to accelerate maturation were identified, then these signals or other molecular modulators of these pathways could be introduced into the culture at specific times by manipulating medium composition. Additionally identification of the defined, cardiac-tissue inspired ECM for hPSC-derived CM maturation could mitigate the need to integrate other cell types into the production hPSC-derived CMs. A summary of the methods to induce maturation, shown in **Figure 1.4**, and their effects on specific CM phenotypes can be seen in **Table 1.2**.

1.3.1 Interactions with fibroblasts

Fibroblasts are a vital cell type for cardiac function and may be essential for cardiac maturation. They are responsible for secretion of growth factors, ECM deposition and remodeling, and even connect to CMs through connexins to aid in electrical signal propagation (55). Several studies have employed different methods and platforms to simulate and incorporate coculture of different fibroblast populations with either hPSC-derived or neonatal CMs. Culturing rat neonatal CMs in rat neonatal cardiac fibroblast-conditioned medium induced proarrhythmic changes (56). After 24 hours in the conditioned medium, the CMs had a prolonged action potential duration and a slower conduction velocity, measured by single-cell electrophysiology, compared to the unconditioned control, suggesting the fibroblast-conditioned medium impeded electrophysiological maturation. This adverse effect was not seen when the CMs were able to interact with the cardiac fibroblasts in a noncontact coculture (56). In contrast, the noncontact coculture appeared to enhance structural maturation of the CMs, increasing CM cell size and expression of β-MHC, suggesting that intercellular crosstalk is important in regulating the signals between the fibroblasts and CMs for CM maturation.

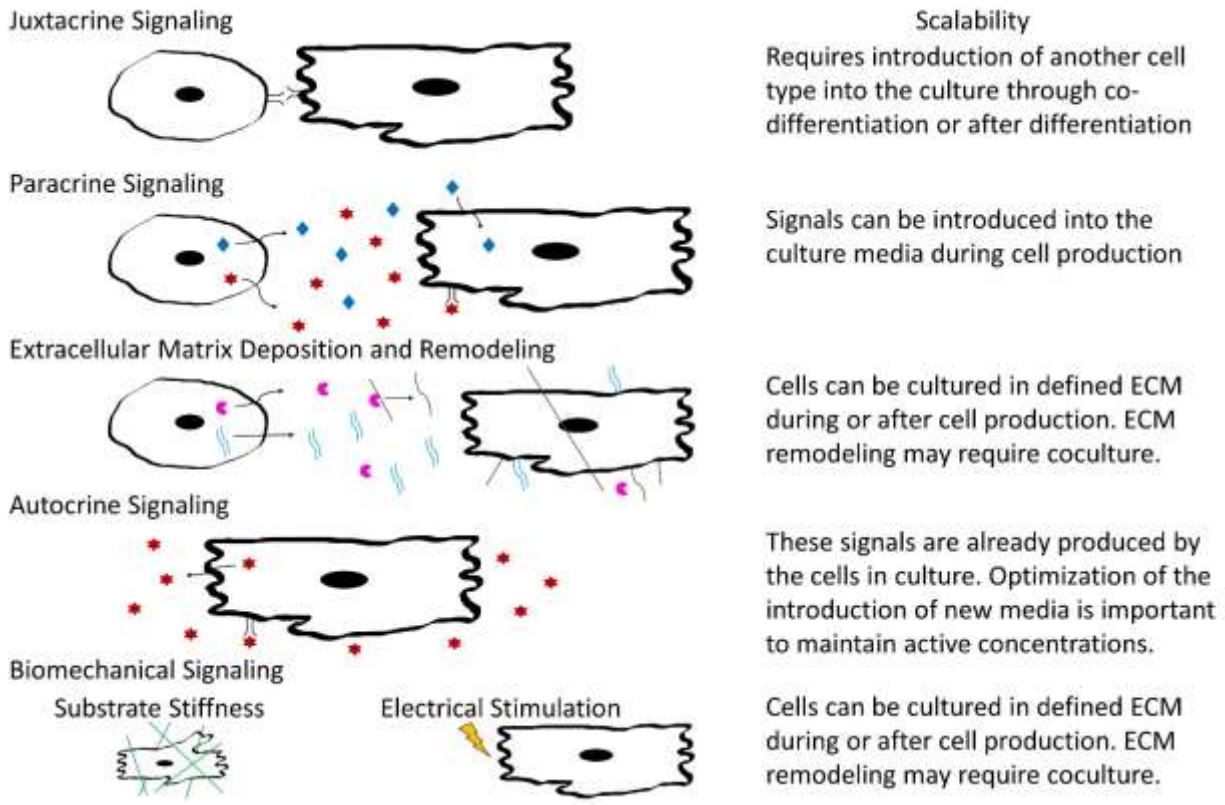

Figure 1.3: Schematic illustrating types of intercellular interactions and their scalability for inclusion into large-scaling manufacturing.

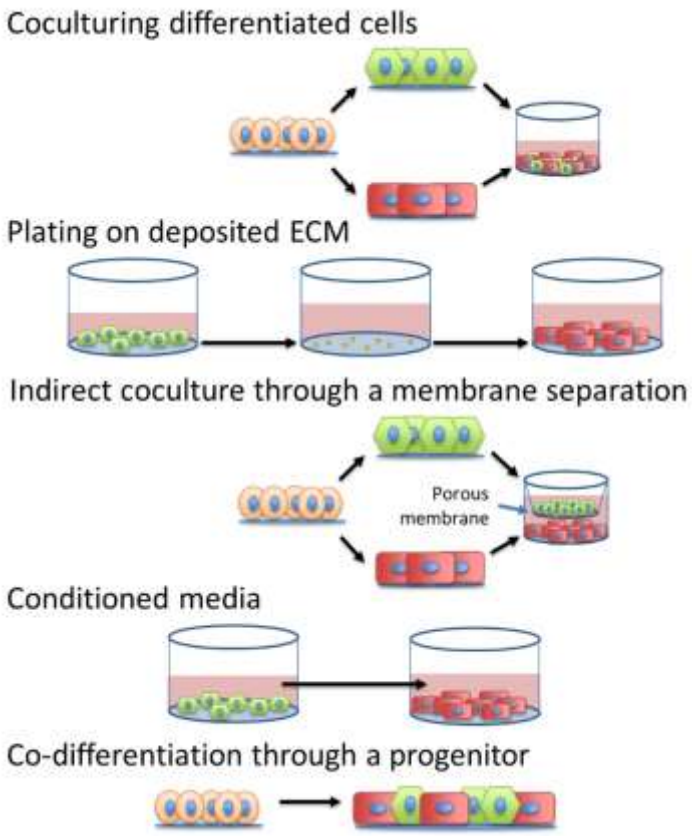

Figure 1.4: Different strategies to introduce intercellular interactions during hPSC-derived CM manufacturing.

Table 1.2: Summary of improvements to maturation phenotypes through different cues. + symbolizes an improvement of maturation, 0 is no significant improvement, - is a decrease in maturation. If left blank, then that type of analysis was not reported.

Methods to Induce hPSC-derived CM Maturation										
	Cell Shape	**Cell Alignment**	**Gap Junctions**	**Sarcomere Structure**	**Sacromeric Gene or Protein Expression**	**cTnI:ssTnI Ratio**	**Electrophysiology**	**Ion channel Gene or Protein Expression**	**Contractility**	**Ca^{2+} Handling**
Cell-secreted factors										
Fibroblast conditioned media (56)	+		**0**				-	-		
Indirect fibroblast coculture (56)							+			
EC-lysates (61)				+						
EC-conditioned media (61)				**0**						
EC-conditioned media (62)									**0**	**0**
Juxtacrine										
Direct fibroblast coculture on fibroblast ECM in comparison to indirect coculture (58)					+					
Direct EC coculture (61)	+	+		+	+					+
Direct EC coculture (62)									+	+
Fibroblast and EC coculture (78)	+	+	+		+			+		+
Fibroblast and EC coculture (79)					+			+	+	+
Direct EC coculture (91)					+	-	**0**	+		+
Extracellular Matrix										
Fibroblast-deposited ECM (58)	+		+		+					
EC-deposited ECM (61)				**0**						
Decellularized adult bovine heart ECM in comparison to decellularized fetal heart (97)					+			+		+
Metabolite and Hormone										
Tri-iodo-l-thyronine (14)	+			+	-			+	+	+
Glucocorticoid signaling (64)				+		**0**			+	+
Galactose and fatty acid carbon source (67)	+	+		+	+	+	+	+	+	+
Biomechanical										
Cyclic stretch (92)	+	+			+			+		
Cyclic Stretch with fibroblasts and ECs present (86)			+		+				+	+
Cyclic stretch (93)	+	+	+		+			+		+
Culture on soft PDMS in comparison to glass (98)			+			+		+		+
Culture on aligned fibers (99)		+		+			+		+	+
Electrical										
Electrical pacing (94)	+				+		+	+		+
Electrical pacing (95)		+	+	+		+		+	+	+

The cardiac ECM is important for distributing mechanical forces, conveying biochemical and biomechanical signals, and providing structural integrity to the surrounding tissue (55). Since it is essential to transmitting signals between CMs and the neighboring tissue, the ECM composition likely impacts the ability of hPSC-derived CMs to mature. Thus, it is likely a direct coculture or culture on fibroblast-derived ECM can influence hPSC-derived CM cell states (57). Indeed, Suhaeri *et al.* developed a scaffold coated with mouse fibroblast-deposited ECM that, when used to culture hESC-derived CMs, caused enhanced maturation as demonstrated by enhanced transcription of *TNNT2,* upregulation of Cx43 and α-actinin expression, and increased cell length-to-width ratio (58). Rat neonatal CMs also exhibited enhanced cardiac gene and protein expression, cell hypertrophy, increased sarcomere length, and more extensive cell multinucleation in both direct contact and noncontact cocultures with fibroblasts while cultured on fibroblast-derived ECM. While the neonatal rat CMs approached adult-like phenotypes with respect to cell shape and electrophysiology, the hESC-derived CMs remained more similar to embryonic CMs in their shape. Minimal differences were seen between the contact and non-contact neonatal CM-fibroblast cocultures on fibroblast-derived ECM (58).

Together these studies demonstrate that a noncontact coculture with fibroblasts and fibroblast-derived ECM can enhance CM maturation and can recapitulate the majority of effects from a direct contact coculture, pointing toward ECM deposition and remodeling along with paracrine secretion being the main methods of interaction between the fibroblasts and CMs for CM maturation. While known paracrine factors could be added to culture media, cell-deposited ECM could be introduced into large-scale production through either direct coculture, co-differentiation, or through pre-depositing ECMs onto the substrate before introducing the CMs into the culture.

No evidence so far indicates the necessity of having direct cell-cell contact between CMs and fibroblasts, though incorporation of fibroblasts directly into culture with CMs would allow the fibroblasts to deposit their ECM and secrete paracrine factors. It is also not yet evident whether cardiac-specific fibroblasts affect CM maturation to a greater degree than fibroblasts harvested from other tissues. Cardiac fibroblasts are largely responsible for synthesizing cardiac ECM components, including collagens I and III which together comprise 91% of the total collagen in the heart (8). The ECM also includes CM-produced collagen IV and other components including collagen V and VI, fibronectin, laminin, elastin, and fibrillin (57). Unlike other fibroblasts, cardiac fibroblasts specifically express DDR2 (57). In addition to other paracrine and juxtacrine interactions, further research should investigate cardiac fibroblasts, in comparison to others found in the body, to determine the specific factors and ECM components they produce to accelerate maturation of hPSC-derived CMs.

1.3.2 Interactions with ECs

As the most numerous cell type in the myocardium besides CMs, ECs are in close contact with CMs throughout heart development, delivering nutrients and removing wastes via the circulatory system (2). EC-derived factors may also regulate development and maturation of CMs. For example, endocardial ECs have been shown to produce neuregulin-1, a paracrine signaling factor that can induce electrophysiological maturation in hPSC-CMs (59, 60). To investigate whether rat arterial ECs could enhance hPSC-derived CM maturation, Lee *et al.* incorporated either EC lysates, EC-generated ECM, or EC-conditioned medium into the CM culture in addition to direct contact coculture of two cell types (61). Both direct coculture and EC lysates enhanced CM maturation, including better-organized sarcomeres, greater cell elongation and alignment, and

improved Ca^{2+} handling, compared to CMs in monoculture. However, EC-conditioned medium and EC-derived ECM had no detectable effect on maturation. Additionally, they found that the EC-induced changes in CM maturity were not replicated by mouse cardiac fibroblast coculture (61). ECs from rat fat, aorta, and heart induced similar effects on CM maturation, suggesting that the EC-derived effects on CM maturation are a general endothelial property. Direct EC coculture and EC lysates induced the CMs to upregulate expression of four specific microRNAs, miR-125b-5p, miR-199a-5p, miR- 221, and miR-222. Transfection of these microRNAs into CMs induced a degree of CM maturation, although not to the same extend as direct EC coculture (61). Adding microRNAs or other genetic targets of maturation pathways may be a facile method to simulate the effects of coculture in a CM manufacturing process, although more research is necessary to determine the mechanisms by which CMs sense and respond to cues produced by other cardiac cell types. Further investigation by Pasquier *et al.* saw improvements in the chronotropy and synchrony of hESC-derived CMs when in direct coculture with E4orf1-transfected human umbilical vein ECs in comparison to both EC-conditioned media and monoculture (62). This study further suggests the importance of juxtacrine signaling between the ECs and CMs for CM maturation. Notably, ECs also may aid in CM survival after transplantation due to their ability to vascularize the tissue and therefore are important to include in cardiac regenerative therapies in addition to possible CM maturation effects.

1.3.3 Hormone and metabolite induction of hPSC-CM maturation

Alternatively, biochemical activation of cardiac maturation pathways may be an effective strategy for manufacturing more mature CMs. Tri-iodo-l-thyronine (T3), a hormone synthesized by the thyroid, has been shown to decrease fetal gene expression and induce an isoform switch

from fetal to adult titin in embryonic rat CMs (63). T3 treatment increased iPSC-derived CM cell size and elongation, increased contractility, and increased sarcomere length after 1 week compared to untreated iPSC-derived CMs when the cells were treated with the compound for a week (14). Interestingly, expression of α-MHC was substantially upregulated following T3 treatment, which may indicate specification to atrial CMs. Kosmidis *et al.* investigated the ability of glucocorticoid signaling, which is known to enhance maturation of all organs in the fetus, to mature hPSC-derived CMs (64). Treating hESC-derived CMs with the synthetic glucocorticoid dexamethasone increased sarcomere length and force of contraction. A combination of dexamethasone and T3 applied to human iPSC-CMs cultured on a Matrigel substrate induced t-tubule network formation and enhanced excitation-contraction coupling (65). Lastly, it may be possible to induce hPSC-derived CM maturation through the metabolites provided in the culture media. Bhute *et al.* found a substantial shift in the metabolism of the hESC-derived CMs as they aged from 1 month to 3 months old *in vitro* (66). Aging in culture significantly upregulated phospholipid metabolism, pantothenate and Coenzyme A metabolism, and fatty acid oxidation and metabolism. It may be possible to induce these changes by altering media formulations. Indeed, Correia *et al.* found that switching to a medium containing galactose and fatty acids as primary carbon sources, rather than of glucose, forced the hPSC-derived CMs to mature at a faster rate (67). These cells demonstrated enhanced contractility, calcium handling, and a more elongated cell shape than CMs cultured in medium containing glucose. Altogether these studies illustrate the potential of regulating hPSC-derived CM maturation via known molecular and metabolic modulators of heart maturation. Addition of galactose and fatty acids along with T3 and dexamethasone could easily be incorporated into large-scale production of hPSC-derived CMs through culture media optimization.

1.4 hPSC-derived CM maturation in microtissues

While the addition of soluble factors or fibroblast-derived ECM may not be sufficient to fully mature hPSC-derived CMs, these strategies represent a step in the right direction. Signaling through direct cell-cell contact is also important for cardiac maturation. Also, incorporating hPSC-derived CMs into a scaffold with other cell types may enhance engraftment and survival *in vivo* (68). For these reasons, cardiac microtissues have been investigated as potential regenerative therapies. To create these microtissues, researchers have combined fibroblasts, SMCs, and ECs with CMs by separately differentiating the cells from stem cells or harvesting them from primary sources, and then constructing the tissue. Initially the strategy to combine multiple cell types into a cardiac microtissue was explored to enhance CM survival and engraftment after transplantation, but effects of intercellular interactions on CM phenotypes were observed in these tissues. Alternatively, it may be possible to use the innate ability of certain CPCs to create a microtissue in which the different cardiac cell types spontaneously organize as they differentiate, which will be discussed in Section 5.

In the past few years, hPSC differentiation protocols have been developed to generate relatively pure populations of multiple cardiac cell types in addition to the CMs described in Section 1.2.1. Pure populations of CD34+ cells, which can give rise to both ECs and SMCs, are obtainable using either MEK/ERK and BMP4 pathway or Wnt pathway activation, followed by magnetic activated cell sorting (MACS) (69, 70). Lui *et al.* used VEGF-A to drive the formation of cardiac-specific ECs from $Isl1^+$ CPCs (71). Purification of CD31+CD144+ cells was achieved by FACS with antibodies for both CD31+ and CD144+ surface markers. Epicardial cells and their derivatives have also been differentiated from hPSCs via an $Isl1^+Nkx2\text{-}5^+$ progenitor. Iyer *et al.* utilized the WNT3A, BMP4 and RA pathways to create WT1+ epicardial cells whereas Bao *et al.*

generated similar cells by stage-specific modulation of the Wnt pathway (72, 73). The resulting epicardial cells were 80-100% pure and could undergo epithelial-to-mesenchymal transition using TGFβ1 together with PDGF-BB or bFGF to generate SMCs and FGF treatment to create fibroblasts (6, 73). Bao *et al.* also demonstrated that hPSC-derived epicardial cells have the capacity to differentiate to cells expressing endothelial markers after VEGF treatment, but this process remains inefficient (74). hPSC-derived epicardial cells may be differentiated to epicardial-derived cells and then combined with hPSC-derived CMs to form cardiac tissues, or hPSC-derived epicardial cells may be directly incorporated into the cardiac tissues.

Initial attempts to generate cardiac tissues often utilized primary cells as a proof of concept to demonstrate the benefits of including these cells into microtissues in comparison to a CM-only graft. For example, Stevens *et al.* found that incorporation of human umbilical vein endothelial cells (HUVECs) and mouse embryonic fibroblasts (MEFs) into spheroids containing hESC-derived CMs greatly enhanced the survival of the CMs after transplantation into nude rat hearts (75). *In vitro*, ECs have the capacity to form tube-like vascular structures, though they are generally unstable and often require specific growth factors and 3D ECM or other scaffolds to form. In the presence of fibroblasts, these vascular-like structures were able to form and were maintained and stabilized without specific growth factor supplementation (76). When MEFs were cocultured with hESC-derived ECs and CMs on Matrigel in poly(lactic-co-glycolic acid) sponges *in vitro*, the stability of the tubes was enhanced and the CMs exhibited increased proliferation and expression of MLC-2v (76). Inclusion of ECs aided CM survival after transplantation of hESC-derived cardiac patches over the anterior cardiac wall of infarcted rat hearts (75, 77). The vascular structures in the patch were able to connect to the host capillaries as shown by the staining of Indian ink that was injected into the inferior vena cava (77) and by the presence of leukocytes and

Ter-119-positive red blood cells inside the vessels (75). It is not entirely clear whether the EC-mediated vascularization improved CM survival by enhancing delivery of oxygen and nutrients to the graft, or if paracrine and juxtacrine signaling influenced CM fate.

Additionally, combining multiple different cardiac cell types into cardiac tissue constructs has elicited greater maturation than individual cell types, suggesting additive or synergistic effects. Vuorenpää *et al.* found that fibroblasts together with ECs helped mature CMs (78). They seeded HUVECs and human foreskin fibroblasts first, allowing the cells to spontaneously form a vascular-like network in the culture dish, before adding iPSC-derived CMs. This caused the resulting CMs to orient longitudinally and to become larger. In a similar experiment, Ravenscoft *et al.* cultured human primary cardiac fibroblasts and ECs with hESC-derived CMs for two weeks (79). The resulting CMs exhibited increased contractile response to drugs targeting the β1-adrenergic receptor, EGFR-1/EGFR-2 receptor, or Na/K+ ATPase and the increased expression of *S100A1, TCAP, PDE3A, NOS3* and *KCND3* in comparison to either a monoculture or the combination of CMs with either ECs or fibroblasts alone. This response to the pharmacological agents was elicited by cardiac-specific fibroblasts and ECs, but not dermal fibroblasts or ECs, further suggesting a unique capacity for cardiac-specific cells in maturing hPSC-derived CMs. Though cardiac fibroblast and EC coculture improved gene expression in the CMs, they were still much more representative of fetal CMs than adult CMs.

Further microtissue design and evaluation should test the ability of hPSC-derived cell types to improve the functionality of hPSC-derived CMs. Production of cardiac tissues containing multiple cell types including ECs, fibroblasts, and possibly SMCs or epicardial cells will need to be investigated and optimized. These cardiac microtissues will likely need additional exogenous stimulation via biochemical and/or biophysical cues to achieve sufficient maturation.

1.5 Creating cardiac tissues via morphogenesis of CPCs

Instead of independently differentiating various cardiac cell types then combining them to create a cardiac microtissue, it may be advantageous to start with a CPC that can form the desired cell types and differentiate these progenitors in such way that they form organized cardiac structures. If differentiation can be spatially and temporally controlled, one may be able to manufacture cardiac tissues similar in composition and structure to the native myocardium, incorporating key factors that impact CM maturation and survival upon engraftment.

The adult heart contains rare populations of adult CPCs that can differentiate into CMs, ECs, SMCs, and fibroblasts (80). Different markers have been used to identify these adult CPCs including Sca-1 and c-kit, with consensus still needing to be reached on each populations' potential to form cardiomyocytes (80-82). Alternatively, CPCs found during development and differentiation of hPSCs to CMs are characterized primarily by the expression of Nkx2.5, Isl1, Flk-1/KDR, and PdgfR-α (20). These hPSC-derived CPCs are multipotent and can further differentiate to epicardial cells, ECs, SMCs, and CMs *in vitro* (71, 73, 83-85). While these CPCs have the capacity to form myocardial cell types, this potential has not yet fully been harnessed to manufacture cardiac tissues *in vitro*. Ruan *et al.* utilized an hPSC-derived $KDR^{+}PDGFR\alpha^{+}$ progenitor to create cardiac tissue constructs, co-differentiating the CPCs in a medium containing VEGF into CMs, SMCs, and ECs, which organized into vascular structures containing lumens (86). Interestingly, 3D differentiation favored CM generation while tissues differentiated in 2D contained a much greater SMC population. One caveat in using the CPCs for engineering cardiac tissues is that it is difficult to fully control the differentiation, with up to 40% of their constructs composed of unidentified cell types (86). Though use of hPSC-derived CPCs may provide a seemingly facile, development-inspired approach for engineering myocardial tissues, progress

must be first made to understand how to expand and control differentiation of these cells *in vitro* to generate sufficient quantities of therapeutically relevant cardiac tissues.

In fact, several recent advances in expanding and differentiating CPCs have opened the possibility of implanting CPCs for cardiac regeneration. Isolating CPCs from cardiac tissue and expand these CPCs *in vitro* is challenging (87). Only recently, Birket *et al.* discovered that by genetically modifying hESCs to allow doxycline-induced *MYC* expression, the CPC population could be maintained for up to 40+ doublings with the addition of IGF-1 and a hedgehog agonist (88). Though the genetic modification to stimulate *MYC* expression may limit the potential to use these cells in regenerative therapies, they will likely prove beneficial to study mechanisms of self-renewal and differentiation fates. Alternatively, two teams have reported methods to reprogram murine fibroblasts into induced CPCs (iCPCs) that can be expanded *in vitro* (15, 89). Lalit *et al.* induced expression of the cardiac transcription factors and chromatin regulators *Mesp1*, *Gata4*, *Tbx5*, *Baf60c*, and *Nkx2-5* in the fibroblasts (15). Zhang's method utilized the small molecules B431542, CHIR99021, parnate, and forskolin together with induced expression of *Oct4* (89, 90). Both methods resulted in Flk-1^{+}PdgfR-α^{+} iCPCs which were purified and then expanded in medium containing Wnt and JAK/STAT pathway activators (15) or containing BMP4, Activin A, a Wnt inhibitor, and an inhibitor of FGF, VEGF, and PDGF signaling (89). When transplanted into mouse hearts, these cells exhibited the capacity to differentiate into SMCs, ECs, and CMs, but did not form teratomas. The expandable iCPCs generated tissues comprised of approximately 60% SMCs, 7% ECs, and 30% CMs (89). This propensity to differentiate to SMCs may be a consequence of the fibroblast origin of the iCPCs. Lastly, reprogramming of fibroblasts to iCPCs has not yet been demonstrated in human cells and further characterization of the resulting CMs need to be done to determine their subtype specificity and maturity. Therapeutic delivery of

reprogrammed iCPCs may eliminate the need to terminally differentiate stem cells to cardiac cell types *in vitro*, but we need a better fundamental understanding of how to control differentiation fates and tissue morphogenesis in order to reliably manufacture structurally organized and functional cardiac tissues from iCPCs.

This concept of co-differentiation was used to direct hESCs to a mixed population of CMs and ECs using culture conditions permissive for differentiation to both cell types (91). Addition of VEGF at the same time as inhibition of Wnt signaling generated a population comprised of ~50% CMs and ~16% cardiac-specific *GATA4*+ ECs by day 10 after initiation of differentiation. It is not clear whether the VEGF directed a cardiac progenitor to an endothelial fate or provided a selective growth advantage to ECs in the differentiating culture. The CMs and ECs were purified then recombined to form a cardiac microtissue with enhanced CM maturity in their ion channel gene expression which was upregulated compared to CMs alone. These microtissues formed from co-differentiated CMs and ECs also exhibited increased sensitivity to the Ca^{2+} inhibitor verapamil and the β-adrenoreceptor agonist isoprenaline, signs of functional maturation. In contrast, the microtissues formed from co-differentiated CMs and ECs contained a lower cTnI:ssTnI ratio than the CMs alone, suggesting that co-differentiation did not induce myofilament maturation.

Co-differentiation allows cross-talk between developing cell types throughout the differentiation process, similar to what occurs in the embryonic heart during development, while combining cells after differentiation may fail to provide intercellular differentiation and maturation cues during the most impactful developmental stages. However, co-differentiation will likely be more difficult to implement in a manufacturing setting because of challenges in controlling the ratio and organization of multiple cell types and the potential need to purify and recombine cells into tissues if they do not spontaneously assemble into appropriate structures. With enough control

of the differentiation and morphogenesis processes, it may be possible to engineer the cells to autonomously form organized cardiac tissue structures, enhancing their function and ability to engraft into an adult heart. Further research will be needed to achieve this level of control through design of effective strategies that permit the formation of structured tissues from mixed populations of differentiating cardiac cells.

1.6 Incorporation of acellular methods to induce hPSC-derived CM maturation

While intercellular interactions play crucial roles in cardiogenesis, providing these signals during differentiation and subsequent culture of hPSC-derived CMs will likely be insufficient to fully mature the CMs. Other microenvironmental cues, including mechanical forces, electrical stimulation, and ECM composition and mechanical properties also regulate CM phenotypes. Here we will discuss how these cues impact hPSC-derived CM phenotypes and how they can integrate into a CM manufacturing process. These cues and their effects on specific CM maturation phenotypes are shown in **Table 1.2.**

The contractile forces generated by the heart are necessary for cardiac homeostasis and impact heart development. To investigate the role of stresses on hPSC-derived CMs, Tulloch *et al.* assessed the effects of cyclic and static stresses on these cells (92). The cells were cast into a gel which was attached to a flexible silicon surface. Mesh tabs were used to introduce static stress whereas the deformable silicon substrate was stretched to induce cyclic stresses. Both cyclic and static stresses induced sarcomere organization, CM enlargement and alignment, and increased expression of *MYH7*, *CACNA1C*, *RYR2*, and *ATP2A2* (92). Cyclic stretch on the CMs cultured with HUVECs did not further enhance maturation in comparison to the monoculture though the cocultured CMs demonstrated increased DNA synthesis (92). By using CPCs to co-differentiate

SMCs, ECs, and CMs together, Ruan et al. tested the effects of cyclic stretching on the resulting cardiac tissue constructs. Cyclic stretch increased the tissue stiffness and, in the hPSC-derived CMs, expression of cTnT, ratio of β-MHC:α-MHC, and cell contractility (86). Alternatively, Mihic *et al.* incorporated hESC-derived CMs into a gelatin sponge which could then be physically stretched and saw increased expression of the proteins Cx43 and MLC-2v and the genes *CACNA1C*, *SCN5A*, *KCNJ2*, *KCNH2*, *MYH7*, and faster Ca2+ handling (93). Incorporation of mechanical stresses into scalable CM manufacturing processes will likely prove challenging, although these cues may be effective when applied to cardiac tissues and might not be necessary during the CM differentiation phase of manufacturing.

Chan *et al.* employed electrical conditioning to simulate the cardiac conduction system signaling that developing myocytes are exposed to in the embryo in an effort to mature hESC-derived CMs (94). Electrically-paced CMs demonstrated increased spontaneous and caffeine-induced calcium flux and upregulated expression of cardiac genes including *SCN5A*, *ATP2A2*, and *KCNH2*, suggesting enhanced electrophysiological changes in ion channel expression. Eng *et al.* further demonstrated the ability of electrical conditioning to enhance CM expression of cTnI and Cx43, and increase the fraction of rapidly depolarizing cells through inducing expression of *KCNH2*, a gene that encodes a potassium channel responsible for the ability of hPSC-derived CMs to adapt their autonomous beating rate to the rate of the stimulation (95). The ability to respond to signaling provided by the conduction system rather than to follow intrinsic pacing may reduce the risk of arrhythmias after cells are implanted.

The composition and mechanical properties of the ECM and cell microenvironment impacts hPSC differentiation and cell phenotypes (96). Decellularized tissues provide 3D scaffolds with the composition and structure of native ECM. Fong *et al.* cultured iPSC-derived CMs in

decellularized fetal and adult bovine hearts in 3D culture (97). The decellularized adult heart ECM was found to be 10-fold stiffer than the decellularized fetal hearts and resulted in more extensive CM maturation, with increased expression of *JCN*, *CACNA1C*, *GJA1*, and *CASQ2*, compared to the CMs in decellularized fetal hearts. Herron *et al.* found that plating iPSC-derived CMs on soft PDMS gels increased cell size, Cx43 and cTnI expression, and CM contractility compared to CMs plated on glass (98). Culture on PDMS with an elastic modulus similar to that of cardiac tissue led to greater activation of β1 integrin receptors than culture on glass. When either the β1 integrin was directly inhibited by a neutralizing antibody or its downstream target, focal adhesion kinase, was inhibited, the CMs demonstrated a decrease in cTnI expression and cell size. This study further suggests the benefits of imitating both the composition of cardiac ECM and the stiffness of native heart tissue to accelerate CM maturation. Similarly, alignment of the ECM components also affects CM maturation. Li *et al.* cultured iPSC-derived CMs on electrospun, aligned nanofibers. CMs cultured on aligned fibers exhibited enhanced alignment, increased expression of MLC-2v and β-MHC, and higher electrical field potentials than CMs on random fibers and flat substrates (99). This highlights the ability of substrate topography to regulate both CM organization and maturation. Thus, one must consider ECM mechanics and organization as well as composition in designing a matrix for manufacturing CMs.

1.7 Current methods to scale up hPSC-derived CM manufacturing

Many recent advances have been made toward up-scaling the production of hPSC-derived CMs. From optimizing the differentiation and identifying how to adjust crucial parameters during the process, the industry is getting closer to being able to reliably produce CMs on a large-scale basis. For example, Tohyama *et al.* recently demonstrated the ability to differentiate hPSC-derived

CMs in monolayer culture in 10-layer, 1.2 L culture flasks with active gas ventilation, creating near a therapeutically relevant number of 1.5-2.8 x 10^9 cells with >66% purity (100).

To reduce the cost of manufacturing, 3D suspension differentiation platforms have been developed. Suspension systems generate higher cell concentrations, reducing the cost of culture medium and the size of reactor needed. Ting *et al.* utilized microcarriers to transition from hESC expansion and differentiation to CMs on a flat 2D substrate to CM production in suspension. (101). Microcarriers have a large surface area per volume and can be coated with different ECMs to facilitate cell attachment, proliferation, and differentiation. With gentle rocking during the stem cell culture and intermittent agitation during the differentiation, they obtained approximately 60% CM purity and about 200 million cells per 15 mL batch. With further development, microcarriers could provide a reliable and inexpensive method to produce clinically-relevant numbers of hPSC-derived CMs. However, the resultant cells would likely have to be separated from the microcarriers prior to clinical use.

Recent advances also have demonstrated the ability to produce hPSC-derived CMs in suspension without microcarriers. For example, Nguyen et al. followed either the Laflamme *et al.* 2007 or Lian *et al.* 2012 directed differentiation protocols to generate CMs, singularized the CMs and plated them in microwells to form 3D aggregates before transferring the cells into a rotary orbital suspension culture (18, 21, 102). By optimization of the cell density in the microwells, they achieved almost 100% α-actinin+ cells in 3D culture. Both Chen *et al.* and Kempf *et al.* seeded undifferentiated hPSC aggregates in reactors to scale up production of hPSC-derived CMs in suspension culture (103, 104). Kempf *et al.* differentiated the hPSCs in a 100 mL stirred tank reactor, generating 40-50 million CMs per batch (104). Chen *et al.* produced 1.5 to 2 billion CMs in a 1 L spinner flask (103). To date, these suspension differentiation platforms have strived to

produce pure populations of CMs. Moving forward, to introduce intercellular interactions in suspension CM manufacturing processes, direct cocultures may be achieved either through co-differentiation or introduction of other cell types during the differentiation. Further, perfusion of media from a reactor containing other cell types could provide a method to introduce conditioned media to simulate coculture conditions. Alternatively an indirect coculture could be achieved through separation of the cell types with a membrane. The use of small molecules and growth factors to mimic intercellular interactions would provide a simpler, easier to scale, and likely more robust and cost-effective alternative to coculture platforms.

To create cardiac patches with mature hPSC-derived CMs, several studies have devised methods to culture the constituent cells on a large scale after differentiation. Shadrin *et al.* developed a method to create cardiospheres, using differentiated and singularized hPSC-derived CMs and culturing them in a hydrogel plug free-floating in medium. After three weeks in culture, the CMs demonstrated increased maturation with highly structured sarcomeres and T-tubules (105). The hydrogels were 36 x 36 mm, a size relevant for clinical application (105). In addition to allowing CM maturation, this method of culturing the CMs in the hydrogels post-differentiation is amenable to both coculture and scale-up. The introduction of other cell types could be easily achieved when encapsulating the cells into the hydrogel. Specific ECM components also could be incorporated into the hydrogel.

Biophysical techniques to maturate hPSC-derived CMs may prove difficult to integrate into a large-scale manufacturing process. Lux *et al.* created a bioreactor that can both provide cyclic mechanical stretch and perfusion of medium to cardiac patches up to 2.5 x 4.5 cm in size (106). Tandon *et al.* developed a portable bioreactor which can both provide perfusion and electrical stimulation to cardiac patches (107). Further engineering is required to scale-up these

types of reactors, to design systems able to transmit electrical and mechanical cues in suspension. A comparison of the methods to scale-up production of mature hPSC-derived CMs is provided in **Table 1.3**.

Research has begun to look at monitoring and controlling the cells during production to ensure the quality of the cell product. Kempf *et al.* investigated the effects of cell density and CHIR concentration on CM yield and purity (108). They found that the CHIR concentration needed to induce CM differentiation correlated with cell density. This suggests that CHIR concentration can be modified to account for differences in growth rates between different cell lines or different batches (109). Metabolic analysis of the media would also allow monitoring of the differentiation and maturation processes. For example, an increase in glycerophosphocholine and the glycerophosphocholine:phosphocholine ratio during maturation may be markers for the maturation state of the hPSC-derived CMs (66).

1.8 Scalable purification of hPSC-derived CMs

After differentiation, hPSC-derived CMs will likely need to undergo a purification process to remove any traces of undifferentiated hPSCs or undesired differentiated cell types, and ensure a consistent product. Antibody-based purification methods are highly selective but costly to scale. Toward a negative-selection process to remove undifferentiated hPSCs, Choo *et al.* developed an antibody, mAB 84, which selectively caused undifferentiated hESCs to die, likely through oncosis (110). This antibody could reduce the tumorigenic potential of cells differentiated from hPSCs, although this has not yet been shown to be a significant problem in preclinical models of hPSC-derived cardiac cell therapies. CM-specific surface markers allow separation of hPSC-derived CMs by MACS and FACs. MACS against SIRPA and VCAM1 has been used to yield >95% pure

CMs (111, 112). However, there is a loss of CM yield following MACS (111). FACS also separates living cells based on expression of specific surface proteins. While it is highly efficient in terms of purity and yield, FACS is costly to scale. To eliminate the necessity of antibodies, Hattori *et al.* discovered that tetramethylrhodamine methyl ester perchlorate, a fluorescent dye that labels mitochondria, could be used to enrich hPSC-derived CMs to 99% purity (113). To enable their high energy utilization rate, CMs contains a large number of mitochondria in comparison to other cell types, with mitochondria comprising 30% of the CM volume (114).

Alternatively, genetic modification could allow purification of hPSC-derived CMs and other cardiac cells. Antibiotic resistance genes that are under the control of a cardiac specific transcriptional regulator enables purification via negative antibiotic selection. For example, a 99% pure population of CMs differentiated from a murine stem cell line expressing aminoglycoside phosphotransferase under control of the *Myh6* promoter was isolated following treatment with G418 (115). Additionally, lineage-specific expression of fluorescent markers would allow FACS without the need for antibodies. Expressing eGFP from the *MYL2* promoter allowed purification of a 95% pure hESC-derived ventricular CM population (116). Miki *et al.* developed microRNA switches that can selectively terminate undesired cell types (117). Upon successful transfection of a specific microRNA switch corresponding to the desired cell type, the switch will induce apoptosis of all cell types except the target. By using microRNA 208a, they were able to enrich iPSC-derived CMs to a 95% purity with a loss of only 10% of the CMs (117). They further demonstrated the ability to use one switch with two targets, microRNA 208a for CMs and 126-3p for ECs, yielding a purified coculture of these two cell types (117). This method may be able to eliminate any non-CMs in tissue patches without disrupting the cellular organization. The main limitation of the microRNA switches and genetic selection methods is the necessity for either

Table 1.3: Comparison of scaling methods for the generation of mature hPSC-derived CMs. + symbolizes minimal engineering to incorporate the maturation method into the bioreactor; - symbolizes significant engineering necessary.

	Bioreactor Capacity					**Ease of Potential Incorporation**						
Scaling Method	Size	Scalability	Purity	Cell Yield	Starting cell type in bioreactor	Mechanical	Electrical	Perfusion	Membrane separated coculture	ECM	Coculture of differentiated cells	Co-differentiation
10-layer tissue culture flasks (100)	1.2L	high	>66%	1.5-2.8B	hPSC	-	-	+	+	+	+	+
Microcarriers (101)	15mL	high	60%	0.2B	hPSC	-	-	+	+	+	+	+
3D cell aggregates (103)	1L	high	>90%	1.5-2B	hPSC	-	-	+	+	-	+	+
Cardiospheres (105)	proof-of-concept	high	Pre-purified	N/A	CMs	-	-	+	+	+	+	-
Perfusable, mechanical stimulation bioreactor (106)	N/A	low	Pre-purified	0.008B	CMs	+	-	+	-	+	+	-
Portable bioreactor (107)	N/A	low	Pre-purified	0.1B	CMs	-	+	+	-	+	+	-

limitation of the microRNA switches and genetic selection methods is the necessity for either transient or permanent genetic modification of these cells, which will have to be thoroughly analyzed to establish safety *in vivo* before their potential use in regenerative medicine.

Lastly, a metabolic selection may be used to purify CMs, taking advantage of their ability to use carbon sources that other cells cannot, such as lactate. Tohyama *et al.* demonstrated that lactate-containing medium can be used to generate 99% pure iPSC-derived CMs (118). This selection method was optimized in concert with differentiation of hPSC-derived CMs such that a pure population of cells was obtained within 20 days after the initiation of differentiation (24). By using a glucose-free medium, a pure CM population can be manufactured in a simple, defined, scalable process.

An overall comparison of the purification methods can be found in **Table 1.4**. After CM purification, the cells could undergo either density gradient or membrane filtration purification to remove any debris from the culture. Both of these methods are conducive to sterile large-scale cell manufacturing (119).

1.9 Preservation of hPSC-derived CMs

Preservation would simplify the supply chain for meeting the clinical demand of hPSC-derived CMs. Typically the cells will be singularized then cryopreserved in a medium that contains a cryoprotectant, such as DMSO, and apoptosis inhibitors. When using the proprietary DMSO-containing cryopreservation solution CryoStor, Xu *et al.* found that the hESC-derived CMs had a recovery rate of 70-77% with similar viability and purity as before freezing (120). To enhance survival, the cells were pretreated with a pro-survival cocktail containing apoptosis inhibitors, K^+ channel modulators, and growth factors for 24 hours prior to cryopreservation (18). Following

implantation into an ischemic rat heart, there were no differences in the sizes of grafts composed of hESC-derived CMs that had or had not undergone cryopreservation (120). Chong *et al.* also found no effect of hESC-derived CM cryopreservation on graft size after implantation of into mice hearts following myocardial infarction (13). DMSO causes cell toxicity and adverse reaction of patients, and thus must be removed from the cells prior to transplantation. DMSO alternatives including trehalose and poly-L-lysine, have been investigated although none have yet proven to effectively replace DMSO in cryopreservation media (121).

Alternatives to cryopreservation have been designed to simplify stabilization of hPSC-derived CMs. Correia *et al.* found that in 3D aggregates, about 70% of hPSC-derived CMs survived after storage at 4°C for up to 7 days (122). Although large scale manufacturing will likely require long-term cryopreservation, hypothermic stabilization may be suitable for transporting cells from a central manufacturing site to the clinic.

1.10 Conclusion

Significant advances have recently been made in manufacturing relatively pure populations of CMs from hPSCs in fully-defined processes, making the use hPSC-derived CMs for heart repair more plausible. The focus of research in this field is shifting to imparting more mature phenotypes in these cells to increase their safety and efficacy following transplantation. Additionally standards need to be defined to both quantify the extent of maturation and determine the level of maturation that is optimal for transplantation. The ratio of cTnI:ssTnI expression was proposed to be such a marker, but it is not yet clear how to assess electrical, mechanical, or metabolic maturation.

Recent efforts to simulate the intercellular interactions found in the heart *in vivo* during hPSC differentiation to CMs *in vitro* have demonstrated the importance of incorporating ECM,

Table 1.4: Purification methods for large-scale production of hPSC-derived CMs.

	Scalability	**Cost**	**Singularization required**	**Purity**	**Multiplexibility**
Fluorescently Activated Cell Sorting- mitochondria dyes (113)	low	low	yes	99%	no
Fluorescently Activated Cell Sorting- eGFP expression (116)	low	low	yes	95%	yes
Magnetically Activated Cell Sorting (111, 112)	medium	high	yes	95%	yes
Metabolic selection (24, 118)	high	low	no	99%	no
Antibiotic selection (115)	high	low	no	99%	yes
Antibody-based negative selection for hPSCs (110)	high	medium	no	98% removal of hPSCs	yes
MicroRNA switches (117)	high	medium	no	95%	yes

juxtacrine, and paracrine interactions between CMs, ECs, and fibroblasts. Of these, fibroblast ECM and EC juxtacrine signaling have been shown to enhance maturation phenotypes in hPSC-derived CMs. In addition, several experiments have pointed toward the necessity to use cardiac-specific cell types to induce maturation with the coculture. This should be further investigated to reveal mechanisms by which fibroblasts and ECs induce specific phenotypes in CMs. These cues could then be engineered into CM manufacturing processes in simpler manner than coculture. Also, efforts to discover genetic and epigenetic regulators of cell state, growth factors, hormones, and metabolites that enhance maturation would facilitate scalable production of hPSC-derived CMs.

Introduction of cardiac intercellular interactions via either microtissues or co-differentiation has been shown to enhance CM survival and engraftment *in vivo* in addition to CM maturation. Thus far the potential to co-differentiate cardiac cells from stem and progenitor cell types has not been investigated in sufficient depth due to insufficient control of these complex differentiation systems. In addition, co-differentiation would likely require purification using methods such as microRNA switches or antibiotic or metabolic selection. The potential of CPCs to form appropriately-structured myocardial tissue is a powerful advantage in developing cardiac regenerative therapies and should be investigated more extensively.

Mechanical and electrical simulation are effective means to accelerate maturation in hPSC-derived CMs but are difficult to incorporate in scalable manufacturing processes. Design of bioreactors to deliver these biophysical cues will likely improve CM and cardiac tissue manufacturing processes. A better mechanistic understanding of mechanotransduction during differentiation and maturation would enable alternative biochemical or genetic strategies to

modulate these pathways during CM manufacturing. Control of ECM organization, stiffness, and structure represents another promising approach to regulate hPSC-derived CM maturation.

To date no single method has proved effective in inducing maturation in hPSC-derived CMs. A combination of factors will likely be necessary to generate CMs of the appropriate maturity for regenerative therapies. Identification of effective strategies will be enabled by studies that relate the effects of maturation cues on specific phenotypes and identify mechanisms by which these signals impart maturation.

Chapter 2: Coculture of ECs with hPSC-derived CPCs Reveals a Differentiation Stage-Specific Enhancement of CM Maturation

2.0 Summary

Cardiomyocytes (CMs) generated from human pluripotent stem cells (hPSCs) are immature in their structure and function, limiting their potential in disease modeling, drug screening, and cardiac cellular therapies. Prior studies have demonstrated that coculture of hPSC-derived CMs with other cardiac cell types, including endothelial cells (ECs), can accelerate CM maturation. This chapter addresses whether the CM differentiation stage at which ECs are introduced affects CM maturation. We cocultured hPSC-derived ECs with hPSC-derived cardiac progenitor cells (CPCs) and CMs, and analyzed molecular and functional attributes of maturation. ECs had a more significant effect on acceleration of maturation when cocultured with CPCs than with CMs. EC coculture with CPCs increased CM size, expression of sarcomere and ion channel genes and proteins, the presence of intracellular membranous extensions, and chronotropic response compared to monoculture. Maturation was accelerated with increasing EC:CPC ratio. This study demonstrates that EC incorporation at the CPC stage of CM differentiation expedites CM maturation, leading to cells that may be better suited for *in vitro* and *in vivo* applications of hPSC-derived CMs.

This section was published in part as "Coculture of Endothelial Cells with Human Pluripotent Stem Cell-Derived Cardiac Progenitors Reveals a Differentiation Stage-Specific Enhancement of Cardiomyocyte Maturation" in the Biotechnology Journal on March 30th 2019.

2.1 Introduction

Cardiac failure affects 6.5 million people in the US annually and accounts for 9% of the total deaths (123). Cell-based therapies represent a promising class of emerging treatments to combat this mortality. Heart attacks often result in heart failure, killing approximately one billion cardiomyocytes (CMs) via hypoxia (10). Adult CMs are minimally proliferative, with only about 1% of the cells proliferating per year in an adult heart (124). Current methods of treatment for heart failure are limited; left ventricular assist devices only provide temporary aid and cardiac transplants are constrained by a shortage of donor hearts (12). The proliferation and differentiation potential of human pluripotent stem cell (hPSC)-derived cardiac cells and tissues provides a novel strategy to restore contractility to a failing heart (125).

Recently, hPSC-derived CMs differentiation methods have been optimized such that a nearly pure population of CMs can be created in fully-defined conditions (25). Scale-up of CM differentiations to produce over one billion CMs at >90% purity has been achieved using microcarriers in a 1L flask (103). When hPSC-derived CMs were injected intramyocardially into major histocompatibility complex-matched or immune-suppressed nonhuman primate hearts, cardiac function after myocardial infarction was significantly enhanced (13, 26, 126). Unfortunately, the implanted CMs caused transient arrhythmias and suffered from poor long-term survival (13, 26, 126). The arrhythmias may result from intrinsic spontaneous electrical signals generated by immature hPSC-derived CMs, which more closely resemble fetal CMs than CMs found in adult hearts (126). For example, hPSC-derived CMs express higher levels of myosin light chain 2a (MLC2a), α-myosin heavy chain (MHC), and slow skeletal troponin I (ssTnI) and lower levels of myosin light chain 2v (MLC2v), β-MHC, and cardiac troponin I (cTnI) than adult ventricular CMs (36). Additionally, expression of channels, regulators, and transporters such as

CACNA1C, *SCN5A*, *HCN4*, *KCNJ2*, *ATP2A2*, *RYR2*, and *GJA1* is generally lower in hPSC-derived CMs than in adult CMs (127). Additionally, hPSC-derived CMs are much smaller and rounder than adult CMs, and lack aligned myofibrils, localized gap junctions, and organized sarcomeres. hPSC-derived CMs spontaneously contract, lack t-tubules, and exhibit slower Ca+2 conduction than adult CMs (28, 43). In adult CMs, gap junctions localize at the cell membrane at the end of the myofibrils, and contain the gap junctional protein Cx43, allowing the flow of ions between adjacent cells. Also, hPSC-derived CMs utilize metabolic pathways similar to those employed in the fetal heart, including glycolysis and glucose oxidation, rather than fatty acid β-oxidation (66). These immature phenotypes limit the potential of hPSC-derived CMs in drug screening and clinical applications.

Several strategies have been shown to induce maturation in hPSC-derived CMs, but thus far no method has yet generated an hPSC-derived CM that fully mimics an adult CM (125). With extended time in culture, hPSC-derived CMs gained more organized sarcomeres and more mature gene expression profiles and electrophysiology after 90 to 120 days (37, 51). Electrical stimulation of hPSC-derived CMs enhanced expression of ion channels, cTnI, and Cx43 (94, 95). Mechanical stimulation induced expression of adult CM genes and proteins and accelerated Ca2+ handling (86, 92, 93). Ronaldson-Bouchard *et al*. reported ultrastructural sarcomere organization, sarcomere spacing of 2.2 μm, and more mature gene expression profiles after 4 weeks of simultaneous and continuous mechanical and electrical conditioning, but the cells did not generate the same contractile forces as adult CMs (128). Culturing CMs on micropatterned or soft substrates had a variety of impacts on maturation, including enhanced structural organization of sarcomeres and myofilaments, increased MLC2v and β-MHC expression, cell size, and contractility (98, 99, 129). Incorporation of electrically conductive materials, through integration in cardiac spheroids or with

the creation of cardiac films on polymer-covered plate, increased the expression of Cx43 and cellular alignment while decreasing the calcium transient time (130, 131). Similarly, biochemical cues such as hormone production or metabolic induction also can induce partial maturation (14, 67).

Heterotypic intercellular interactions also impact CM maturation. Coculture of mesenchymal stem cells with induced pluripotent stem cell (iPSC)-derived CMs increased CM contractility and sarcomere organization and alignment (132). This effect was recapitulated with EC-derived exosomes containing proteins and microRNAs (132). Similarly, fibroblasts have been shown to induce hPSC-derived CM maturation, including elevated cardiac troponin T (cTnT), Cx43, and α-actinin protein expression and contractility through both soluble factors and extracellular matrix protein production (58, 133).

To induce CM maturation and increase CM survival after implantation, hPSC-derived CMs have been cocultured with endothelial cells (ECs) (76). ECs are abundantly found in the myocardium, with each CM in direct contact with at least one capillary (134). Recently rat ECs and human umbilical vein ECs (HUVECs) were shown to induce structural and electrical maturation when cocultured hPSC-derived CMs; these effects were partially attributed to the transfer of microRNAs via gap junctions between the ECs and CMs (61). ECs isolated from fat, aorta, and heart had similar effects on cocultured CMs. A similar study found that direct contact was required for ECs to enhance maturation in cocultured hPSC-derived CMs (62). Giacomelli *et al*. cocultured purified hPSC-derived ECs and CMs, and found that ECs enhanced the CM chronotropic response to isoprenaline (91).

In addition to these binary cocultures, cardiac tissues comprised of hPSC-derived CMs, ECs, and stromal cells have been constructed. Construction of cardiac patches containing mouse

embryonic fibroblasts and hPSC-derived ECs and CMs led to tube-like structures and increased MLC2v expression in the CMs (76). Another group implanted patches composed of these three cell types into rat hearts and found that the vascular-like structures integrated with host capillaries when the patches were implanted onto the surface of rat hearts (75). The incorporation of fibroblasts and ECs enhanced transplanted CM survival compared to patches containing only CMs (75). Another study found that culturing iPSC-derived CMs with human foreskin fibroblasts and HUVECs increased CM size (78). Coculture with both primary cardiac fibroblasts and ECs increased hPSC-derived CM response to drugs such as isoprenaline, in comparison to monocultured CMs, EC and CM cocultures, and fibroblast and CM cocultures (79). These microtissues displayed increased contractility, Ca2+ handling, and CM-specific gene expression. Interestingly, dermal fibroblasts and ECs did not induce CM maturation.

CM differentiation and the migration of ECs into the developing heart occur in concert. For example, an endocardial tube has formed next to the myocardial layer by the Hamburg Hamilton (HH) stage 8 of chick embryo development (135). At stage HH13, endocardial-lined spaces have appeared within the myocardium. CMs begin spontaneously contracting at stage HH10 though vascularization of the myocardium does not occur until 6 days after the initiation of beating (135). The proximity of ECs in the endocardium to the developing CMs in the myocardium may be crucial in providing the CPCs and CMs with intercellular interactions vital for CM maturation. In developmental biology, the endocardium has been shown to impact myocardial development through pathways such as FGF signaling, neuregulin, and NOTCH signaling which affect myocardial proliferation, trabeculation of the myocardium, and cardiac development gene expression (52, 53, 59, 60). Through these pathways and other yet unidentified mechanisms, ECs may be assisting CM maturation.

Here we addressed whether EC effects on hPSC-derived CM maturation is influenced by the state of development of the CMs at which the coculture is initiated. We investigated whether hPSC-derived ECs can induce CM maturation when the ECs are cocultured with hPSC-derived cardiac progenitor cells (CPCs) or with beating CMs. We found that culturing CPCs with ECs generated larger CMs with elevated cTnI, cTnT, and MLC2v protein expression, with greatest effects at a 3:1 EC:CPC ratio. In contrast, EC coculture had little effect on beating CMs. Additionally, electrically active intracellular membrane formation increased when CPCs were cocultured with ECs. Both CPCs and CMs exhibited greater chronotropic responses when cultured with ECs. Together these results suggest that ECs have differentiation stage-specific effects on maturation of hPSC-derived CMs.

2.2 Materials and methods

2.2.1 hPSC culture with CM and EC differentiation

hPSC lines were maintained in mTeSR1 (STEMCELL Technologies; Vancouver, Canada) on Matrigel-coated (BD Biosciences; Franklin Lakes, NJ) culture plates (Corning; Corning, NY) using versene (ThermoFisher; Waltham, MA) or ACCUTASE™ (Innovative Cell Technology; San Diego, CA) for passaging. H9 human embryonic stem cells (hESCs) were differentiated to CPCs via the GiWi protocol (22, 136, 137). In brief, on day 0 cells were treated with 8-12 μM CHIR99021 (Selleckchem; Houston, TX) for 24 hours in RPMI (ThermoFisher) medium supplemented with B27 minus insulin (ThermoFisher). On day 3 of the differentiation, 5 μM IWP2 (Tocris; Bristol, UK) was added to the medium for two days. On day 6, the cells were frozen for future use in the coculture experiments, with test wells maintained in culture in RPMI/B27 containing insulin (ThermoFisher) for at least 5 days to verify their CM differentiation potential.

For the EC differentiation, the protocol from Bao *et al*. was followed using the H1 hESC line, 6-9-9 iPSC line, and 19-9-11 iPSC line (21, 136). To initiate differentiation, undifferentiated cells were treated with 6 μM CHIR99021 for two days in LaSR medium (Advanced DMEM F12 (ThermoFisher) supplemented with 60 μg/mL ascorbic acid (Sigma; St. Louis, MO) and 2.5 mM Glutamax (ThermoFisher)). On day 5, CD34+CD31+ endothelial progenitor cells were purified using the EasySep FITC Positive Selection Kit (STEMCELL Technologies) for magnetic activated cell sorting (MACS) on CD34. Purified EC progenitors (EPCs) were plated on either 1 mg/mL gelatin (Sigma) or 10 μg/mL fibronectin (Sigma) coated, polystyrene, tissue culture plates and cultured in EGM-2 (Lonza; Basel, Switzerland) supplemented with 5 μM Y-27632 (Selleckchem). The ECs were then passaged using ACCUTASE™ when near ~90% confluent, plated with Y-27632 in EGM-2, and maintained in EGM-2 medium.

2.2.2 Coculture of ECs, CPCs, and CMs

To initiate EC:CPC cocultures, cells were plated in the following ratios with 160 x 10^3 cells/cm^2 total added to each well of a 12-well plate: 1:3, 1:1, 3:1, 0:1. Cells were plated on Matrigel in EGM-2 with 5 μM Y-27632 and maintained in EGM-2 with the medium changed daily. Similarly EC:CM cocultures were initiated with 160 x 10^3 total cells at a 1:1 ratio. Upon thawing, the D6 CPCs were either seeded in EGM-2 medium with 5 μM Y-27932 with or without ECs or seeded in DMEM with 10% FBS and 5 μM Y-27932. The cells plated in DMEM with 10% FBS were then maintained in RPMI with B27 until D13-D18 (when beating was observed). At this point, the CMs were singularized with ACCUTASE™ and plated with or without ECs in EGM-2 medium with 5 μM Y-27632, then maintained in culture for two weeks with daily medium changes. For the transwell cocultures, the 400 x 10^3 MACS-purified EC progenitors (EPCs) were

plated in the transwell on a 3.0 μm polycarbonate membrane coated in collagen IV and fibronectin. The transwell were coated Matrigel for the CPCs. The main wells of a 12-well plate were coated in Matrigel and CPCs were plated at a density of 250 x 10^3 cells/cm^2 in DMEM with 10% FBS with 5 μM Y-27632. After allowing one day for cell attachment, the transwell was placed in the main well and the medium was changed daily with EGM-2 and cultured for seven days. ACCUTASE™ was used to singularize the cells for further analysis. For confocal microscopy, cells were replated onto Matrigel-coated glass plates (Cellvis; Mountain View, CA) or slides (LabTek; Grand Rapids, MI). For cell size analysis, the cells were replated onto gelatin-coated tissue culture plates at a density of 40 x 10^3 cell/cm^2.

2.2.3 Flow cytometry

After singularization with ACCUTASE™, cells were fixed in 1% paraformaldehyde for 20 minutes. Primary antibodies were diluted in flow buffer (5% wt/vol BSA (ThermoFisher) in PBS containing 0.1% Triton X-100 (Sigma)) according to **Supplementary Table 1** and added to fixed cells overnight at 4 °C. Secondary antibodies (1:1000 dilution in flow buffer) were incubated for 30 minutes at room temperature prior to analysis. Samples were run on a BD FACSCalibur flow cytometer. H9 hESCs were used to make CPCs and CMs and 19-9-11 and H1 hPSCs were used to make ECs for flow cytometry analysis. Statistical analysis was performed using one-way ANOVA with Tukey's HSD post hoc analysis, Student's t-test, Mann-Whitney test, or the Kruskal-Wallis test with Dunn's post hoc analysis.

2.2.4 Immunochemistry and confocal microscopy

Cells were fixed in 4% paraformaldehyde for 15 minutes before incubation with primary antibody diluted (**Supplementary Table 1**) in a blocking buffer containing 5% wt/vol non-fat dry milk and 0.4% Triton X-100 (Biorad; Hercules, CA) in PBS at 4 °C overnight. Secondary antibodies were added (1:1000 dilution in blocking buffer) for at least 20 minutes at room temperature. Nuclei were stained with 0.4 μL/mL Hoechst in PBS for 5 minutes. For confocal imaging, gold antifade reagent with DAPI (ThermoFisher) was used to seal the slides. Images were taken either with an inverted Olympus IX70 microscope or with a Nikon A1R confocal microscope.

T-tubule analysis was performed by incubating live cells with 30 μM di-8-anepps (ThermoFisher) and 2.5 μL/mL of Pluronic F-127 (ThermoFisher) for 5 minutes at 4 °C. eGFP and di-8-anepps were excited with the 488nm laser on a Nikon A1R confocal microscope. eGFP emission was collected a 450/50 bandpass filter, and di-8-anepps emission with a 595/50 bandpass filter. Comparison of the immunochemistry data between cocultures and monoculture controls was performed using Student's t-test.

2.2.5 FACS, RNA extraction, and qPCR

CPCs differentiated from H9-hTnnTZ-pGZ-D2, a hESC line which expresses GFP under control of the CM-specific *TNNT2* promoter, facilitated separation of CMs from EC cocultures (138). After using ACCUTASE™ to singularize the cells from the two week cultures, cells were suspended in versene containing 1% FBS (ThermoFisher) and 5 μM Y-27632 and kept on ice. 300 nM DAPI (ThermoFisher) was added to the flow buffer with the samples at least five minutes before flow activated cell sorting (FACS) to eliminate dead cells during sort. After gating out the

eGFP- cells, dead cells, and doublets, using the forward and side scatter area, eGFP+ cells were sorted directly into lysis buffer using a BD FACSAria cytometer. Immediately following the sort, total RNA was extracted using the RNEasy Micro kit (Qiagen; Venlo, Netherlands). Cells from three separate differentiations and cocultures were used to account for variation in the differentiated cells. The RNA was then converted to cDNA using the RT SuperScript III First-Strand kit (Invitrogen; Carlsbad, CA). qPCR was carried out with the PowerUP SYBR green master mix (ThermoFisher) and run for 45 cycles with annealing temperatures between 58-63 °C on an AriaMx Real-Time PCR System (see **Supplementary Table 2** for further information of primer sequences). To normalize for the amount of cDNA loaded, averaged CT values of VIRMA and ZNF384 were used as two housekeeping genes. Relative gene expression was calculated using the ΔΔCt method, with normalization to the monoculture control for each differentiation. Significance was determined via the Kruskal-Wallis test with Dunn's post hoc analysis between cocultures and controls.

2.2.6 Multielectrode array analysis

To obtain multielectrode array (MEA) recordings, monocultures and coculture were initiated on glass MEA plates coated with poly-D-lysine (Sigma) and Matrigel, with a total cell count of 160 x 10^3 cell/cm^2. After two weeks, initial recordings with the MEA were taken for 100 seconds using the MEA2100 system (ALA Scientific; Farmingdale, NY) before the addition of 0.5 µL of 0.01 mM isoprenaline (Sigma). The cells were placed in the incubator for 15 minutes before an additional recording was taken. This was repeated with escalating isoprenaline doses (up to 500 µM) until recordings at all concentrations were made. Analysis of the MEA data was done with Student's t-test.

2.3 Results

2.3.1 Coculture of hPSC-derived ECs and CPCs increased cardiac protein expression and cell size in the resulting CMs

During development ECs play crucial roles in the formation of cardiac tissue via many potential routes, including providing juxtacrine and paracrine factors such as Notch1, Fgf9, neuregulin-1, and nitric oxide (52, 53, 59, 60, 139). ECs have also been shown to enhance maturation of hPSC-derived CMs *in vitro* (61, 62, 91). The goal of this study was to determine whether hPSC-derived ECs affect maturation of hPSC-derived CMs when cocultured at different stages of differentiation, specifically comparing the effect of ECs on CPCs and early stage CMs. Since ECs are present at early stages of heart development, we hypothesized that hPSC-derived ECs would impact maturation phenotypes of hPSC-derived CPCs and CMs *in vitro*. To first test the impact of EC coculture on CPCs, hPSCs were differentiated to D6 CPCs via the GiWi protocol (22). CPCs were frozen, with test wells maintained to ensure the capacity to differentiate to CMs. After culture for at least 4 additional days, these CPCs formed a population of spontaneously contracting cells with greater than 90% of cells expressing cTnT, demonstrating their high CM differentiation potential (**Figure 2.1A**). The CPCs expressed ISL1 and VEGR2, consistent with multipotent cardiac progenitors (**Supplementary Figure 2.1A-B**) (73). Endothelial progenitor cells were differentiated from hPSCs using the protocol developed by Bao *et al*. and purified via magnetic activated cell sorting for CD34-expressing cells to obtain a progenitor population of at least 90% CD34+/CD31+ cells (**Figure 2.1B**) (73). These progenitors were expanded in EGM-2 for at least five days, yielding nearly pure ECs that expressed membrane-localized CD31 and VE-cadherin along with cytoplasmic vWF but no longer expressed CD34 (**Figure 2.1C-D**). The ECs were then maintained for up to five passages in EGM-2. The two cell types were co-plated at 160

x 10^3 cells/cm^2 on Matrigel-coated tissue culture plates with EC:CPC ratios of 1:3, 1:1, and 3:1, placing the two cell types in direct contact with each other to allow both juxtacrine and paracrine interactions (**Figure 2.1E**). A CPC monoculture also plated at 160 x 10^3 cells/cm^2 was used as a control to determine if the ECs enhance maturation of the resulting CMs. Brightfield images taken one day after plating the 1:1 EC:CPC coculture and the CPC monoculture control show cell attachment and formation of a confluent monolayers in both conditions (**Supplementary Figure 2.1C**). EGM-2 medium, changed daily, was used for both monoculture and coculture experiments. Other media, including RPMI/B27, caused the ECs to undergo an endothelial-to-mesenchymal transition to smooth muscle-like cells whereas the CMs survived and maintained their identity in EGM-2 medium (data not shown). After the two weeks in coculture, the percentage of VE-cadherin+ cells and cTnT+ cells in the culture was assessed via flow cytometry, and the final cell population approximately maintained the EC:CM cell ratios initially seeded, with the presence of small populations of other unidentified cell types (**Figure 2.1F**). Interestingly, 7.4 ± 1.0% VE-cadherin+ cells were present in the CPC monoculture control, suggesting that some endothelial progenitors or ECs exist in the CM differentiation. However, there were significantly fewer ECs in the monoculture control than the 24.7 ± 4.7% VE-cadherin-expressing cells in the 3:1 EC:CPC coculture ($p<0.05$).

During heart development, CMs begin to express cTnI at the late fetal or early neonatal stage (73). Induction of this protein has been elusive in hPSC-derived CMs and cTnI expression has been suggested as a molecular benchmark for CM maturity (140). To determine whether ECs induced cTnI expression in hPSC-derived CMs, we used flow cytometry to assess the co-expression of cTnI and cTnT+ cells after two weeks of coculture, and calculated the percent of cTnI+ cells within the cTnT+ cell population. With the addition of ECs, the percentage of cTnT+

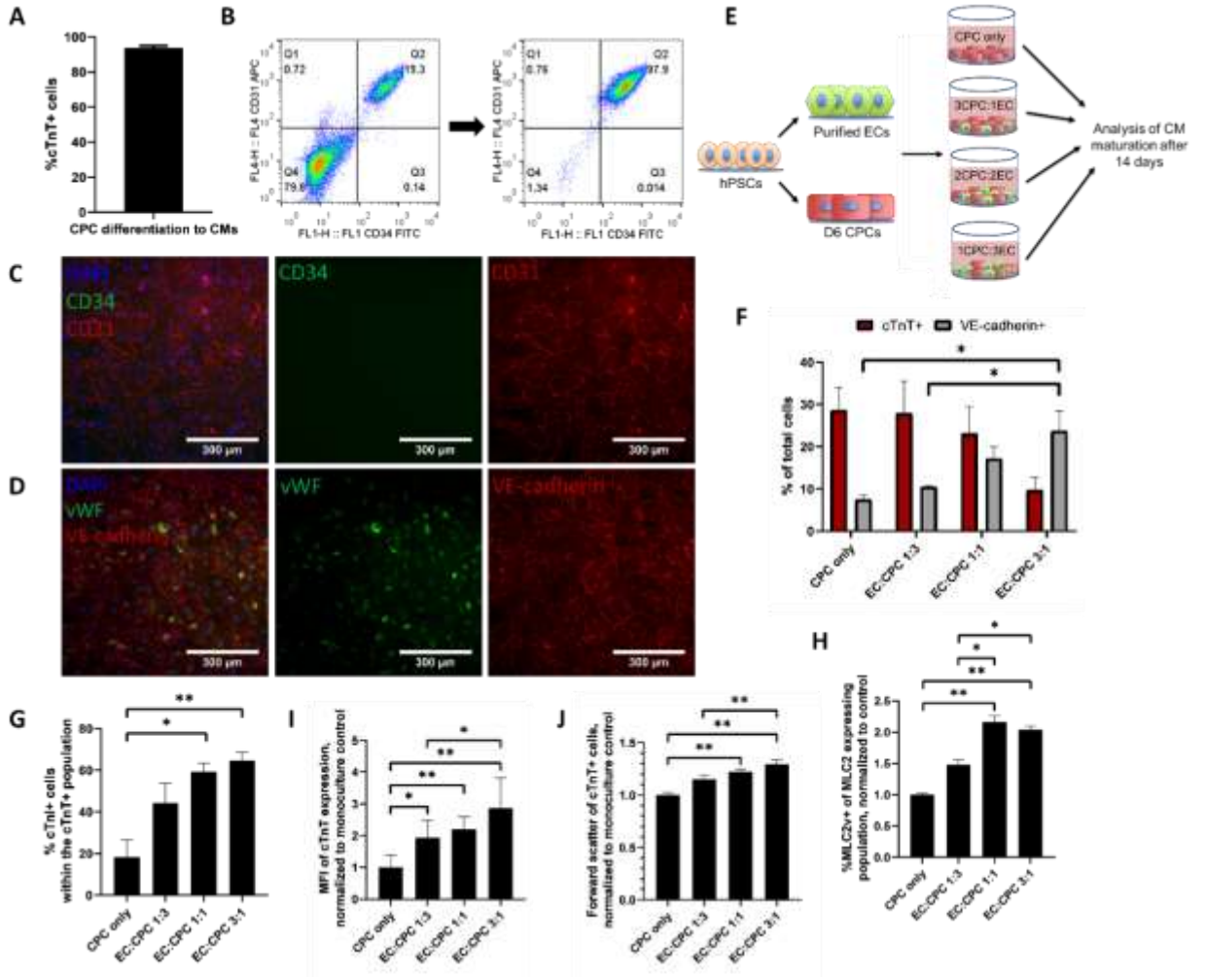

Figure 2.1: Cocultures of ECs and CPCs induced phenotypes in the resultant CMs that are associated with CM maturation. **(A)** H9 hESC-derived CPCs were differentiated to CMs via the GiWi protocol and the percentage of cells expressing cTnT was quantified by flow cytometry. **(B)** H1s and 19-9-11s were differentiated to EPCs by two days of CHIR99021 treatment followed by three days in culture, then purified by MACS for CD34 expression. CD34 and CD31 expression were determined by flow cytometry before (left) and after (right) MACS. **(C-D)** EPCs derived from 19-9-11 iPSCs were cultured in EGM-2 medium for five or more days, passaging when confluent. Before coculture, the cells were immunostained for **(C)** CD34 (green) and CD31 (red) or **(D)** vWF (green) and VE-cadherin (red) with DAPI (blue) to verify their identity prior to the coculture. **(E)** Schematic illustrating how hPSC-derived CPCs and ECs were cocultured for two weeks at a varying ratio with a constant 160 x 10^3 cells/well. **(F)** After two weeks, monoculture and coculture populations were analyzed for the percentage of cells expressing VE-cadherin and cTnT by flow cytometry. cTnT+ cells in the indicated monoculture and cocultures were analyzed via flow cytometry for **(G)** the percentage of cTnT+ cells expressing cTnI, **(I)** the median fluorescence intensity (MFI) of cTnT in cTnT+ cells, normalized to the monoculture, and **(J)** forward scatter of cTnT+ cells, normalized to the monoculture. **(H)** The cells in monoculture and cocultures were costained simultaneously for expression of both MLC2a and MLC2v by flow cytometry and the percent of MLC2v+ cells were calculated from the total cells expressing either MLC2 isotype. For each differentiation, the MLC2v percentages were normalized to the monoculture control. Data represent mean ± SEM of three independent differentiations with at least two experimental replicates each. Comparison of percentage of cells expressing VE-cadherin, cTnT, MLC2a/v, and cTnI was performed using ANOVA with Tukey's HSD post hoc analysis, N=3 (*

$p<0.05$, ** $p<0.01$). cTnT MFI, forward scatter, and normalized %MLC2v values were normalized to the CPC monoculture in each differentiation, and comparisons were performed using the Kruskal-Wallis test with post hoc Dunn analysis, $N\geq8$ (* $p<0.05$, ** $p<0.005$).

CMs expressing cTnI+ increased from 18.4 ± 8.2% in the monoculture to 59.4 ± 4.1% and 64.7 ± 3.0% cells in the 1:1 and 3:1 EC:CM ratios ($p<0.05$) (**Figure 2.1G**). To verify the specificity of the cTnI antibody used in this study, three-month old CMs were immunostained to demonstrate expression and localization of cTnI to myofilaments. As shown in **Supplementary Figure 2.1D-F**, the cTnT and cTnI antibodies colocalized in a striated pattern throughout the CMs and the cTnI did not stain cTnT+ day 10 CMs nor undifferentiated hESCs.

Expression of MLC2v is induced during ventricular CM development (36). The atrial MLC2 isoform, MLC2a, is expressed in embryonic ventricular CMs and is downregulated after induction of MLC2v (32). At day 14, the monoculture CPC control contained 15.3 ± 4.4% MLC2v+ CMs while the 1:1 and 3:1 EC:CPC cultures contained 29.9 ± 5.5% and 28.9 ± 4.9% MLC2v+ cells respectively (**Supplementary Figure 2.1G**). When the MLC2v percentages were normalized to the monoculture control in each condition, the 1:1 and 3:1 EC:CPC cultures contained a greater percentage of MLC2v+ CM populations by 2.16 and 2.04-fold respectively ($p<0.005$) as shown in **Figure 2.1H**, indicating that EC coculture accelerated induction of MLC2v. While cTnT is expressed early in CM differentiation, the expression level increases throughout development and thus may be used as another marker of CM maturation (141-143). To further investigate the influence of ECs on CM maturation, the degree of cTnT expression was measured in the cTnT+ CMs by the median fluorescence intensity (MFI) via flow cytometry. cTnT MFI was 1.9 ± 0.95-fold greater ($p<0.001$) in CMs from 3:1 EC:CPC samples compared to CMs in the monoculture control (**Figure 2.1I**). Additionally the size of CMs is known to increase during development (37). Via assessment of forward scatter by flow cytometry, which increases with cell volume, the size of resulting CMs was seen to increase significantly after coculture with ECs (**Figure 2.1I-J**). Overall, the addition of ECs to CPC cultures increased CM size and induced

expression of structural markers of maturation. The 3:1 EC:CM ratio resulted in the greatest percentage of cells expressing cTnI and MLC2v, the highest cTnT expression level, and the largest CMs.

To narrow down the potential methods of intercellular interactions between EPCs and CPCs that induce maturation, iPSC-derived EPCs and hPSC-derived CPCs were cocultured via transwells or co-plating for 7 days, focusing on differences that are essential during the intial formation of the hPSC-derived CMs. EPCs were used to further model interactions in the developing myocardium. The transwells limit cell-cell interaction to solely excreted paracrine factors whereas co-plating allows for a combination of paracrine signaling, juxtacrine signaling, and ECM modifications. As shown in **Supplementary Figure 2.2A**, 400 x 10^3 MACS-purified EPCs were plated in the transwell with 10^6 CPCs plated in the main well compartment. As a control, CPCs were plated on the membranes, in addition to the CPC in the main well. After the 7 days of coculture in EGM-2, the CPCs in the main compartment formed ~80% cTnT+ CMs and did not significant differ in percent of cTnT+ cells between the control and the coculture as shown in **Supplementary Figure 2.2B**. On the transwell after the 7 days in culture, the EPCs formed nearly pure ECs as shown by immunostaining, with junctional CD31 and VE-cadherin, minimal staining for α-SMA, a marker for smooth muscle cells, and no remaining CD34, a marker for EPCs (**Supplementary Figure 2.2C-D**). Using flow cytometry, the cells from the CPCs in the main well were analyzed, and no change in cTnT expression, cell size, nor MLC2v expression was detected (**Supplementary Figure 2.2E-G**).

To compare the transwell experiment to co-plated cell condition, the iPSC-derived EPCs and CPCs were co-plated in a 1:1 ratio as shown in **Supplementary Figure 2.3A**. There was a significant decrease, from 77.6 ± 1.6% to 47.4 ± 7.5%, in the percent cTnT+ cells found after one

week in the coculture compared to the monoculture (**Supplementary Figure 2.3B**; $p<0.05$). Correspondingly, there was a slight increase in cTnT expression from 1.00 ± 0.08 to 1.26 ± 0.21 and a significant ($p<0.05$), though small, increase in forward scatter from 1.000 ± 0.002 to 1.031 ± 0.015 between the monoculture and coculture CMs (**Supplementary Figure 2.3C-E**). To verify the results of these EPC/CPC co-plated cocultures, further replicates should be performed and the presence of ECs in the coculture should be validated after seven days. The increase in CM cell size in the co-plating coculture, which is not seen in the transwell cocultures, may indicate that physiological maturation effects are aided by juxtacrine signaling or ECM remodeling, and not exclusively paracrine signaling. It is possible the difference in seeding densities and total ratio of ECs the CPCs in the cocultures allowed the ECs to have a greater impact on the CMs in the co-plating experiment and should be further investigated. Longer coculture time may yield the same level of CM maturation by the EPCs as the ECs, shown in **Figure 2.1**, and future experiments should be extended to 14 days to determine if culture time impacts the CM maturation.

2.3.2 CM-specific protein expression induced by coculture with ECs is dependent on the stage of CM development at which coculture is initiated

In EC cocultures, we used either early beating hPSC-derived CMs, obtained between days 13 and 18 of the differentiation, or pre-CM D6 CPCs as shown in **Figure 2.2A**. To generate CMs, hPSC-derived CPCs were maintained in RPMI/B27 medium for ~9 additional days. When coculture was initiated, the cells were plated at a density of 160 x 10^3 cells/cm^2 in EGM-2 medium. The cells were plated as a monoculture or in a 1:1 ratio of ECs to the CPCs or CMs. Cells were then maintained in monoculture or coculture for two weeks before analysis (**Figure 2.2B**). After two weeks the monocultures contained approximately a 1:2 EC:CM ratio whereas the 1:1 seeded

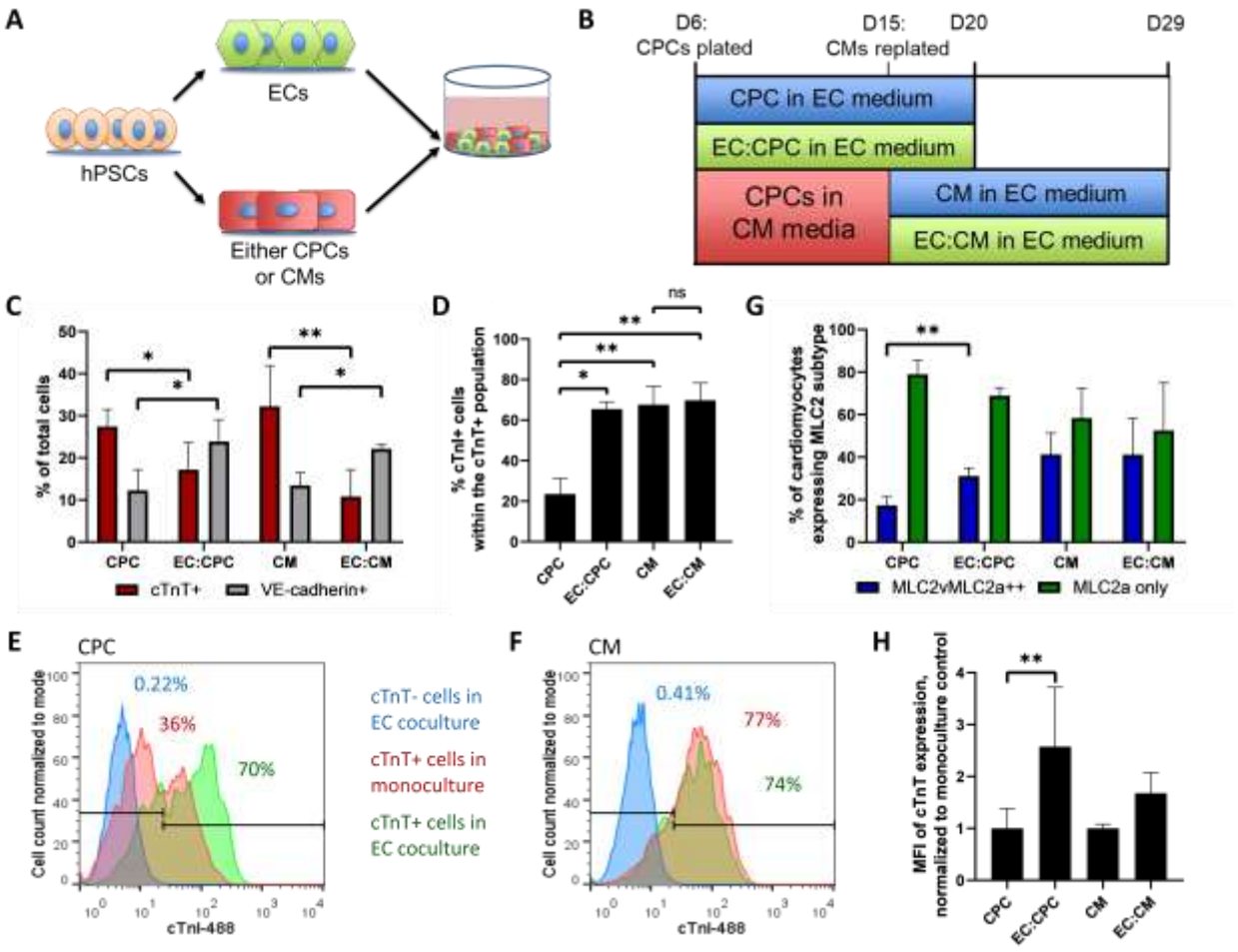

Figure 2.2: Comparison of induction of CM maturation properties when hPSC-derived ECs were cocultured with hPSC-derived CPCs and CMs. **(A)** Schematic illustrating how hPSC-derived ECs were cocultured with either CPCs or CMs. **(B)** The timeline in which the EC cocultures were induced and maintained in EGM-2 for two weeks before analysis and compared to their time-matched monoculture controls. **(C)** After two weeks in culture, the indicated monoculture and coculture samples were analyzed for the percentage of cells expressing cTnT and VE-cadherin by flow cytometry. **(D)** After two weeks in culture the percentage of cTnT+ cells expressing cTnI was determined by flow cytometry. Representative flow cytometry histograms are shown for **(E)** the cTnT+ cells in the CPC monoculture (red) and the EC:CPC coculture (green) and the cTnT- cells in the EC:CPC (blue), and **(F)** the cTnT+ cells in the CM monoculture (red) and the EC:CM coculture (green) and the cTnT- cells in the EC:CPC (blue). The numbers indicate the percent of cTnI+ cells in the corresponding samples. **(G)** Cells in the cocultures were costained and analyzed for expression of both MLC2a and MLC2v by flow cytometry, and the percent of each were calculated based on the total number cells expressing either MLC2v or MLC2a. **(H)** The median fluorescence intensity of cTnT in cTnT+ cells was quantified by flow cytometry. Data represent mean ± SEM of three independent differentiations with at least two experimental replicates each. Comparisons of VE-cadherin, cTnT, and MLC2a/v expression between cocultures and monocultures were performed using Student t-test, N=3 (* $p<0.05$, ** $p<0.01$). Comparisons of percentage of cells expressing cTnI were performed using one-way ANOVA with Tukey's HSD post hoc analysis, N=3 (* $p<0.05$, ** $p<0.01$). cTnT MFI values were normalized to the monoculture and statistical comparisons were performed using the two-way Mann-Whitney test, N≥8 (* $p<0.05$, ** $p<0.005$).

cocultures contained approximately 2:1 EC:CM, perhaps as a result of greater proliferation of ECs than CMs. The EC:CPC coculture contained a significantly higher percentage of VE-cadherin+ cells and a lower percentage of cTnT+ cells compared to the monoculture control (**Figure 2.2C**; $p<0.05$), consistent with observations in **Figure 2.1**. Similarly, the EC:CM coculture also contained a significantly higher percentage of VE-cadherin+ cells compared to the monoculture control ($p<0.005$). Immunostaining for VE-cadherin and MLC2a after two weeks of coculture of the CPC, EC:CPC, CM, and EC:CM samples demonstrated the presence of ECs and CMs in the wells (**Supplementary Figure 2.4A**). In all conditions, the ECs did not display any notable organization but were evenly dispersed throughout the plate. The CPC and CM monocultures were comparable in the final EC percentage and organization, as were both EC coculture conditions and are therefore are suitable for comparison of the impact of the incorporation of the ECs into the cultures on the resulting CMs.

Next, we determined if the stages of CM differentiation (CPCs vs. beating CMs) impacts the ability of ECs to induce the expression of key proteins indicative of CM maturation. To compare induction of CM maturation via the switch in troponin I expression to the cardiac isoform, the percentage of cTnI+ CMs was examined after two weeks in coculture. A significantly greater percentage of cTnT+ cells in the EC:CPC coculture expressed cTnI ($65.5 \pm 6.4\%$) as compared to the monoculture control ($23.5 \pm 4.0\%$, $p<0.05$) (**Figure 2.2D-F**). The percentage of cTnI+ cells within the cTnT+ population was not significantly different between the CM monoculture and EC:CM conditions ($67.6 \pm 9.1\%$ and $69.8 \pm 8.5\%$). This demonstrates that ECs may accelerate the rate at which cTnI expression is initiated when coculture is initiated prior to CM commitment. To see if this acceleration of cTnI expression is representative of other markers of CM maturation, we also assessed the expression of MLC2v in the CMs in the CPC, EC:CPC, CM, and EC:CM

conditions after two week in culture. Consistent with results shown in **Figure 2.1**, initiating EC coculture with the CPCs led to a significant increase in the percentage of CMs that were MLC2v+ compared to the monoculture control ($p<0.005$) (**Figure 2.2G**). However in the CM and CM:EC samples, MLC2v expression was not affected by EC addition. This supports the hypothesis that the CM differentiation stage at which the interaction with ECs is incorporated affects the ability of ECs to accelerate the induction of CM maturation. We next measured the expression level of cTnT in the cTnT+ cells to determine if EC coculture also increases cTnT expression when coculture is initiated with CMs. The MFI of cTnT demonstrated a significant increase in the cTnT expression in the CPC coculture compared to its control, but not in the CM coculture (**Figure 2.2H**, **Supplementary Figure 2.4B**). Overall, ECs accelerated production of structural markers of CM maturation when coculture was initiated while the cardiac cells were in their progenitor state but not with already beating CMs.

2.3.3 EC coculture with CPCs induced changes in CM morphology

Early hPSC-derived CMs are small, round cells (144). In extended culture they grow and elongate over time, but they do not become as large or rod-shaped as adult CMs (37, 51). To assess whether EC coculture with CPCs or CMs affects the resultant CM cell size, we first measured forward scatter by flow cytometry. CMs from the EC:CPC coculture forward-scattered light significantly more than CMs differentiated in monoculture (**Figure 2.3A**), consistent with a larger cell volume. To directly measure CM size, cells were replated after two weeks in monoculture or coculture and immunostained for cTnT. Image J was used to quantify the cell area, perimeter, and circularity of cTnT+ cells (**Supplementary Figure 2.5A**). Consistent with the forward scatter results, CMs from the EC:CPC coculture had a 33 ± 13% greater cell area than CPCs differentiated

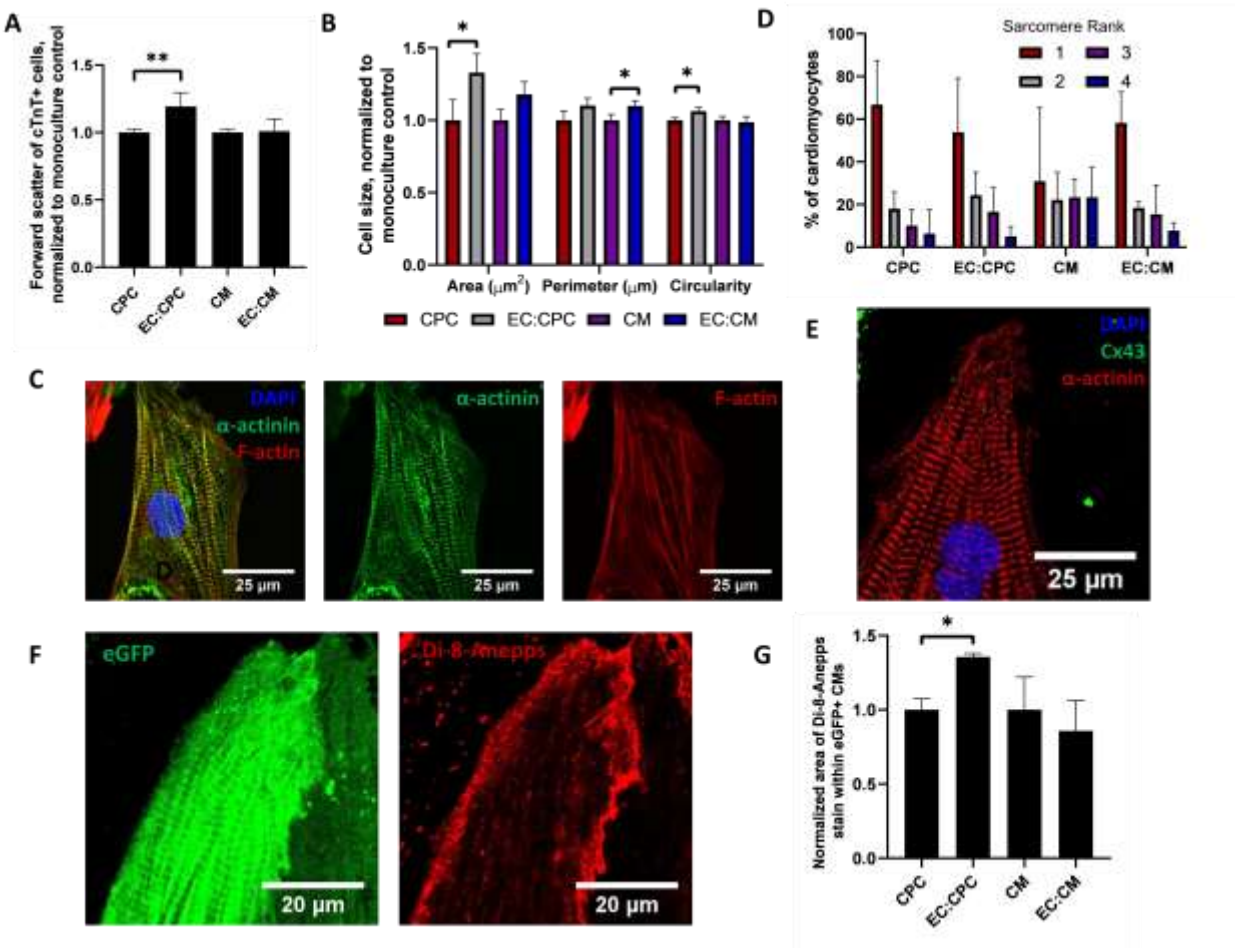

Figure 2.3: Cocultures of hPSC-derived ECs with CPCs, but not CMs, induced a more adult-like phenotype in the CMs after two weeks in culture. **(A)** The forward scatter of cTnT+ cells in the indicated monoculture and coculture samples was measured by flow cytometry after two weeks in culture. Data represent mean ± SEM of three independent differentiations with at least two experimental replicates each. Forward scatter values were normalized to the CPC monoculture in each differentiation and comparisons were performed using the two-way Mann-Whitney test, N≥8 (** $p<0.005$). **(B)** CM area, CM perimeter, and CM circularity of cTnT+ cells in the indicated monoculture and coculture samples were quantified by analyzing at least 40 cells per experimental replicate using ImageJ after replating two week samples onto gelatin-coated plates and culturing for 3 days. Values were normalized to the monoculture for each differentiation. Data represent mean ± SD of three independent differentiations with three experimental replicates each. Comparisons between corresponding cocultures and monocultures were performed using Student t-test, N=3 (* $p<0.05$). **(C)** H9 hESC-derived CPCs and CMs with or without hPSC-derived ECs were cultured for two weeks before replating on Matrigel-covered glass slides and immunostained for α-actinin (green) and phalloidin (red) with DAPI (blue) to compare sarcomere organization. **(D)** Blinded images of sarcomeres stained as described in panel (C) were ranked for their organization based on the following criteria: 1, no visible sarcomere structure; 2, some sarcomere organization; 3, H zones and Z lines visible in areas with some sarcomere organization; 4, near perfect sarcomeres with clear H zones, Z lines, and thick myofibrils**.** The percentage of CMs containing each rank in the indicated monoculture and coculture samples is plotted. **(E)** After replating the CPC, EC:CPC, CM, and CM:EC cultures after the two weeks in culture, cells were also stained for Cx43 (green), α-actinin (red), and DAPI (blue) to assess gap junction formation and localization.

(F-G) hESCs expressing eGFP under the *TNNT2* promoter were differentiated to CPCs and CMs and cultured in the indicated monocultures or with hPSC-derived ECs for two weeks. The cells were then replated on glass slides and were then stained with di-8-anepps to identify membranous extensions into the intracellular area of the CMs. **(F)** A high magnification image of an eGFP+ (green) CM is shown to illustrate the faintly striated di-8-anepps stain (red). **(G)** The percentage of the cell area, determined by eGFP, stained by di-8-anepps was quantified in ImageJ. Values were normalized to the monoculture for each differentiation (1.59% and 2.23% for the CPC and CM monocultures, respectively). Data represent mean ± SD of three independent differentiations for the CM and EC:CM data and two independent differentiations for the CPC and EC:CPC data. Cocultures were compared to monocultures using Student's t-test (* $p<0.05$).

in monoculture (**Figure 2.3B**; $p<0.05$). The cTnT+ cells in the EC:CPC cocultures displayed a 6.1 ± 3.1% greater circularity than the CMs from a monoculture control ($p<0.05$). This increase in circularity is inconsistent with increased structural maturation, which was interesting considering the ECs induced other structural markers of CM maturation. Both the EC:CPC and EC:CM cultures exhibited a greater perimeter than CMs in monoculture control of 10% (± 5% and 3% respectively) which could signify CM elongation. The raw values without normalization in each differentiation are provided in **Supplementary Figure 2.5B-D**.

Additionally, adult CMs have organized, aligned sarcomeres and myofibrils in addition to gap junctions localized to the intercalated discs, which together coordinate the direction and timing of contractions between CMs. The organization and alignment of sarcomeres within the CMs were analyzed for the presence of H zones and Z lines, and sarcomere length was measured on the replated cells by α-actinin immunofluorescence and phalloidin staining for F-actin. No significant differences in the organization of the sarcomeres and myofibrils were seen (**Figure 2.3C-D**). To examine differences in sarcomere structure induced by EC coculture, at least 75 cells in each condition over three separate differentiations were analyzed for their organization (examples in **Supplementary Figure 2.5E**). In all conditions, CMs exhibited a wide variety of sarcomeric structures, demonstrating some of the CMs in all conditions had developed to contain organized sarcomeres and myofibrils. Also during heart development, sarcomere spacing increases to ~2.2 μm from 1.6 μm (145). For every cell in which at least 11 Z lines in a row were visible, sarcomere length was measured. There was no significant change seen in the sarcomere length between the CPC, EC:CPC, CM, or CM:EC cultures. The average lengths ranged between 1.58 μm and 1.79 μm, indicating immature sarcomere spacing in all conditions (**Supplementary Figure 2.5F**). Finally, gap junction localization was visualized in CMs by immunostaining for Cx43 and α-

actinin (**Figure 2.3E**). We did not see a difference in Cx43 localization between the CPC, EC:CPC, CM, and EC:CM cultures. Overall, culturing ECs with CPCs yielded larger CMs compared to the CPC culture without ECs, though no additional structural organization was observed and the coculture seemed to decrease the amount of elongation in the CMs. In contrast, ECs had very little effect when cocultured with beating CMs, leading to a small increase in CM perimeter but no significant change in area or circularity.

Along with organized sarcomeres and localized gap junctions, t-tubules are another structural feature of adult CMs. In rats, formation of t-tubules begins after birth and are fully developed after a month (141). However, in hPSC-derived CMs, t-tubules are rarely seen, and this lack has been suggested to contribute to irregular Ca2+ handling in hPSC-derived CMs (37, 132). CMs and CPCs were generated from the H9-hTnnTZ-pGZ-D2, an hESC line that expresses eGFP under the *TNNT2* promoter, and used in monoculture and coculture configurations with hPSC-derived ECs as illustrated in **Figures 2.2A-B**. Live cells were stained with di-8-anepps (**Figure 2.3F**), a lipophilic membrane dye that fluoresces upon changes in the membrane potential and can be used to identify the CM membrane and extensions of the membrane into the cell (41). Over two separate differentiations, 43 eGFP+ cells in the CPC monoculture and 51 in the EC:CPC coculture were imaged. For the CM cultures, 71 eGFP+ cells were imaged in the monoculture and 78 in the EC-CM coculture over three differentiations. The percentage of the cell area stained with di-8-anepps was quantified for each CM analyzed (**Supplementary Figure 2.5H**). After normalizing to the monoculture control within each differentiation, we found that significantly more intracellular areas were stained by di-8-anepps in the EC:CPC coculture compared to the CPC monoculture (**Figure 2.3G**). Alternatively, the EC:CM coculture did not show any difference in di-8-anepps staining compared to the CM monoculture. The di-8-anepps staining demonstrates

that EC coculture can induce the formation of membrane extensions in CMs only when the culture is instigated early in the differentiation. These extensions may accelerate t-tubule formation although bona fide t-tubules were not observed in any of the experimental conditions.

2.3.4 Upregulation of CM-specific genes was induced by the coculture of ECs with CPCs

Genes encoding sarcomeric proteins, ion channels, and regulators of said channels are upregulated during CM differentiation and maturation (14). By analyzing relative mRNA abundance between the CPC and EC:CPC cultures, we further addressed whether EC coculture induces CM maturation at the early stage of differentiation. We cultured CPCs or CMs derived from H9-hTnnTZ-pGZ-D2 hESCs with hPSC-derived ECs for two weeks. We then used FACS to collect eGFP+ CMs for RNA extraction, using at least two experimental replicates across three differentiations, and analyzed gene expression via qPCR in **Figure 2.4** for the CPCs and **Supplementary Figure 2.6** for the CMs. *MYL2* expression was significantly upregulated in the EC:CPC coculture sample ($p<0.01$), consistent with the increase in MLC2v protein levels in the EC:CPC coculture shown in **Figures 2.2H** and **Figure 2.3G**. A significant decrease ($p<0.05$) in *TNNI1* (ssTnI) and an increase in *TNNI3* (cTnT) in the EC:CPC coculture is also consistent with increased cTnI expression in this sample. Myosin heavy chain isoform switches from predominantly α-MHC (*MYH6*) to β-MHC (*MYH7*) during human ventricular CM development (147). A decrease in *MYH6* and a significant increase ($p<0.01$) in *MYH7* provide additional evidence for accelerated CM maturation in the EC:CPC coculture compared to the CPC monoculture. Interestingly an increase in *GJA1* (Cx43) expression was also observed in the coculture sample ($p<0.05$), even though no any changes in gap junction organization were observed (**Figure 2.4F**). Finally, CMs from the EC:CPC coculture exhibited higher expression of

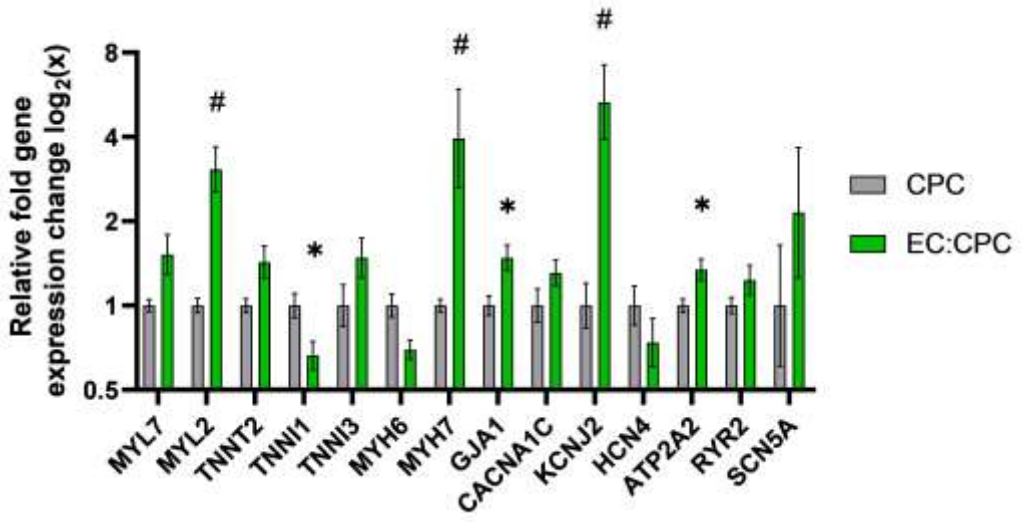

Figure 2.4: CMs from EC:CPC cocultures express genes associated with CM maturation. hESCs expressing eGFP under the *TNNT2* promoter were differentiated to CPCs, and maintained as CPC monocultures or cocultured with hPSC-derived ECs for two weeks. Then, eGFP+ cells were purified via FACS and expression of the indicated genes was quantified by qPCR. Values were normalized to the average of the expression of *VIRMA* and *ZNF384*, two housekeeping genes. Fold change values were calculated via the ΔΔCt method. Data represent mean ± SEM of at least six replicates taken from three independent differentiations with at least two qPCR experimental replicates each. The values were normalized to the CPC monoculture in each differentiation and statistical comparisons were performed using the two-way Mann-Whitney test, $N \geq 6$ (* $p<0.05$, # $p<0.01$).

KCNJ2 and *ATP2A2*, genes encoding a potassium-gated channel and an intercellular ATP pump, respectively. Alternatively, the ECs only significantly increased *KCNJ2* expression in the EC:CM coculture in comparison to the CM control as shown in **Supplementary Figure 2.6**. Summarizing this gene expression data, coculture of ECs with only CPCs resulted in upregulation of several genes involved in CM sarcomere formation and electromechanical coupling.

2.3.5 ECs promoted a CM chronotropic response from a β-adrenoreceptor agonist

hPSC-derived CMs are less electromechanically mature than adult CMs, as seen by lower upstroke and conduction velocities, reduced excitation-contraction coupling, and a higher resting membrane potential (43, 37, 41). These are in part due to their lower expression of specific ion channels and regulators along with the expression of different ion channel isoforms (148). Also, hPSC-derived CMs express lower levels of β-adrenoreceptors than adult CMs (149). Isoprenaline, a β-adrenoceptor agonist, generates a positive chronotropic response in CMs (150). The extent of this response has been shown to be affected by CM maturation, with 10 day hPSC-derived CMs having smaller increase in beating rate when exposed to isoprenaline in comparison to 80 day CMs (151). We initiated culture of CPC, EC:CPC, CM, and EC:CM on the MEAs. After two weeks, we measured changes in the time between each beat (RR interval) upon exposure to a range (0-500 nM) of isoprenaline concentrations. Example MEA recordings are shown for each sample with and without 500 nM isoprenaline in **Supplementary Figure 2.7A-D**. As shown in **Figure 2.5A**, there was no significant decrease in RR interval in EC:CPC and monoculture samples after isoprenaline treatments in part due to the high variability in the replicates. Alternatively, the EC:CM coculture required only 50 nM isoprenaline to result in a statistically significant decrease in RR interval ($p<0.01$), compared to 500 nM for the CM monoculture (**Figure 2.5B**).

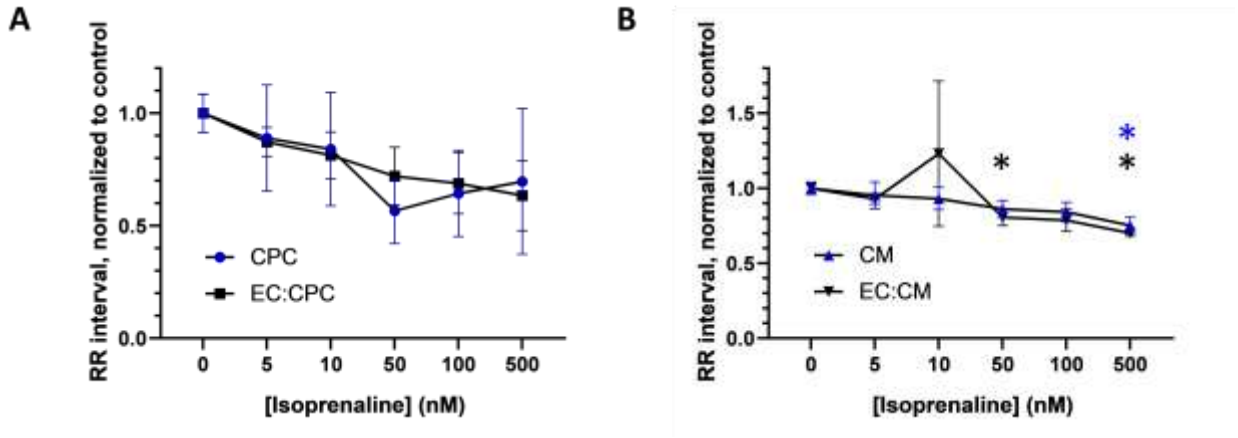

Figure 2.5: EC coculture increased CM response to isoprenaline in CMs. Monocultures and cocultures were maintained on Matrigel-coated multielectrode arrays for two weeks. The RR interval was measured for **(A)** H9 hESC-derived CPC monocultures or cocultures with H1 hESC-derived ECs and **(B)** H9 hESC-derived CMs monocultures or cocultures with H1 hESC-derived ECs as a function of isoprenaline concentration. Recordings were first acquired for the control condition lacking isoprenaline, then increasing doses of isoprenaline were added for 15 min before each recording. Data for each electrode were normalized to the untreated control. Data represent mean ± SD of RR intervals for two biological replicates. Comparisons between cocultures and monocultures were performed using Student t-test, N=2 (* $p<0.05$).

Incorporation of ECs into only the CM cultures significantly decreased the RR interval, suggesting that ECs enhanced the positive chronotropic response of CMs when cocultured with beating CMs.

2.4 Discussion

To determine the ability of ECs to impact CM maturation when coculture is initiated with cardiac progenitors, we seeded ECs and CPCs together in the ratios of 1:3, 1:1, and 3:1 along with a CPC monoculture. We observed an increase in the percentage of CMs that expressed MLC2v and cTnI, the expression of cTnT per cell and the size of CMs from the EC:CPC coculture compared to CMs from CPC monoculture. The extent of CM maturation depended upon the ratio of ECs to CPCs, with the greatest induction of maturation observed at a 3:1 EC:CPC ratio. Congruously, this ratio is similar to the ~2:1 ratio in which ECs and CMs are found in adult hearts (2). CPC:EC coculture enhanced the expression of *MYL2*, *TNNI1*, *MYH7*, *GJA1*, *KCNJ2*, and *ATP2A2*, which indicates CM maturation. Alternatively, we did not see an induction of any of these genes except for *KCNJ2* when the ECs coculture was initiated with beating CMs. We did not detect an increase Cx43 localization to longitudinal termini of the cells, even though the expression of the gene was upregulated. There was a slight, but not statistically significant, increase in the sarcomere organization when CPCs were cocultured with ECs. When the CPCs were cocultured with EPCs for 7 days, a similar but smaller induction in CM cell size and cTnT expression was found with co-plated cells but not with the cells in transwell, hinting that the maturation inducing signals are reliant on juxtacrine signaling.

Next, to determine if the induction of maturation when ECs were cocultured with CPCs was unique to the stage of the cells in the CM differentiation at which coculture was initiated, we compared the effects of coculturing the ECs with either young, beating CMs or with CPCs. When

the coculture was initiated with beating CMs, we did not see a significant impact on cell size or expression of cTnT, cTnI, and MLC2v. This lack of cTnI or cTnT induction is consistent with the lack of *TNNI3* or *TNNT2* induction reported by Giacomelli *et al*. when they cocultured hPSC-derived CMs in spheroids with or without ECs (91). Additionally the presence of membranous extensions, which might be t-tubule precursors, was enhanced by EC coculture only when the coculture was initiated with CPCs, but not CMs. However, ECs increased sensitivity of CMs to the β-adrenoreceptor agonist, isoprenaline, when coculture was initiated with only beating CMs. Similar enhancement in isoprenaline sensitivity was observed by Giacomelli *et al*. in EC:CM spheroids and by Ravenscroft *et al*. in hESC-derived CMs with coculture of both human primary cardiac fibroblasts and ECs (91, 79).

Based on our results, it is apparent that inducing EC coculture at the CPC stage resulted in greater acceleration of maturation than initiating EC coculture with beating CMs. This is consistent with a study performed by Ronaldson-Bouchard *et al*., where they found that the stage at which electrical stimulation is applied to hPSC-derived CMs impacted the extent of maturation achieved (128). Electrical pacing of day 12 CMs induced greater sarcomere organization, upregulation of genes expressed in adult CMs, and enhanced electrophysiological maturation compared to pacing day 28 CMs. The additional induction of isoprenaline sensitivity in the EC:CM coculture may also point to the importance for EC-derived signals to be continued out from the D20 CMs when the EC:CPC coculture to D29, the point at which the EC:CM coculture was assessed.

It is possible that the tissue specificity of ECs may be vital to induce the hPSC-derived CM development or maturation. In Ravenscroft's coculture system, human primary dermal fibroblasts and ECs were found not to enhance the response to drugs in comparison their cardiac-specific counterparts (79). When Nolan *et al*. engrafted generic, stem cell-derived ECs into mouse kidneys

and livers, they found that the ECs acquired the expression of markers specific to the tissue in which the cells were engrafted (152). The hPSC-derived ECs used in this study arise from a mesoderm progenitor but lack tissue and vessel-type specificity, which may result from developmental immaturity (153). It would be interesting to determine whether cardiac specificity is induced in these hPSC-derived ECs cocultured with hPSC-derived CPCs or CMs and if this specification has an impact on the observed CM maturation.

We observed the appearance of small populations of ECs in the CPC and CM monoculture controls. This may be attributed to the fact that ECs and CPCs arise from the same mesodermal population as CPCs, or the differentiation of ISL1+ CPCs to ECs (23). Indeed, ECs have been found as a byproduct of small molecule-induced CM differentiation (154-156). It is possible that our use of EGM-2, an EC growth medium, for our cocultures selectively expanded the EC population that arose during CM differentiation. Our data indicates that these "contaminating" ECs may in fact be beneficial to CM maturation.

Our results suggest the potential of ECs to influence CM development and maturation in a developmental stage-specific manner. For example, the endocardium influences myocardial development through pathways such as FGF signaling, neuregulin, and NOTCH signaling (52, 53, 59, 60). In addition to these paracrine signals, ECs have been shown to induce partial maturation via juxtacrine signaling through microRNA transfer via gap junctions (61). It is yet unclear which of these pathways and other yet unidentified mechanisms, also including biomechanical signaling and ECM remodeling in addition to juxtacrine and paracrine signaling, may mediate CM maturation caused by EC coculture with CPCs. Additionally, incorporating EC:CPC interactions during CM manufacturing may accelerate production of more mature cells. The maturation phenotypes seen in this study were only in the increased expression of some CM proteins and RNA

along with some structural organization and sensitivity to isoprenaline, demonstrating that full maturation of the cocultured CMs has not been achieved. It is likely that other signals will be necessary to induce full maturation of hPSC-derived CMs, such as the incorporation of other cell types or the design of a novel ECM in which to culture the CPCs. Further research should investigate the mechanisms by which the cocultured ECs induce hPSC-derived CM maturation. Identification of the biochemical and biophysical interactions between the ECs and CPCs that induce CM maturation may facilitate efforts to manufacture mature CMs without EC coculture.

In conclusion, coculturing hPSC-derived ECs and CPCs accelerated acquisition of CM maturation properties, including gene and protein expression, cell size, and development of t-tubule-like membrane extensions. This induction of maturation required initiation of EC coculture at the CPC differentiation stage, before spontaneous contraction was initiated.

Chapter 3: Modeling Myocardial and Epicardial Interactions during Heart Development Induces hPSC-derived Cardiomyocyte Maturation

3.0 Summary

Chapter 3 models the interaction of epicardial cells (EpiCs) with cardiac progenitor cells (CPCs) and the integration of EpiC-derived cells into the myocardium to investigate their impact on cardiomyocyte (CM) maturation. EpiCs form the epicardium, the outer layer of the heart, surrounding the myocardium and undergo an epithelial to mesenchymal transition (EMT) to create fibroblasts and smooth muscle cells in the myocardium. EpiCs have been shown to interact with cardiomyocytes during heart development and provide essential signals for proper myocardium formation, yet little is known about their impact on CM maturation. We differentiated human pluripotent stem cells (hPSCs) to both CPCs and EpiCs using protocols optimized previously in the Palecek lab. The TGF-β inhibitor, A83-01, induces proliferation of EpiCs and allows the cells to be maintained, without which they undergo EMT. We cocultured EpiCs and CPCs in both the presence and the absence of A83-01 for two weeks. The two cocultures each induced their own unique phenotypic changes in the resultant CMs indicative of CM maturation. This demonstrates the importance of investigating the interactions of different cell types on CM maturation to identify unique signaling pathways for identification and inclusion in CM manufacturing.

3.1 Introduction

As discussed throughout Section 1, myocardial infarctions are a growing issue for which human pluripotent stem cell (hPSC)-derived cardiomyocytes (CMs) could serve as a potential therapeutic. Additionally, these cells can be used for drug screening, disease modeling, and cardiac

toxicity tests. Highly efficient, fully-defined protocols have been developed recently to create hPSC-derived CMs (21-27). However these cells are immature in phenotype, mimicking more closely the cells found in embryos than those in adult hearts (27, 125). This immaturity is seen in the functionality of the hPSC-derived CMs, resulting in arrhythmias when implanted in primates (13, 26).

Epicardial cells (EpiCs) form the outer barrier of the heart. During development, they originate from the proepicardium and begin a migration to cover the heart immediately following the looping and beginning of contraction of the embryonic heart tube (135). The EpiCs then migrate into the myocardium, through a matrix-rich barrier called the subepicardium, to form fibroblasts (FBs), smooth muscle cells (SMCs), and potentially endothelial cells (ECs) (74, 157, 158). EpiCs play a key role in the development of the myocardium. Prevention of epicardial outgrowth caused a change in the conduction of the heart in embryonic chickens (159). Elimination of EpiC-derived cells caused a decrease in CM proliferation, mechanical coupling, and electrical coupling in embryonic mice models (160). Additionally, developmental biology studies have found that EpiCs interact with CMs through paracrine signals (161). These include fibroblast growth factors (FGF) and retinoic acid (RA) (162, 163). They influence myocardial morphogenesis and when eliminated, resulted in embryonic lethality in mice. For example, FGF9 depletion from epicardial cells or CM-specific FGF receptor knockouts in mice caused a decrease in CM proliferation and malformation of the heart (163). These interactions demonstrate the importance of epicardial-derived signals in embryonic heart formation.

Minimal research has investigated the impact that EpiCs have specifically on hPSC-derived CM maturation. Bian *et al.* designed EpiC mimetics from elasteromeric molds to have same alignment as the epicardium (164). These mimetics were shown to induce hPSC-derived CM

maturation in the increase in CMs alignment along with adult-like conduction velocity and the formation of t-tubules. Other research has more focused on the impact that EpiC-derived cells has on CM maturation since these cells are found throughout the myocardium. For example, Weeke-Klimp *et al.* used EpiC-derived cells from embryonic quail eggs and cocultured them with neonatal mouse CMs and found that the coculture induces CM maturation in the CM alignment and increase in Cx43, cTnI, and α-actinin expression (160). Moreover, FBs have been shown to induce elevated cardiac troponin T (cTnT), Cx43, and α-actinin protein expression and contractility in hPSC-derived CMs (58, 133). This induction of maturation was caused specifically by soluble signals and FB-deposited ECM. Thus far SMCs have only been cocultured with hPSC-derived CMs in efforts to create multi-cellular tissue patches with ECs to increase CM survival after transplantation (76, 86). In Section 2, we demonstrated the ability for ECs to also induce CM maturation in cell size and the induction of many genes and proteins such as cTnI and cTnT in hPSC-derived CMs when cocultured with CPCs. Together these demonstrate the ability for EpiC-derived cells and even the physical structure of the epicardium to induce hPSC-derived CM maturation, but it is yet unknown if EpiCs and the process of EMT of these EpiCs during heart development has any impact on CM maturation.

Recent protocols have been optimized to generate hPSC-derived EpiCs and prevent the initiation of EMT within the EpiCs through using TGF-β inhibitors (72, 73). By combining hPSC-derived CM progenitors (CPCs) with hPSC-derived EpiCs, the interactions of these cell types during heart development can be modeled. We cocultured these two cell types in the presence and absence of the TGF-β inhibitor, A83-01, to prevent EMT and compared the resulting changes in maturation of the CMs that arise from the CPCs. In the presence of A83-01, the EpiCs maintained their WT1+ expression whereas, without the inhibitor, a calponin+ population was identified and

lacked any WT1+ population, indicating that the EpiCs underwent EMT. After the seven day coculture, the cells were analyzed for phenotypic changes indicative in CM maturation, including cTnT expression CM cell size. In the coculture with A83-01, the CMs had only a larger MLC2v+ CM population compared to a monoculture control. Alternatively in the coculture without A83-01, the CMs only were larger cells with more cells expressing cTnI. Together these results indicate that both EpiCs and EpiCs undergoing EMT can induce hPSC-derived CM maturation, each specifically targeting different CM phenotypes.

3.2 Materials and methods

3.2.1 hPSC culture with CPC and EpiC differentiations

H9 human embryonic stem cells (hESCs) were cultured on Matrigel-coated (BD Biosciences) tissue culture plates in mTeSR1 (STEMCELL Technologies) and passaged every three days with Versene (ThermoFisher) (136). To differentiate to CPCs, the H9 cells singularized with ACCUTASE™ (Innovative Cell Technology) for 7 minutes, quenched in media, and seeded at 265 x 10^3 cells/cm^2 on Matrigel-coated plates in mTeSR1 with 5 μM Y-27632 following the protocol from Lian *et al.* (22). The next day, D-1 of the differentiation, the media is changed to only mTeSR1. On D0, the media is switched to RPMI with 10 mL B27 minus insulin per 500 mL RPMI (RPMI/B27-) and with 12 μM CHIR99021 (Selleckchem) (22). The media is changed on D1 with only RPMI/B27- and again on D3 with half of the current media, half fresh RPMI/B27- and 5 μM IWP2 (Tocris). On D5 the media is changed again with RPMI/B27-. On D6, CPCs have formed and the cells are either continued in culture with RPMI and B27 with insulin or treated with ACCUTASE™ for 5 minutes for freezing in 10% DMSO or for continuation to the EpiC differentiation.

For the EpiC differentiation, the protocol from Bao *et al.* was followed (73). In brief, the CPCs were plated at density of 50 x 10^3 cells/cm^2 on gelatin-coated tissue culture plates in RPMI with 20% FBS and 5 μM Y-27632. For the following two days, the medium is changed every day using LaSR medium (500 mL Advanced DMEM with 6.25 mL Glutamax and 0.03 g ascorbic acid) with 2 μM CHIR99021. For the next three days, the media is changed daily with only LaSR. At this point EpiCs have been obtained and can be passaged on gelatin-coated plates using Versene with the addition of 5 μM Y-27632, 0.5 μM A83-01 (Stemgent), and 1% FBS in the LaSR medium. After plating, the cells are maintained in the LaSR medium with 0.5 μM A83-01. EpiCs were maintained and used for further experiments for up to 8 passages. Further passaging of the EpiCs was done using Versene.

For the 14 day culture of the EpiCs, H9-derived EpiCs were plated on gelatin-coated plates at a density of 50 x 10^3 cells/cm^2 in LaSR medium with 0.5 μM A83-01, 5 μM Y27632, and 1% FBS. The medium was then switched to LaSR basal medium or with 10 ng/mL bFGF, 0.5 μM A83-01, or 5 ng/mL TGF-β1 (R&D Systems) and changed every two days for 14 days before immunostaining.

3.2.2 Coculture of CPCs and EpiCs

The H9-derived CPCs were thawed and plated in monoculture or in 1:1 ratio with H9-derived EpiCs on gelatin-coated plates at a density of 250 x 10^3 cells/cm^2 in DMEM with 10% FBS and 5 μM Y-27632. The media was changed after one day to the LaSR media alone or with 0.5 μM A83-01. This media was changed every two days for 14 days. Then the cells were singularized with ACCUTASE™ for at least 30 minutes and quenched with DMEM/F12. The cells

were then counted before being replated for immunostaining in DMEM with 10% FBS with 5 μM Y-27632 or for flow cytometery.

3.2.3 Flow cytometry

After singularization, the cells were fixed using 1% paraformaldehyde for 20 minutes followed by 90% methanol on the cells for 10 minutes for permeabilization. Next, the cells were resuspended in diluted primary antibodies, shown in **Supplementary Table 1**, in flow buffer containing 5% wt/vol BSA (ThermoFisher) and 0.1% Triton X-100 (Sigma) in PBS at 4 °C overnight. Secondaries were also diluted (1:1000) in the flow buffer and added to the cells for 30 minutes at room temperature. Samples were run on a BD FACSCalibur flow cytometer and statistical analysis was done using the Student's t-test.

3.2.4 Immunochemistry

The cells were fixed with 4% paraformaldehyde for 15 minutes. After washing with PBS, the primary antibodies (shown in **Supplementary Table 1**) were diluted in milk buffer containing 5% wt/vol non-fat dry milk and 0.4% Triton X-100 (Biorad; Hercules, CA) in PBS at 4 °C overnight on a rocker. Next, after three washes with PBS, the secondary antibodies were added in a 1:1000 dilution for 20 minutes at room temperature. Finally nuclei were stained using 0.4 μL/mL Hoechst in PBS and the solution was added to the cells for 5 minutes at room temperature. Images were taken either with an inverted Olympus IX70 microscope.

3.3 Results

3.3.1 Coculture of EpiCs and CPCs

Little is currently known about the impact of EpiCs and their derivatives on the maturation ability on hPSC-derived CMs. We have previously shown in Section 2 that EC interactions with CM progenitors can affect the ability for CMs to mature, either through speeding up the maturation or by interacting with the cells at a point where they have higher sensitivity to these interactions. EpiCs have been shown *in vivo* to impact heart development (165). Our hypothesis is that providing the interactions originating from EpiCs during heart development to CPCs will further induce CM maturation. Using the protocols to make EpiCs from Bao *et al.* (shown in **Figure 3.1A**) and to make CMs from Lian *et al.*, H9 hESCs were differentiated to relatively pure EpiCs and CMs, shown by the >95% WT1+ cell population from the EpiC differentiation and by >90% cTnT+ cells from the CM differentiation in **Figure 3.1B-C** (73, 22).

Following the same procedure as outlined in Section 3.2, CPCs were obtained from D6 in the CM differentiation and frozen, with one well continuing on for testing on their ability to form pure CMs. The CPCs were thawed and plated at a density of 250 x 10^3 cells/cm^2, either in a monoculture or coculture with EpiCs in a 1:1 ratio as shown in **Figure 3.2A**. The cells were maintained for 14 days in LaSR medium with or without A83-01 as shown in **Figure 3.2B**. Without A83-01, the EpiCs have been shown to undergo EMT, a process seen during heart development in which myocardial SMCs, FBs, and ECs are formed (72, 73). Prior to analysis, pictures were taken from each condition shown in **Supplementary Figure 3.1**. In the monocultures, the CPCs formed a thick layer of cells and which, in the condition without A8301, began to peel off the plate before the two weeks were up seemly due to the intense contractions of the CMs. In the basal medium coculture, the CPCs appeared to form denser areas which were beating, surrounded by other

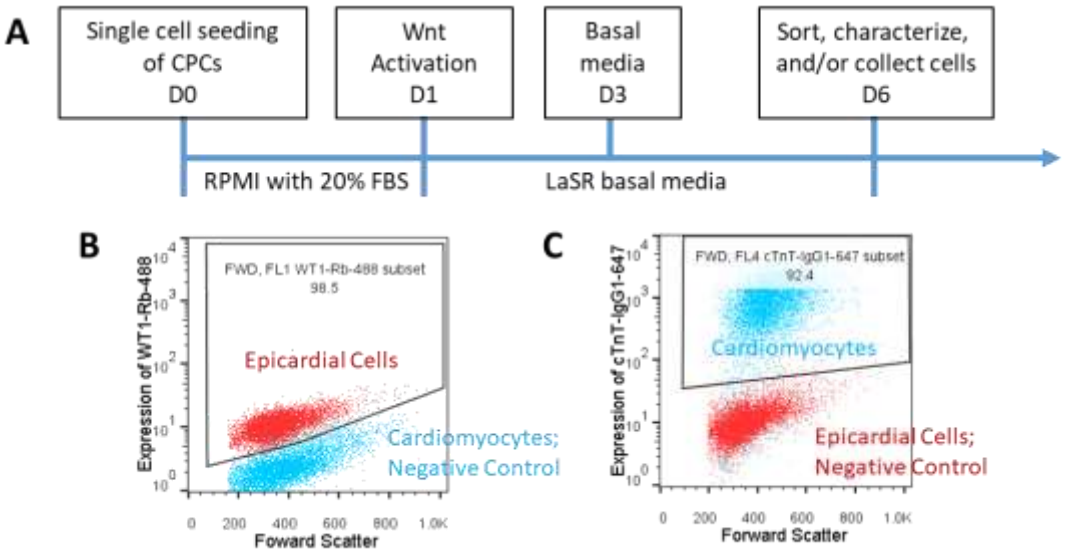

Figure 3.1: H9 hESCs were differentiated to pure EpiCs and CMs. **(A)** Differentiation protocol to make EpiCs from hPSC-derived CPCs. In short, CPCs were treated with the Wnt activator, 2 μM CHIR99021, for two days after seeding on gelatin-coated plates. On from D3 to D6, LaSR basal media without any small molecules is changed daily. By D6, WT1+ EpiCs have formed and can be maintained and passaged in LaSR with a TGF-β inhibitor, 0.5 μM A83-01. **(B, C)** Passage 4 H9-derived EpiCs and D20 H9-derived CMs are labeled with antibodies to WT1 (B) and cTnT (C) and analyzed via flow cytometry.

non-beating cells. Similarly, in the A83-01 treated coculture, the beating areas were exclusively found within the almost spheroid-like clusters of cells tended to detach throughout the two weeks. Around the clusters were cells that appeared more epicardial in shape. After the two weeks in culture, the cells were singularized with ACCUTASE™ and the numbers of cells were counted manually using a hemocytometer. Since much greater numbers of cells were found in the CPC/Epi coculture in A8301 (~2.3 x 10^6 cells/well in comparison to the 0.54 to 1.25 x 10^6 cells/well in the other conditions), the cardiomyocytes were costained for MF20, to identify the CMs, and Ki67 to determine if the coculture impacted the proliferation of the CMs as shown in **Figure 3.2C**. Only a significantly higher percent of Ki67+ CMs were found in the coculture of the CPCs with EpiCs in the presence of A8301 ($p<0.05$). This difference may be caused in part by the proliferative signals that EpiCs have been shown to produce *in vivo* to induce CM proliferation (163).

To determine the identity of the cells in the cultures after two weeks, the percent of cells expressing cTnT, WT1, or calponin from each condition was assessed via flow cytometry (shown in **Figure 3.2D**). Calponin can be used as a marker of SMCs and FBs as it has been shown to be highly expressed in SMCs, with low expression found in FBs (166). In the monocultures, significantly more WT1+ cells were found with the addition of A83-01 to the medium than in the basal medium (9.3 ± 1.6% vs 1.2 ± 0.9% respectively, $p<0.01$). Significantly more calponin+ cells were found between the monoculture and coculture conditions in the basal medium (8.0 ± 4.5% vs. 18.2 ± 2.2% respectively, $p<0.05$) with a negligible difference in the cTnT+ of 93.7 ± 4.1% in comparison to 87.5 ± 5.1%, respectively. With A83-01, the coculture had a higher WT1+ percent than the monoculture (9.3 ± 1.6% vs. 41.6 ± 8.7%, $p<0.01$) with a corresponding decrease in cTnT+ from 83.5 ± 4.8% to 44.8 ± 16.2% with the addition of EpiCs ($p<0.05$). This demonstrates that the EpiCs were maintained in the coculture with the A83-01 and may have caused the

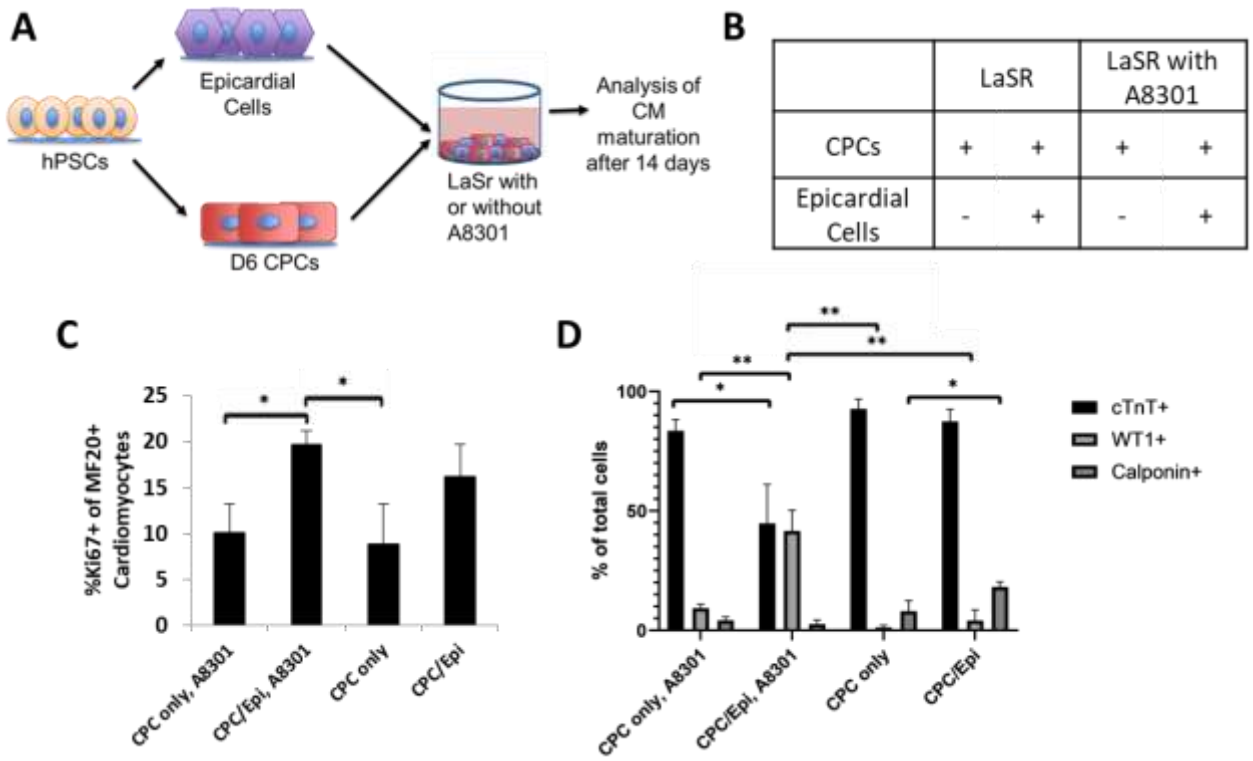

Figure 3.2: Coculture of H9 hESC-derived EpiCs and CPCs. **(A)** Schematic of the co-plating of the EpiCs and CPCs in LaSR medium with or without 0.5 μM A83-01. The cells were kept in culture for two weeks before analysis of the EpiCs impact on the CM maturation. **(B)** Table of the four resulting conditions for the coculture experiment, showing the CPC monoculture controls in addition to the CPC cocultued with EpiCs. **(C-D)** After the H9-derived CPCs and EpiCs were cocultured for two weeks in a 12-well tissue culture plate. The cocultured cells were analyzed after the two weeks via flow cytometry for the coexpression of Ki67 and MF20 (**C**) and the markers cTnT, WT1, and calponin, and the percent of the total cell population for each was calculated (**D**). The hemocytometer and flow data represent mean ± standard deviation of three samples taken from three independent differentiations and cocultures. The values were normalized to EpiC controls for each differentiation and statistical comparisons were performed using ANOVA with Tukey's test post hoc, N=3 (* $p<0.05$, ** $p<0.01$).

proliferation of a minor population of EpiCs from the plated CPCs. Without the A83-01, the coculture of EpiCs with CPCs resulted in an increase from 8.0% to 18.2% in the calponin+ population without an increase in WT1%, likely indicating the EpiCs underwent EMT.

3.3.2 Cardiac protein expression and cell size are increased in CPCs cocultures with EpiCs and EpiCs undergoing EMT

To assess the maturation effects of the EpiCs on the resulting CMs, the cocultured cells were analyzed via flow cytometry for the expression of proteins related to maturation state. In comparison to embryonic and hPSC-derived CMs, adult CMs have higher cTnT expression (141-143). Using cTnT to identify the CMs, the median fluorescence intensity or MFI of cTnT was analyzed within the CMs with normalizing to an EpiC control in **Figure 3.3A**. The MFI slightly increased from 110 ± 32 to 181 ± 28 with the addition of the EpiCs in the A83-01. No significant change was found between the monocultures due to the addition of the A83-01 nor between the monoculture and cocultures without the A83-01. Additionally, the CMs undergo a transition in which the cells switch from primarily expressing the atrial version of the myosin light chain protein, MLC2a, to ventricular version, MLC2v (32). By co-labeling the cells with MLC2a and MLC2v as markers of CMs, the percentages of MLC2v+ CMs were determined via flow cytometry after the two week cocultures in **Figure 3.3B**. A significant increase in MLC2v+ CMs was found when the EpiCs were cocultured with the CPCs in A83-01 in comparison to the A83-01 monoculture (46.3 ± 10.8% vs. 20.1 ± 3.6%, $p<0.01$). No change was found with or without the A83-01 in monoculture nor with the basal media coculture. This demonstrates that the EpiCs, when their identity is maintained and not allowed to undergo EMT, will cause the induction of MLC2v expression in the CMs derived from the CPCs, indicating their ability to induce hPSC-derived

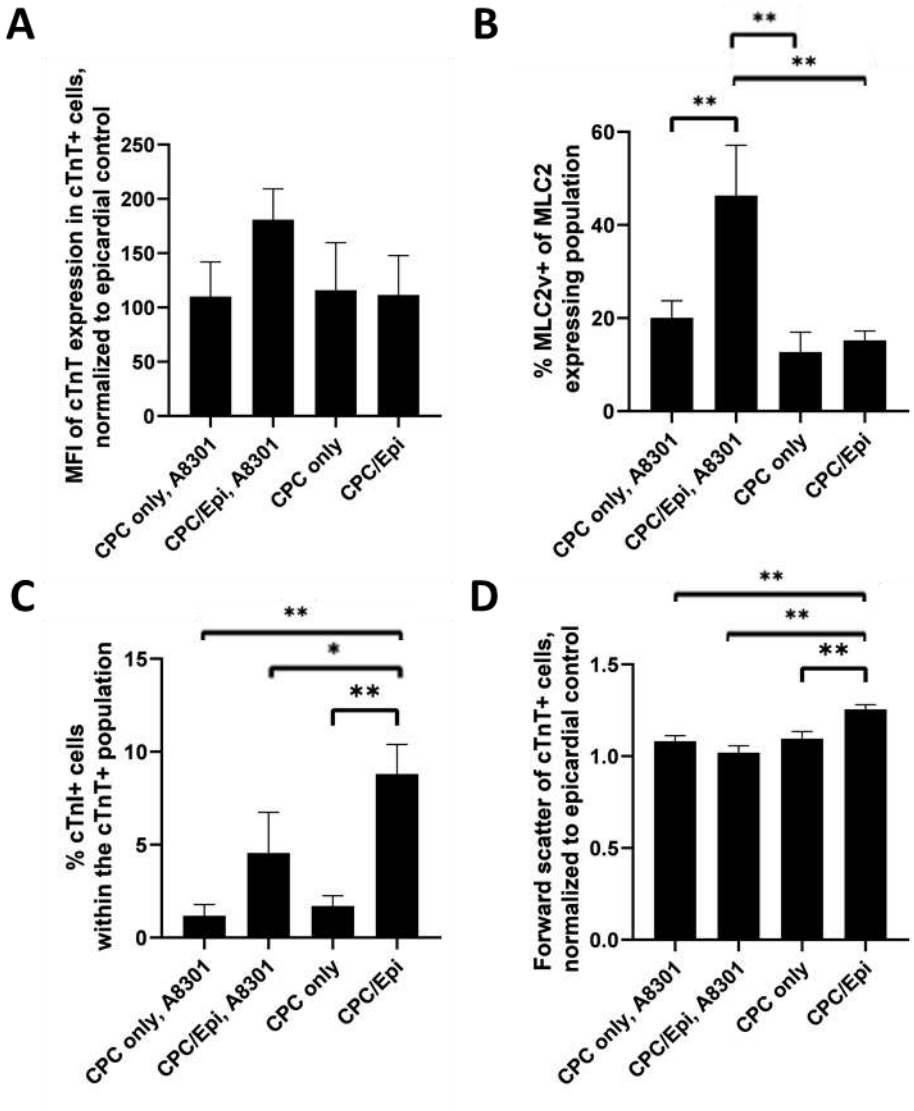

Figure 3.3: Maturation of CMs through coculture of EpiC and EpiC-derived cells with CPCs. H9 hESC-derived CPCs and EpiCs were cocultured on gelatin-coated plates for two weeks in LaSR basal medium with or without 0.5 μM A83-01. The cells were singularized and analyzed via flow cytometry after antibody labeling. Monocultures are labeled CPC only, cocultures are labeled CPC/Epi. **(A)** The median fluorescence intensity (MFI) of cTnT within the cTnT+ cells was normalized to an EpiC sample run at the same time. **(B)** The percent of cells expressing MLC2v was calculated from the total number of cells expressing either MLC2a or MLC2v. **(C)** The percent of cTnI+ cells was calculated from the cTnT+ CM population. **(D)** The forward scatter of the cTnT+ cells was normalized to the EpiC control sample. The data represent mean ± standard deviation of three samples taken from three independent differentiations and cocultures. The values were normalized to EpiC controls for each differentiation and statistical comparisons were performed using ANOVA with Tukey's test post hoc, N=3 (* $p<0.05$, ** $p<0.01$)

CM maturation. This maturation was specific to the EpiC coculture in A83-01 and not found in the EpiC basal medium coculture.

Troponin I also switches from the slow skeletal to the cardiac isoform, cTnI, in late stage development of the heart (140). To determine if troponin I isoform protein expression is impacted by coculture using flow cytometry, the cells were co-labeled for cTnT and cTnI, allowing the percent of cTnI+ CMs to be identified in **Figure 3.3C**. Very few of the CMs expressed cTnI in the different conditions, however there was a slight but significant increase from 1.7 ± 0.5% cTnI+ CMs to 8.8 ± 1.6% with the addition of the EpiCs in the LaSR basal medium ($p<0.01$). Similarly, when CMs mature throughout development, the cell elongate and become larger (37). By using the forward scatter from flow cytometry, a rough measurement of the cell size can be determined. The cells were labeled with a cTnT antibody and the median of the forward scatter of the CMs were analyzed in **Figure 3.3D**. The CMs resulting from the cocultured EpiCs with the CPCs in the LaSR basal medium had significantly higher forward scatter than the monoculture control after normalizing to the forward scatter of an EpiC sample (1.26 ± 0.02 vs. 1.09 ± 0.04, $p<0.01$). This demonstrates that specifically the EpiCs when undergoing EMT throughout their coculture with CPCs, promote the expression of cTnI and an increase in cell size from the resulting CMs, indicative of CM maturation.

3.3.3 Induction of EMT in EpiCs

During the two week coculture, the EpiCs appeared to undergo EMT when cultured in the LaSR basal media. To further reinforce the idea that the calponin+ cells found in the basal media coculture after two weeks originated from the EpiCs and not from the CPCs, H9-derived EpiCs were cultured for 14 days without passaging in LaSR medium alone or with either 10 ng/mL bFGF,

5 ng/mL TGF-β1, or 0.5 μM A83-01. Previously, it has been shown that culture of EpiCs with bFGF causes the cells to undergo EMT to form FBs (73). Alternatively when TGF-β1 was added to the medium, the EpiCs became SMCs (73). By using these proteins to induce EMT as a positive control, the identity of the cells in the LaSR basal medium may be identified.

After two weeks of culture, the cells were fixed and stained with the mesenchymal cell-marker vimentin, a smooth muscle cell marker (calponin), an EpiC marker (WT1), a SMC and myofibroblast marker (α-SMA), and a junctional endothelial marker (VE-cadherin) (166-168). As shown in **Figure 3.4A-C**, the cells maintained in A83-01 had minimal to no expression of α-SMA or VE-cadherin, lower expression of calponin, and high expression of nuclear-localized WT1 and vimentin. The lower expression of calponin and expression of vimentin with the continued expression of WT1, is indicative of the cells in A83-01 after two weeks being EpiC beginning to undergo EMT. In the bFGF containing media, the cells were positive for α-SMA, vimentin, and calponin, though the calponin expression was lower than found in the basal media and TGF-β1 conditions. Although calponin is considered a marker for SMCs, it is also expressed at a lower amount in FBs (166). These results indicate that after bFGF treatment, the EpiCs became myofibroblasts or FBs though further markers will be needed to differentiate them from SMCs. This matches the results found by Bao *et al.* when they treated EpiCs with bFGF, yielding vimentin+ FBs (73). The basal media and TGF-β1 conditions yielded similar staining and morphology of the cells, with expression of vimentin and α-SMA, high expression of calponin, and lacking expression of WT1 and VE-cadherin. These results are phenotypically found in SMCs and TGF-β1 had previously been shown to create SMCs from EpiCs (73). Altogether this points to the EpiCs undergoing EMT to a SMC-like cell type when in culture for two weeks in the LaSR basal medium.

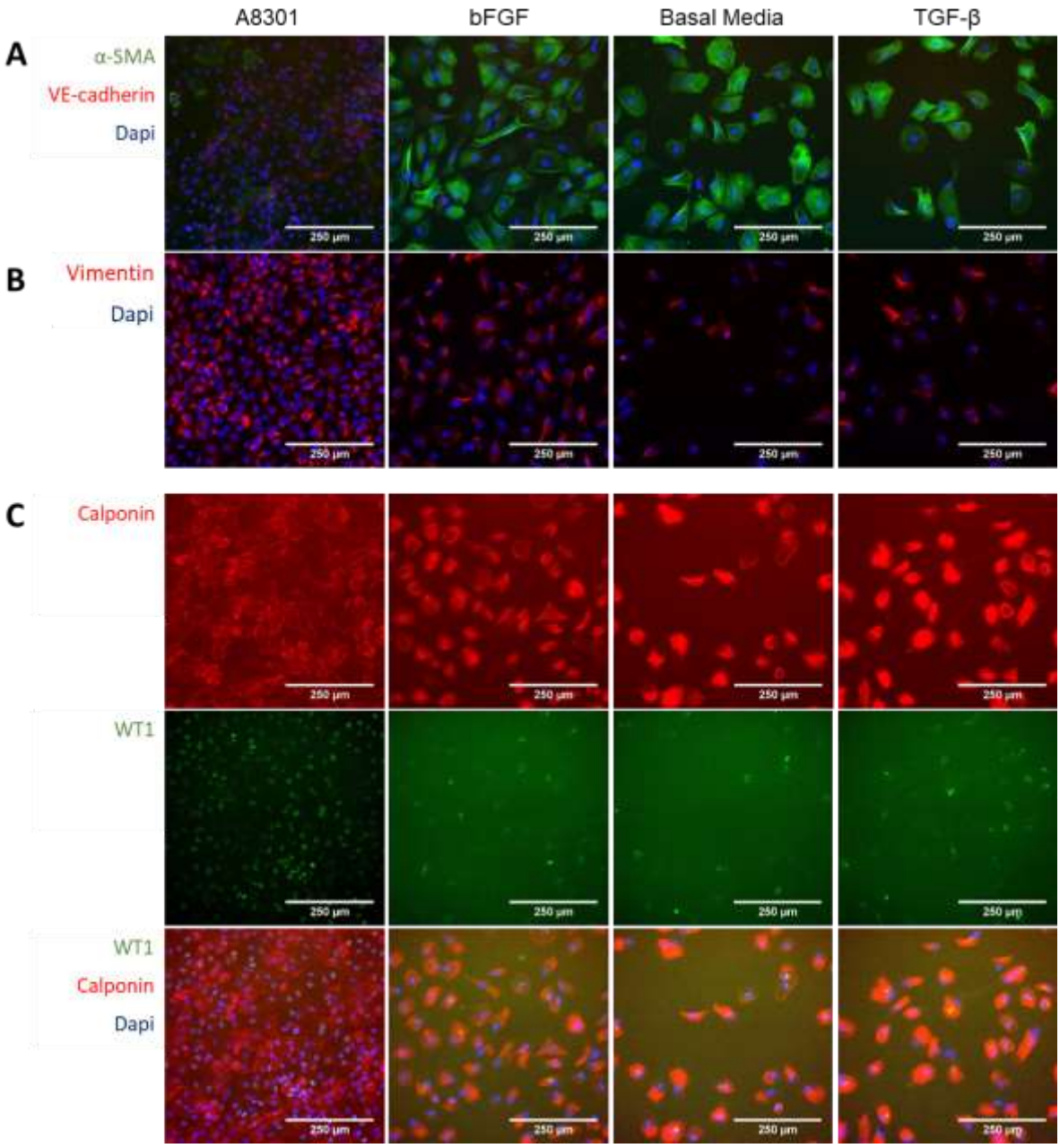

Figure 3.4: Culture of H9-derived EpiCs in LaSR basal medium alone, with bFGF, or with TGF-β1 induces EMT. H9-derived EpiCs were plated on gelatin-coated plates at a density of 50 x 10^3 cells/cm^2 in LaSR medium with 0.5 µM A83-01, 5 µM Y27632, and 1% FBS. The medium was then switched to LaSR basal medium or with 10 ng/mL bFGF, 0.5 µM A83-01, or 5 ng/mL TGF-β1 and changed every two days. After 14 days, the cells were fixed and immunostained for **(A)** α-SMA (green) and VE-cadherin (green) **(B)** vimentin (red) **(C)** WT1 (green) and calponin (red) with Dapi staining on all (blue).

3.4 Discussion

Coculture of EpiCs with CPCs, with and without the presence of the TGF-β inhibitor, A83-01, induced phenotypic changes in the resulting CMs indicative of CM maturation. With A83-01, the EpiC fate was maintained as shown by the significant increase of WT1+ cells in the coculture after two weeks compared to the monoculture, allowing interactions between the epicardium and the CMs in the myocardium to be modeled. This interaction led to the increase in the percent of MLC2v+ CMs. Without the A83-01, the EpiCs underwent EMT as shown by the lack of WT1+ cells in the coculture after two weeks and the increase in calponin+ cells compared to the monoculture. This models stages of heart development in which EpiCs undergo EMT in the myocardium in the presence of CMs. The EMT coculture yielded more mature CMs in the increase in the percent of CMs expressing cTnI and the cell size of the CMs. Additional effects from the cocultures should be analyzed using other assays to determine the impact on sarcomere organization, cellular alignment, ion channel expression, localization of gap junctions.

There is also an increase in hPSC-derived CM proliferation with coculture in the A83-01 medium, contributing to the ~50% increase in the number of cells found after the two week coculture. This proliferation may be induced by the EpiCs which are known to produce RA and other signaling factors that cause CM proliferation in the developing heart (162, 165). Further investigation should be done to determine if this effect may be caused solely by soluble factors secreted by the EpiCs or through some other interaction with the EpiCs. Identification of this proliferative effect may increase yield in the production of mature CMs from hPSCs for cellular manufacturing of cardiac patches.

The hPSC-derived EpiCs that underwent EMT in the coculture with hPSC-derived CPCs require further characterization to identify the cell types that were formed. EpiCs have been shown

to form FBs, SMCs, and potentially ECs in the myocardium during heart development (73, 74). When in monoculture for two weeks in LaSR medium, the EpiCs formed cells that closer mimicked the marker expression of EpiCs directed to a SMC-like fate. Additional markers should be used to differentiate these cells from myofibroblasts, a similar but distinctly different cell type found in the heart in response to heart disease (169). Follow-up research should be done to confirm the same transition of the EpiCs to SMC-like cells is found after the two weeks in coculture with CPCs and that these cells are originating from the EpiCs and not from the CPCs. Once the identity of these EpiC-derived cells is determined, coculture of these cells should be done directly with the CPCs to demonstrate if the maturation-inducing effects are partially caused by the EpiCs undergoing EMT or exclusively from the formation of these EpiC-derived cells within the coculture. Lastly, investigation should be done to determine if the effects from the EpiC cocultures with and without A83-01 on the hPSC-derived maturation could be combined. Utilization of these cells in combination with other cells types that have been shown to induce hPSC-derived CM maturation, such as ECs and FBs, should be done to assess if these cell types influence each other to further interact with CMs via alternative pathways than when in a two cell coculture.

In conclusion, we have demonstrated the ability for EpiCs to induce CM maturation, in the induction of MLC2v but not cTnI or CM cell size when coculture with CPCs when the EpiC fate is retained, and the induction of cTnI and CM cell size yet neither MLC2v or cTnT when the EpiCs are allowed to undergo EMT. The differences in phenotypic changes in the CMs further demonstrate the importance of the different interactions from other cell types that the CMs and their progenitors experience during heart development. This simplistic EpiC-CPC coculture model may be useful for screening small molecules and proteins that may inhibit these maturation-inducing interactions, allowing the pathways through which they interact to be recognized.

Analyzing the isotype-switching of MLC2a to MLC2v and ssTnI to cTnI via flow cytometry would allow for higher throughput assessment of the CM maturity, though all maturation phenotypic changes may not be captured. Once identified, the changes in these pathways could be integrated into hPSC-derived CM manufacturing without the need for the EpiCs present.

Chapter 4: Conclusions

In this thesis, we sought to improve the properties of hPSC-derived CMs so that they are more adult-like and may be used in regenerative medicine therapies. Toward this goal, we cocultured hPSC-derived CPCs with hPSC-derived ECs to determine the ability of ECs to induce CM maturation. By coculturing the cell types in different ratios, we found that a EC:CPC ratio of 3:1 yielded the greatest induction of cTnT, cTnI, MLC2v, and cell size in the resulting CMs indicative of CM maturation. We additionally investigated the importance in differentiation stage of the CMs in which the EC coculture should be initiated. We compared EC cocultured with either CPCs or beating CMs and found that after two weeks, the EC coculture had the higher impact on the CPCs, further increasing the presence of t tubule-like extensions and CM gene expression in addition to a heightened expression of cTnT, cTnI, MLC2v, and cell size. This difference in the induction of maturation reveals a differentiation stage-specific response of the CMs to the interaction with ECs. Future work should test other maturation-inducing methods such as electrical or mechanical stimulation on CPCs to determine if this stage-specific response applies to other signals in addition to those generated by ECs.

Next, we investigated the importance of including epicardial-myocardial interactions during development on hPSC-derived CM maturation. hPSC-derived EpiCs were cocultured with hPSC-derived CPCs for two weeks in the presence and absence of a TGF-β inhibitor, A83-01, to control the EpiCs in the initiation of EMT. The presence of WT1% cells were maintained in the coculture with the inhibitor, but WT1+ cells were not found in the coculture without A83-01, instead the coculture had a 10% increase in the population of calponin+ cells compared to the monoculture control. The EpiC cocultures with and without A83-01 each induced phenotypic changes in the resulting CMs indicative of CM maturation. With the A83-01 coculture, the CMs

had a larger percent of them expressed MLC2v and maintained the proliferation of the CMs, though no changes to cTnI expression or cell size was identified. Alternatively, without the A83-01, the CPCs became larger CMs with a higher percent expressing cTnI in the coculture, but no changes in cTnT nor MLC2v expression were seen. This demonstrates that both the EpiC coculture and the resultant coculture from the EpiCs undergoing EMT cause different phenotypes likely due to the induction of different pathways within the differentiating CPCs. Further characterization of the calponin+ cells in the coculture without A83-01 should be done to determine if these cells originate from the EpiCs and to fully identify them as either SMCs or FBs. This cell type should then be used in coculture with CPCs to determine whether the presence of these cells are inducing the CM maturation or if the EpiCs undergoing EMT is partially responsible. Additional assays should also be done to fully characterize the hPSC-derived CMs to identify other phenotypic changes indicative of CM maturation.

Altogether these results demonstrate the importance of different cell types in providing specific maturation-inducing signals. Each of the cocultures with ECs, EpiCs, and EpiCs undergoing EMT produced their own profile of changes in CM maturation, likely indicating that the different cell types are producing their own unique combination of factors through which they interact with the hPSC-derived CPCs and CMs. Additionally, these EpiCs, ECs, and EpiC-derived cells should be cocultured together with the CPCs to more fully model the developing heart and incorporate possible interactions between these support cell types that may regulate the intercellular signals received by the hPSC-derived CPCs and CMs. These cocultures should also be done in 3D, to more accurately represent the biomechanical and biochemical environments found *in vivo* (168). For example, even 3D culture of exclusively hPSC-derived CMs has been shown to induce maturation as shown by their metabolic profiles (169). The correct combination

of signals may further activate additional phenotypic changes within the CMs and induce the most maturation.

Current efforts to upscale the production of hPSC-derived CMs have focused on creating a pure CM population to be used for cardiac tissue repair (103, 104, 125). This allows the cost of the manufacturing of the cells to be minimized, eliminating the need for extensive purification steps while maximizing the quantity of CMs produced. However, production of pure hPSC-CMs prevents maturation-inducing intercellular interactions with other cell types. Future work should focus on identifying the mechanisms through which the cells interact so that small molecule inhibitors and activators can be incorporated into the bioreactor. This would allow direct targeting of pathways to induce CM maturation without the added difficulty and expense of introducing other cell types into the manufacturing process.

Lastly, the switch in isotype from ssTnI to cTnI has been proposed as an indicator of CM maturation (35). Exclusive use of this switch as a marker would have neglected to find any maturation-inducing signals from the EpiC coculture with CPCs treated with the TGF-β inhibitor. This further reaffirms the need to develop a standardized panel of proteins or other phenotypic changes to screen for CM maturation.

Chapter 5: Appendices

5.0 Funding

This study was supported by NIH grant R01EB007534 and NSF grants 1547225, 1743346, and 1648035. KD was supported by a NIH Chemistry Biology Interface Training Grant (NIGMS T32 GM008505). Confocal microscopy was performed at the University of Wisconsin-Madison Biochemistry Optical Core, which was established with support from the University of Wisconsin-Madison Department of Biochemistry Endowment. FACS was performed at the University of Wisconsin Carbone Cancer Center Support Grant P30 CA014520, using the BD FACS AriaII BSL-2 Cell Sorter ("Jill") which is supported by the Multi-color Benchtop Flow Cytometer Grant (1S10RR025483-01).

5.1 Supporting Information

Supplementary Table 1: Primary antibodies and stains for flow cytometry (FC) and immunostaining (IS)

Antibody/Stain	Source	Application
Cardiac troponin T	Lab Vision, mouse IgG1, 13–11, ms-295-p1	1:200 (FC, IS)
VE-cadherin	Santa Cruz, mouse IgG1, F-8, sc9989	1:100 (FC, IS)
MLC2a	Synaptic Systems, mouse IgG2b, 311011, 56F5	1:200 (FC, IS)
MLC2v	ProteinTech Group, rabbit IgG, PTG10906-1-AP	1:200 (FC)
Cardiac troponin I	Abcam, rabbit IgG, ab47003	1:400 (FC, IS)
ISL1	DSHB, mouse IgG2b, 39.4D5-s	1:20 (IS)
VEGFR2	Santa Cruz, mouse IgG1, sc-6251, A-3	1:200 (IS)
α-actinin	Sigma, mouse IgG1, EA-53	1:500 (IS)
CD31-APC	Miltenyi Biotec, mouse IgG1, AC128	1:50 (FC, IS)
CD34-FITC	Miltenyi Biotec, mouse IgG2a, AC136	1:50 (FC, IS)
von Willebrand factor	Dako, rabbit IgG, A008202-5	1:500 (IS)
Connexin-43	Abcam, rabbit IgG, ab11370	1:1000 (IS)
Phalloidin Dylight 594 conjugate (F-actin)	Invitrogen, 21836	1:50 (IS)
WT1	Abcam, rabbit IgG, ab89901	1:250 (FC, IS)
Vimentin	Sigma-Aldrich, mouse IgG1, V6630, V9	1:200 (IS)
Calponin	Abcam, mouse IgG1, ab700, CALP	1:200 (IS)
α-SMA	Lab Vision, mouse IgG2a, 1A4, ms-133-p	1:100 (IS)

Supplementary Table 2: Primer pairs used to analyze gene expression via qPCR

Gene	Forward primer (5'-3')	Reverse primer (5'-3')	Annealing Temperature	Product Length
TNNT2	TTCACCAAAGATCTGCTCCTCGCT	TTATTACTGGTGTGGAGTGGGTGTGG	58°C	166
MYL2	ACATCATCACCCACGGAGAAGAGA	ATTGGAACATGGCCTCTGGATGGA	58°C	247
TNNI1	ACTCTGTCCTGTCCGAGAAA	ATGCGTGTCCTGGTTC	60°C	240
GAPDH	CTGATTTGGTCGTATTGGGC	TGGAAGATGGTGATGGGATT	60°C	207
MYH7	CGCATCAAGGAGCTCACCTA	CTCCTCATTCAAGCCCTTCGT	60°C	270
HCN4	AATGCCAGGGAAAGGCGAG	CTCCGGCTTCAGTTGCGAAT	60°C	102
ATP2A2	CCAACCCTGTGCATGACTGA	GAAATGTGGCGACTTGGCTG	63°C	253
RYR2	AGCCAGTGTCATCCACCAAC	ATGGCCTGACAAGAAGTCCTTA	63°C	120
KCNJ2	TCCGAGGTCAACAGCTTCAC	TTGGGCATTCATCCGTGACA	60°C	97
CACNA1C	TTCAAATGGTGTAGCCGCC	TGCCTCCTCGAGTGAAACTG	60°C	93
GJA1	TGGTAAGGTGAAAATGCGAGG	GCACTCAAGCTGAATCCATAGAT	60°C	123
MYH6	CTCCGTGAAGGGATAACCAGG	CCTTCTCTGACTTGCGGAGG	60°C	97
SCN5A	CCTGGGCAATGTCTCAGCCTTA	TGCCTTAGGTTGCCCATGAAG	63°C	201
MYL7	GGAGTTCAAAGAAGCCTTCAGC	CTCCTCTGGGACACTCACCT	60°C	112
VIRMA	CGAGCGCTGAGCAAAGTTCT	CAGGCTTCCCAACCTATCGAA	60°C	218
ZNF384	AATCTGCAGTCCCACAGACG	ACTGTGTGCGTAGACAGGTG	60°C	116

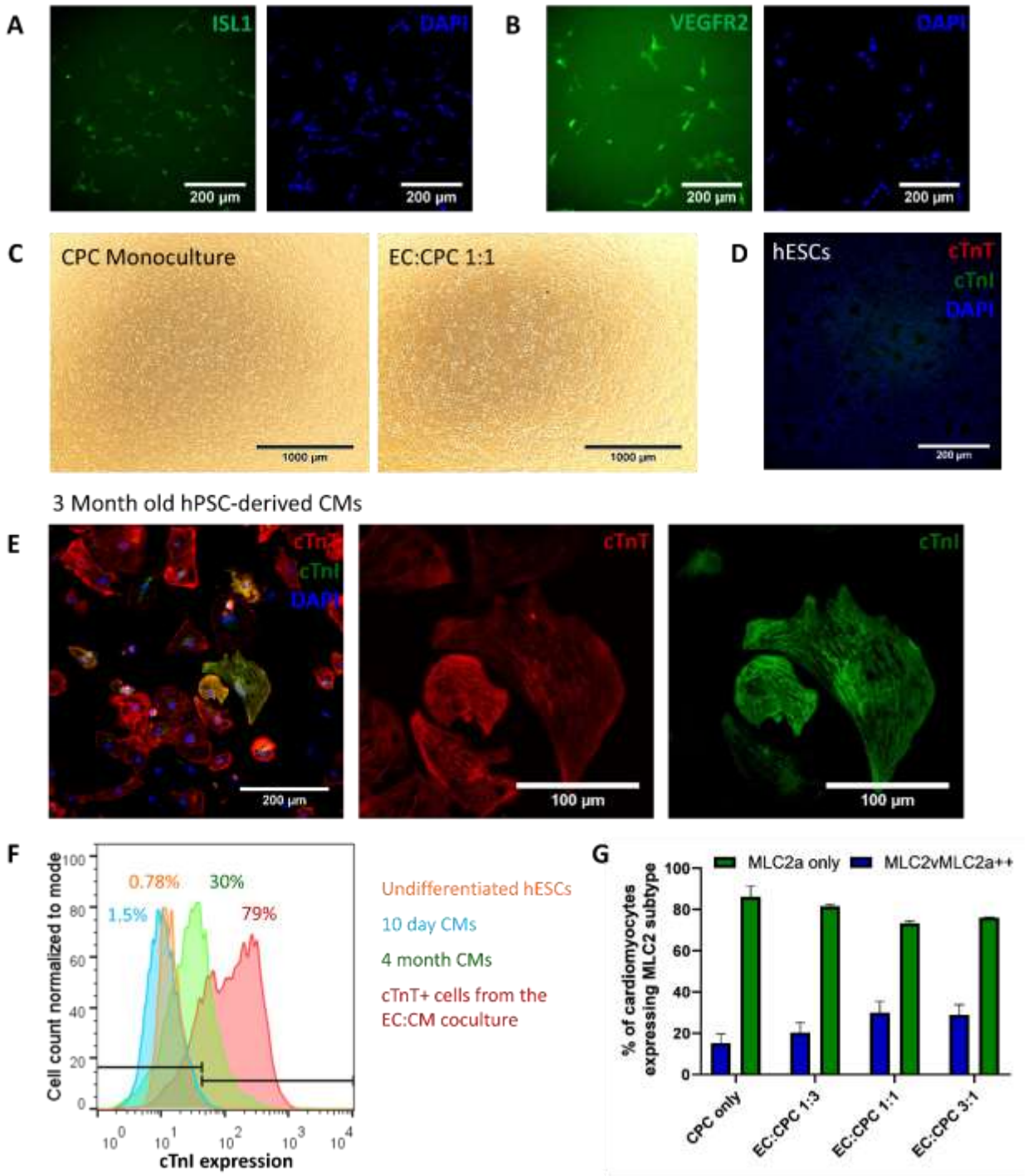

Supplementary Figure 2.1: Coculture of CPCs and ECs, and cTnI antibody specificity. **(A-B)** H9 hESC-derived CPCs were plated on Matrigel at 30 x 10^3 cells/cm^2 and fixed after one day. The CPCs were immunostained for **(A)** ISL1 (left, green) with DAPI (right, blue) and **(B)** VEGFR2 (left, green) with DAPI (right, blue). **(C)** hPSC-derived CPC and EC:CPC cocultures were seeded on Matrigel at 160 x 10^3 cells/well and brightfield images were taken the next day to assess cell attachment and confluency. **(D-E)** Immunostaining of cTnI (green) and cTnT (red) with DAPI (blue) of H9 hESCs (D) and 3 month old hPSC-derived CMs (E). **(F)** H9 hESCs, 10 day hESC-derived CMs, 4 month hESC-derived CMs, and cTnT+ cells from a two week hPSC-derived CM:EC coculture were compared for cTnI expression via flow cytometry.

The indicated gate was set such that less than 1% of the undifferentiated hESCs were counted as cTnI+. Numbers above the histograms indicate the fraction of cells in that population in the cTnI+ gated region. **(G)** The cells in monoculture and cocultures were analyzed simultaneously for expression of both MLC2a and MLC2v by flow cytometry and the percentage of MLC2v and MLC2a cells were calculated based on the total number cells expressing either MLC2v or MLC2a. Data represent mean ± SEM of three independent differentiations with at least two experimental replicates each. Comparison of percentage of MLC2a/v cells was performed using ANOVA with Tukey's HSD post hoc analysis, N=3 (* $p<0.05$, ** $p<0.01$) with no significance found.

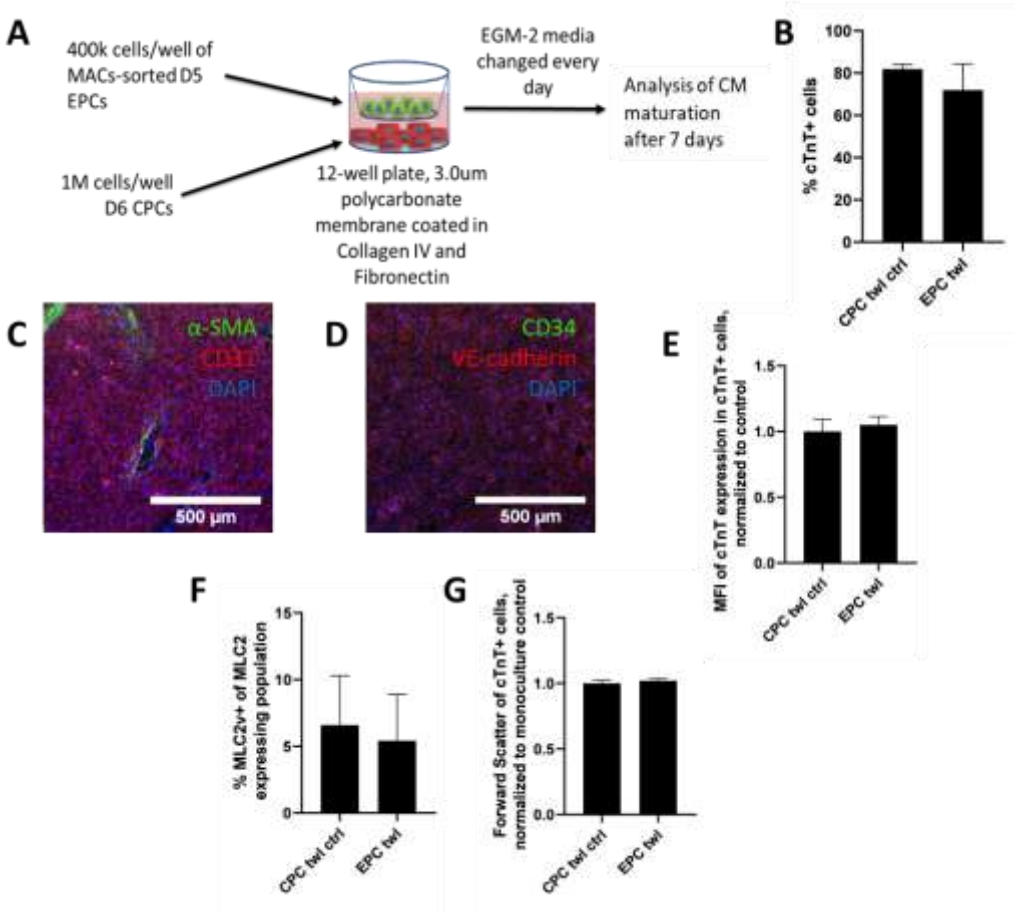

Supplementary Figure 2.2: Transwell cocultures of EPCs and CPCs did not impact phenotypes in the resultant CMs that are associated with CM maturation. **(A)** Schematic illustrating coculture of H9 and 19-9-11 hPSC-derived CPCs with MACS-purified 19-9-11 and 6-9-9 iPSC-derived EPCs (labeled "EPC twl") for seven days in EGM-2 media. For the control, labeled "CPC twl ctrl", CPCs were placed in the transwell instead of the EPCs in addition to having the CPCs in the main well. **(B)** After one week, populations from the CPCs in the main well were analyzed for the percentage of cells expressing cTnT by flow cytometry. The EPCs in transwell were analyzed via immunostaining for the expression of **(C)** α-SMA (green) and CD31 (red) or **(D)** CD34 (green) and VE-cadherin (red), both with DAPI in blue. cTnT+ cells were analyzed via flow cytometry for **(E)** the median fluorescence intensity (MFI) of cTnT in cTnT+ cells and for **(G)** forward scatter of cTnT+ cells, both normalized to the monoculture. **(F)** The cells in monoculture and coculture were costained simultaneously for expression of both MLC2a and MLC2v by flow cytometry and the percent of MLC2v+ cells were calculated from the total cells expressing either MLC2 isotype. Data represent mean ± standard deviation of three independent differentiations with three experimental replicates each. Comparison of flow cytometry data was performed using the Student's t-test, N=3.

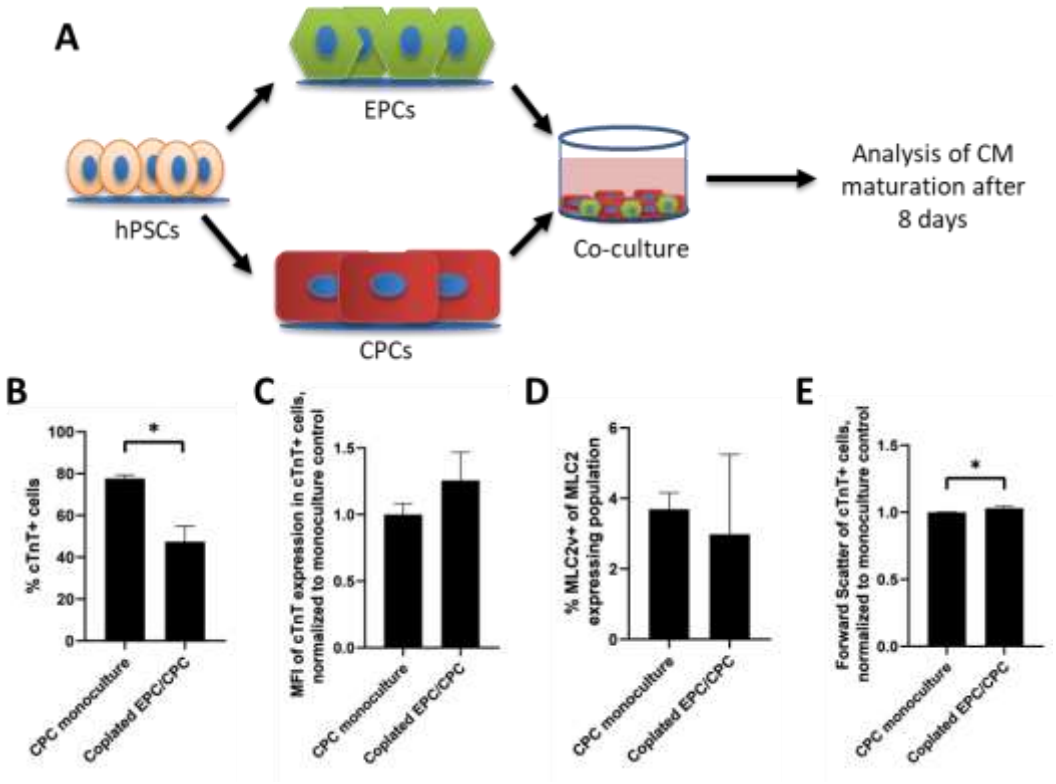

Supplementary Figure 2.3: Co-plating EPCs and CPCs only induced a significant increase in the cell size of the resultant CMs. **(A)** Schematic illustrating co-plated coculture of H9 hESC-derived CPCs on matrigel with MACS-purified 19-9-11 iPSC-derived EPCs for seven days in EGM-2 medium at an overall seeding density of 160 x 10^3 cells/cm^2. For the control, CPCs were plated as a monoculture with 160 x 10^3 cells/cm^2 and maintained in EGM-2 medium. **(B)** After one week, populations from the CPCs were analyzed for the percentage of cells expressing cTnT by flow cytometry. CMs in the monoculture and coculture were analyzed via flow cytometry for **(C)** the median fluorescence intensity (MFI) of cTnT and **(E)** forward scatter of cTnT+ cells, both normalized to the monoculture. **(D)** The cells in monoculture and coculture were costained simultaneously for expression of both MLC2a and MLC2v by flow cytometry and the percent of MLC2v+ cells were calculated from the total cells expressing either MLC2 isotype. Data represent mean ± standard deviation of one differentiation with three experimental replicates. Comparison of flow cytometry data was performed using the Student's t-test, n=3.

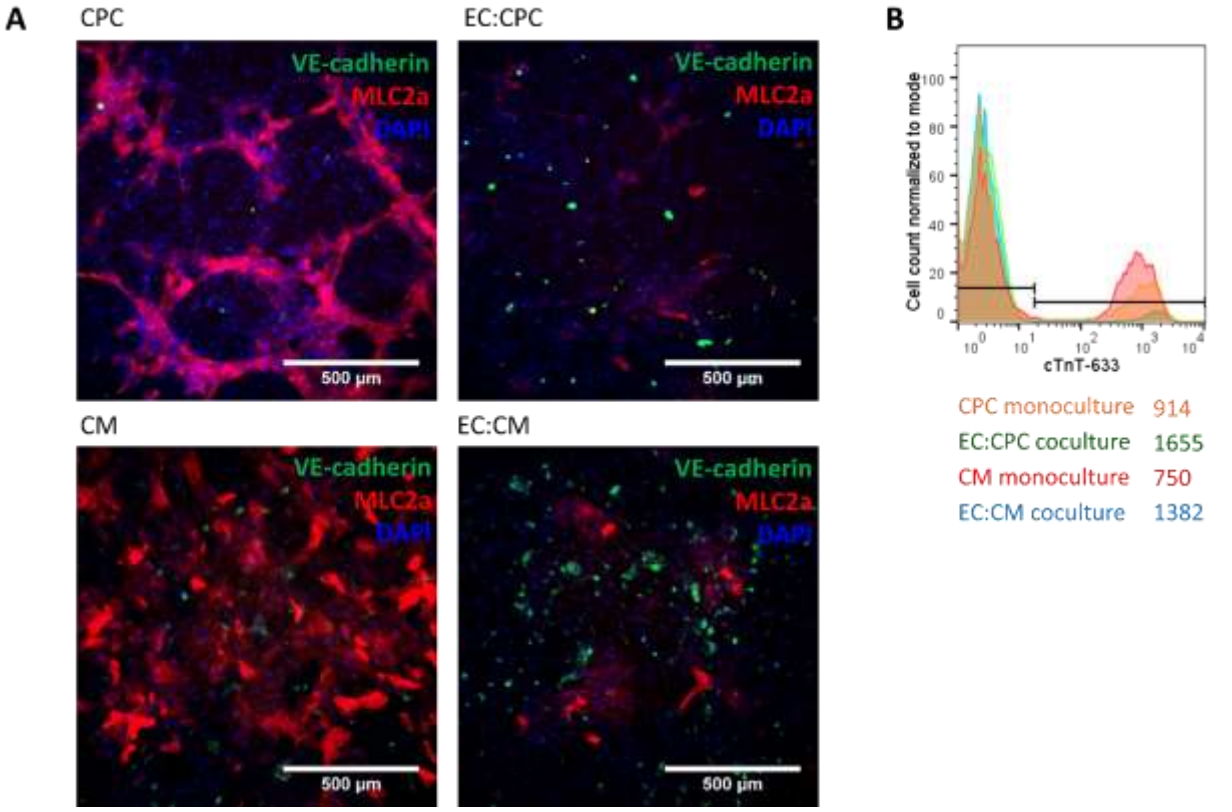

Supplementary Figure 2.4: Organization of H9 hESC-derived CPCs and CMs with or without H1 hESC-derived ECs after two weeks in culture, and example mean fluorescence intensity of cTnT. **(A)** Example representative immunostaining images for VE-cadherin (green), MLC2a (red), and DAPI (blue) after two weeks in culture for the indicated monocultures and cocultures. **(B)** Example flow cytometry histograms of cTnT expression in the cTnT+ cells within the indicated monocultures and cocultures after two weeks. Numbers below the graph indicate the mean fluorescence intensity (MFI) of that population.

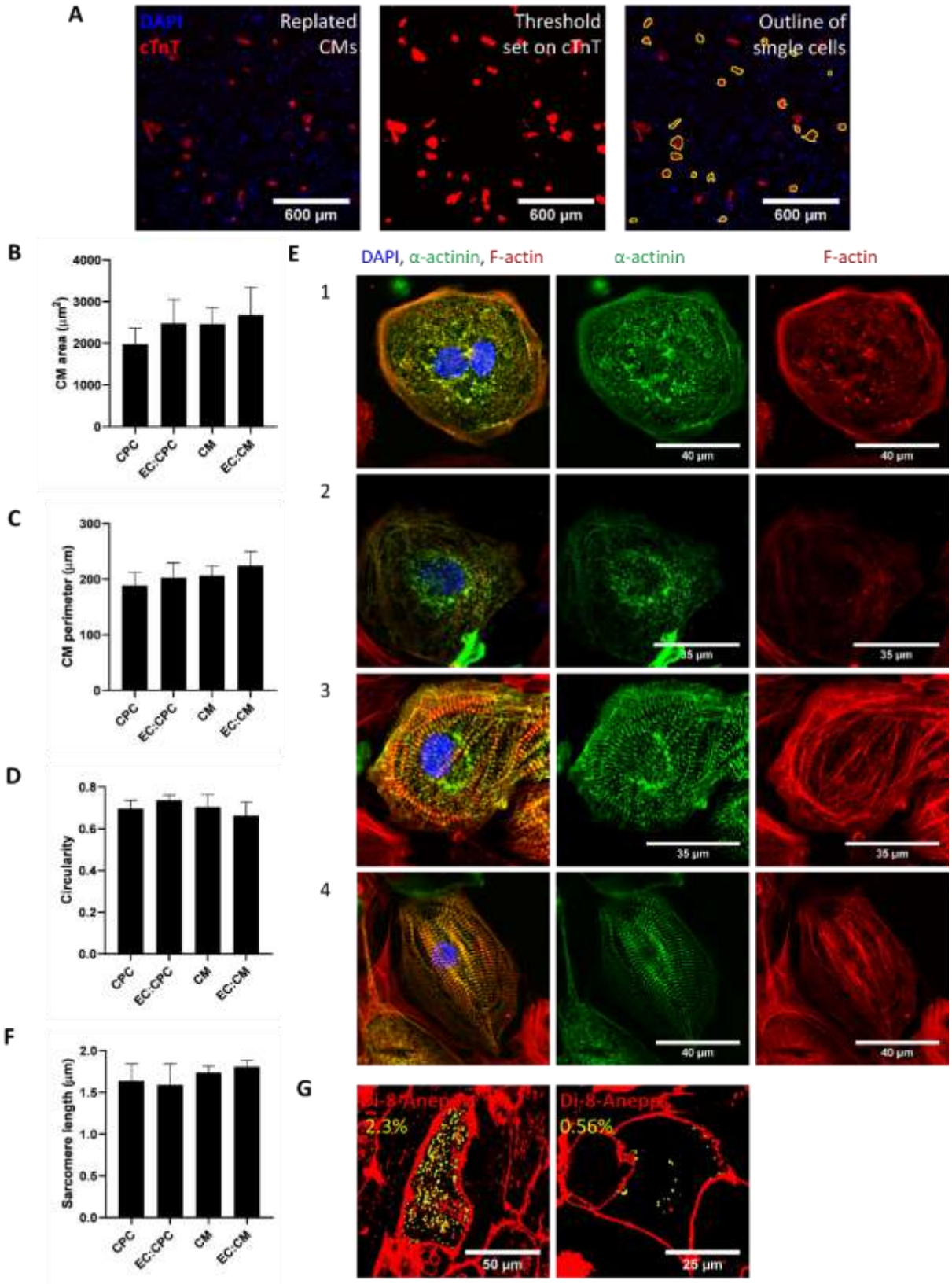
A
DAPI
cTnT
Replated CMs
600 μm
Threshold set on cTnT
600 μm
Outline of single cells
600 μm
B
CM area (μm²)
4000
3000
2000
1000
0
CPC
EC:CPC
CM
EC:CM
C
CM perimeter (μm)
300
200
100
0
CPC
EC:CPC
CM
EC:CM
D
Circularity
0.8
0.6
0.4
0.2
0.0
CPC
EC:CPC
CM
EC:CM
F
Sarcomere length (μm)
2.0
1.5
1.0
0.5
0.0
CPC
EC:CPC
CM
EC:CM
E
DAPI, α-actinin, F-actin
α-actinin
F-actin
1
2
3
4
40 μm
35 μm
G
2.3%
0.56%
50 μm
25 μm

Supplementary Figure 2.5: Analysis of CM morphology and sarcomere structure of CPC, EC:CPC, CM, and CM:EC hPSC-derived cultures. **(A)** Demonstration of the process to identify CMs for morphology analysis. Cells from 2 week monocultures or cocultures were dissociated and replated onto gelatin-coated plates, and cultured for an additional 3 days. Cells were then fixed and stained for cTnT expression to identify CMs. The left image shows a representative cTnT and DAPI co-stain for hPSC-derived EC:CPC coculture after replating onto gelatin-coated tissue culture plates. A binary mask was applied to the image based on a cTnT threshold (middle image). These masks were used to calculate cell area, perimeter, and circularity in ImageJ. Manual screening to remove inclusion of partial or multiple, touching cells from the calculations was done. The right image shows the calculated cell borders (yellow) on the cTnT (red) and DAPI (blue) co-stained cells. **(B-D)** Quantification of **(B)** CM area, **(C)** CM perimeter, and **(D)** CM circularity of cTnT+ cells in the indicated monoculture and coculture samples. Data represent mean ± SD of three independent differentiations with three experimental replicates each. **(E)** Examples of the ranking of sarcomere structure in the CMs immunostained for α-actinin (green) and F-actin (red) with the criteria: 1, no visible sarcomere structure; 2, some sarcomere organization; 3, H zones and Z lines visible in areas with some sarcomere organization; 4, near perfect sarcomeres with clear H zones, Z lines, and thick myofibrils. **(F)** Sarcomere length was assessed for α-actinin+ cells that displayed at least 10 sarcomeres (11 α-actinin lines) in a row. Data represent mean ± SD of all cells measured, N>20 in each of the indicated monoculture and coculture samples. **(G)** hESCs expressing eGFP under the *TNNT2* promoter were differentiated to CPCs, ECs and CMs and cultured in the indicated monocultures or cocultures for two weeks. The cells were replated on Matrigel-coated glass slides after culture for two weeks and were then stained with di-8-anepps to identify membranous extensions into the intracellular area of the CMs. The percentage of the eGFP+ cell area also stained by di-8-anepps was quantified in ImageJ by applying a binary mask based on a di-8-anepps threshold. Any di-8-anepps areas touching the cell boundary were excluded from analysis. Di-8-anepps spots larger than 1μm^2 were excluded from the calculation to minimize vesicles from the calculation. The image show examples of di-8-anepps staining after application of the binary mask of a high percent area stain (left) and low percent area (right) both originating from the CM monoculture. The yellow circles are the positively stained di-8-anepps areas recognized by ImageJ. The numbers on the images represent the percent of total area circled by ImageJ within the entire cell area.

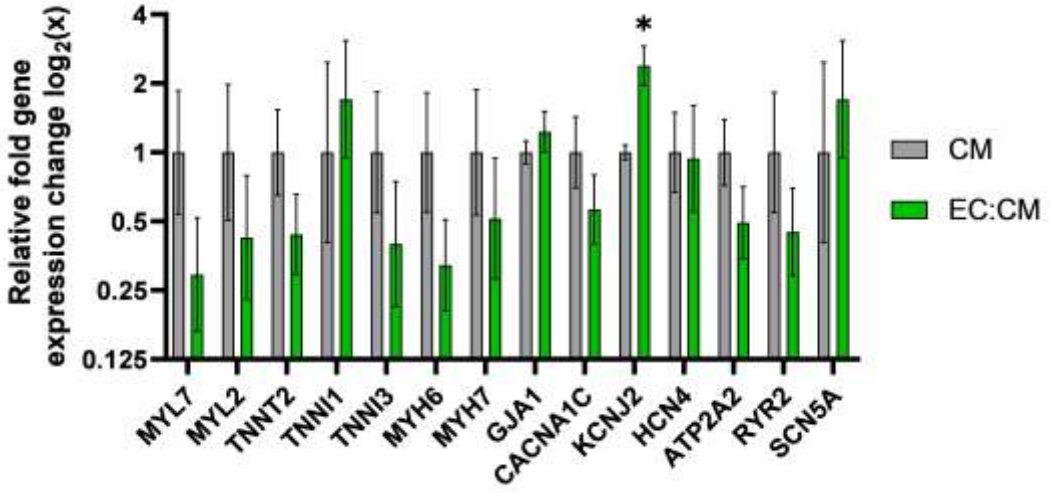

Supplementary Figure 2.6: CMs from EC:CM cocultures do not have higher expression of genes associated with CM maturation. hESCs expressing eGFP under the TNNT2 promoter were differentiated to CPCs, cultured in RPMI/B27 media for 9 days, then maintained as CM monocultures or cocultured with hPSC-derived ECs for two weeks. Next, eGFP+ cells were purified via FACS and expression of the indicated genes was quantified by qPCR. Values were normalized to the average of the expression of VIRMA and ZNF384, two housekeeping genes. Fold change values were calculated via the ΔΔCt method. Data represent mean ± SEM of at least seven replicates taken over three independent differentiations with at least two qPCR experimental replicates each. The values were normalized to the CPC monoculture in each differentiation and statistical comparisons were performed using the two-way Mann-Whitney test, $N \geq 7$ (* $p<0.05$, # $p<0.01$).

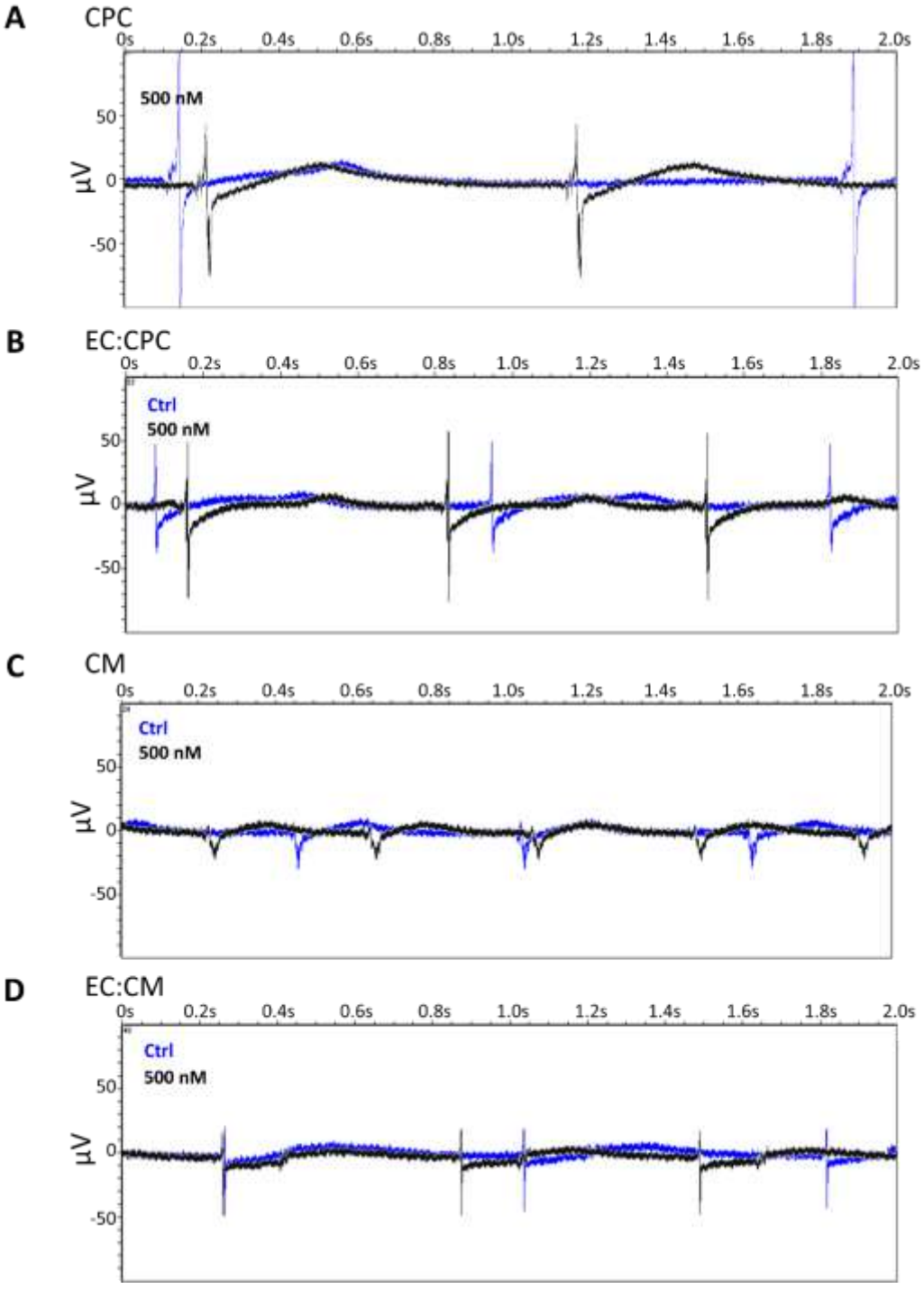

Supplementary Figure 2.7: Example representative MEA measurements from H9 hESCs-derived CPCs and CMs in monoculture or in coculture with H1 hESC-derived ECs, as indicated, after two weeks of culture on a microelectrode array. Traces show signal of a single electrode before (blue) and 15 minutes after (black) treatment with 500 nM isoprenaline.

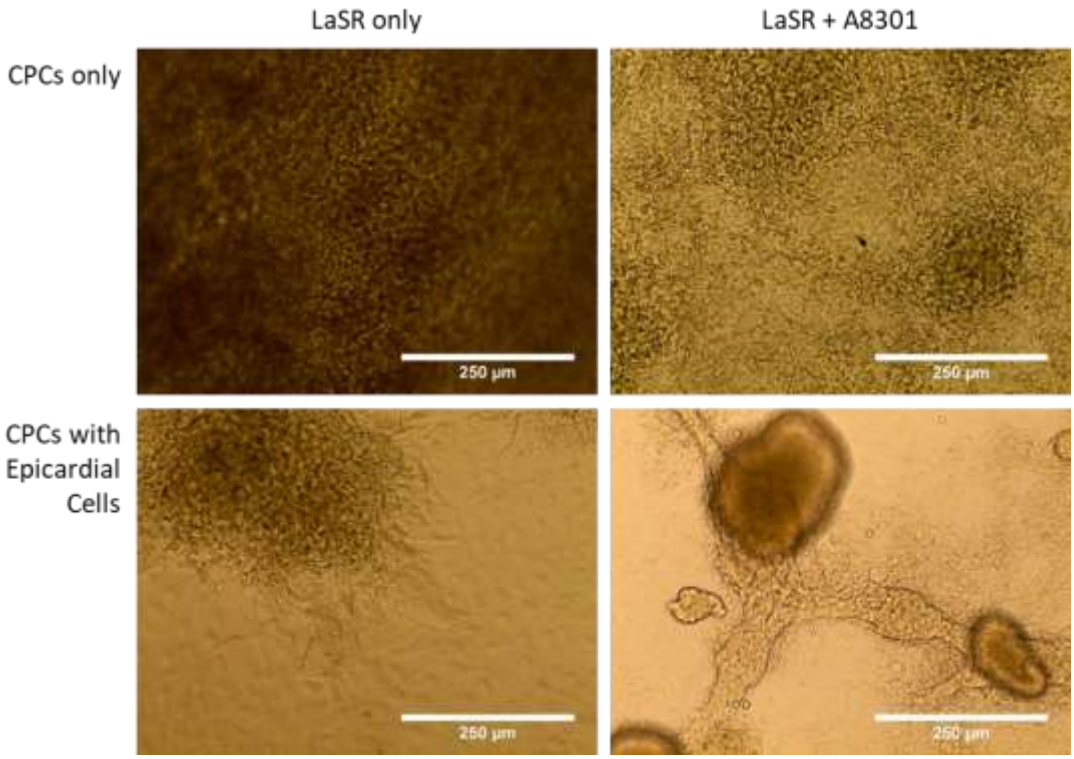

Supplementary Figure 3.1: Changes in morphology occur between the monocultured H9-derived CPCs and the cocultured epicardial cells and CPCs with and without A83-01. H9-derived CPCs and epicardial cells were plated at a density of 250 x 10^3 cells/cm^2 on gelatin-coated plates as a monoculture of CPCs or coculture. They were maintained in LaSR basal media with or without 0.5 µM A83-01. After two weeks, brightfield images were taken of the resulting cells.

5.2 References

1. Hirsch E, Nagai R, Thum T. Heterocellular signalling and crosstalk in the heart in ischaemia and heart failure. *Cardiovasc Res* (2014) 102(2):191–3. doi: 10.1093/cvr/cvu073

2. Pinto AR, Ilinykh A, Ivey MJ, Kuwabara JT, D'antoni ML, Debuque R, et al. Revisiting cardiac cellular composition. *Circ Res* (2016) 118(3):400–409. doi: 10.1161/CIRCRESAHA.115.307778

3. Barth AS, Merk S, Arnoldi E, Zwermann L, Kloos P, Gebauer M, et al.. Functional profiling of human atrial and ventricular gene expression. *Pflugers Archiv* (2005) 450(4):201–208. doi: 10.1007/s00424-005-1404-8

4. Lee JH, Protze SI, Laksman Z, Backx PH, Keller GM, Lee JH, et al. Human Pluripotent Stem Cell-Derived Atrial and Ventricular Cardiomyocytes Develop from Distinct Mesoderm Populations. *Cell Stem Cell* (2017) 21(2):179–194.e4. doi: 10.1016/j.stem.2017.07.003

5. Synnergren J, Heins N, Brolen G, Eriksson G, Lindahl A, Hyllner J, Olsson B, et al. Transcriptional profiling of human embryonic stem cells differentiating to definitive and primitive endoderm and further toward the hepatic lineage. *Stem Cells Dev* (2010) 19:961–978. doi: 10.1002/hep.28886

6. Witty AD, Mihic A, Tam RY, Fisher S, Mikryukov A, Shoichet MS, et al. Generation of the epicardial lineage from human pluripotent stem cells. *Nat Biotechnol* (2014) 32(10):1026–35. doi: 10.1038/nbt.3002

7. Katz TC, Singh MK, Degenhardt K, Rivera-feliciano J. Distinct Compartments of the Proepicardial Organ Give Rise to Coronary Vascular Endothelial Cells. *Dev Cell* (2012) 22(3):639–650. doi: 10.1016/j.devcel.2012.01.012.

8. Bax NM, van Marion MH, Shah B, Goumans MJ, Bouten CVC, van der Schaft DWJ. Matrix production and remodeling capacity of cardiomyocyte progenitor cells during in vitro differentiation. *J Mol and Cell Cardiol* (2012) 53(4):497–508. doi: 10.1016/j.yjmcc.2012.07.003

9. Cardiovascular diseases (CVDs) [Internet]. World Health Organization; 2017 May [cited 2017 Dec 15]. Available from http://www.who.int/mediacentre/factsheets/fs317/en/

10. van Berlo JH, Molkentin JD. An emerging consensus on cardiac regeneration. *Nat Med* (2014) 20(12):1386–1393. doi: 10.1038/nm.3764

11. Laflamme MA, Murry CE. Heart regeneration. *Nature* (2011) 473(7347):326–35. doi: 10.1038/nature10147

12. Rojas SV, Avsar M, Uribarri A, Hanke JS, Haverich A, Schmitto JD. A new era of ventricular assist device surgery: less invasive procedures. *Minerva Chir*. (2015) 70(1):63-8.

13. Chong JJH, Yang X, Don CW, Minami E, Liu YW, Weyers JJ, et al. Human embryonic-stem-cell-derived cardiomyocytes regenerate non-human primate hearts. *Nature* (2014) 510(7504):273–7. doi: 10.1038/nature13233

14. Yang X, Rodriguez M, Pabon L, Fischer KA, Reinecke H, Regnier M, et al. Tri-iodo-l-thyronine promotes the maturation of human cardiomyocytes-derived from induced pluripotent stem cells. *J Mol Cell Cardiol* (2014) 72:296–304. doi: 10.1016/j.yjmcc.2014.04.005

15. Lalit PA, Salick MR, Nelson DO, Squirrell JM, Shafer CM, Patel NG, et al. Lineage Reprogramming of Fibroblasts into Proliferative Induced Cardiac Progenitor Cells by Defined Factors. *Cell Stem Cell* (2016) 18(3):354–367. doi: 10.1016/j.stem.2015.12.001

16. Kehat I, Kenyagin-Karsenti D. Human embryonic stem cells can differentiate into myocytes with structural and functional properties of cardiomyocytes. *J Clin Invest* (2001) 108(3):407–414. doi: 10.1172/JCI200112131

17. He J, Ma Y, Lee Y, Thomson JA, Kamp TJ. Human Embryonic Stem Cells Develop Into Multiple Types of Cardiac Myocytes Action Potential Characterization. *Circ Res* (2003) 93:32–39. doi: 10.1161/01.RES.0000080317.92718.99

18. Laflamme M, Chen KY, Naumova AV, Muskheli V, Fugate J, Dupras SK, et al. Cardiomyocytes derived from human embryonic stem cells in pro-survival factors enhance function of infarcted rat hearts. *Nat Biotechnol* (2007) 25(9):1015–1024. doi: 10.1038/nbt1327

19. Yang L, Soonpaa MH, Adler ED, Roepke TK, Kattman SJ, Kennedy M, et al. Human cardiovascular progenitor cells develop from a KDR+ embryonic-stem-cell-derived population. *Nature* (2008) 453(7194):524–528. doi: 10.1038/nature06894

20. Kattman SJ, Witty AD, Gagliardi M, Dubois NC, Niapour M, Hotta A, et al. Stage-specific optimization of activin/nodal and BMP signaling promotes cardiac differentiation of mouse and human pluripotent stem cell lines. *Cell Stem Cell* (2011) 8(2):228–240. doi: 10.1016/j.stem.2010.12.008

21. Lian X, Hsiao C, Wilson G, Zhu K, Hazeltine LB, Azarin SM, et al. Robust cardiomyocyte differentiation from human pluripotent stem cells via temporal modulation of canonical Wnt signaling. *Proc Natl Acad Sci U S A* (2012) 109(27):E1848-57. doi: 10.1073/pnas.1200250109

22. Lian X, Zhang J, Azarin SM, Zhu K, Hazeltine LB, Bao X, et al. Directed cardiomyocyte differentiation from human pluripotent stem cells by modulating Wnt/β-catenin signaling under fully defined conditions. *Nat Protoc* (2013) 8(1):162–75. doi: 10.1038/nprot.2012.150

23. Palpant NJ, Pabon L, Friedman CE, Roberts M, Hadland B, Zaunbrecher RJ, et al. Generating high-purity cardiac and endothelial derivatives from patterned mesoderm using human pluripotent stem cells. *Nat Protoc* (2016) 12(1):15–31. doi: 10.1038/nprot.2016.153

24. Burridge PW, Matsa E, Shukla P, Lin ZC, Churko JM, Ebert AD, et al. Chemically defined generation of human cardiomyocytes. *Nat Methods* (2014) 11(8):855–860. doi: 10.1038/nmeth.2999

25. Lian X, Bao X, Zilberter M, Westman M, Fisahn A. Chemically defined albumin-free human cardiomyocyte generation. *Nat Methods* (2015) 12(7):595–596. doi: 10.1038/nmeth.3448

26. Shiba Y, Gomibuchi T, Seto T, Wada Y, Ichimura H, Tanaka Y, et al. Allogeneic transplantation of iPS cell-derived cardiomyocytes regenerates primate hearts. *Nature* (2016) 538(7625):388–391. doi: 10.1038/nature19815

27. Fijnvandraat AC, van Ginneken AC, de Boer PA, et al. Cardiomyocytes derived from embryonic stem cells resemble cardiomyocytes of the embryonic heart tube. *Cardiovasc Res* (2003) 58(2):399–409

28. Lieu DK, Liu J, Siu C, Mcnerney GP, Tse H, Abu-khalil A, et al. Absence of Transverse Tubules Contributes to Non-Uniform Ca 2 + Wavefronts in Mouse and Human Embryonic Stem Cell – Derived Cardiomyocytes. *Stem Cells Dev* (2009) 18(10):1493–1500. doi: 10.1089/scd.2009.0052

29. Mollova M, Bersell K, Walsh S, Savla J, Tanmoy L, Park S. Cardiomyocyte proliferation contributes to heart growth in young humans. *Proc Natl Acad Sci U S A* (2012) 110(4):1–6. doi: 10.1073/pnas.1214608110

30. Snir M, Kehat I, Gepstein A, Coleman R, Itskovitz-Eldor J, Livne E, et al. Assessment of the ultrastructural and proliferative properties of human embryonic stem cell-derived cardiomyocytes. *Am J Physiol Heart Circ Physiol* (2003) 285:H2355–H2363. doi: 10.1152/ajpheart.00020.2003

31. Gerdes AM, Kellerman SE, Moore JA, Muffly KE, Clark LC, Reaves PY, et al. Structural remodeling of cardiac myocytes in patients with ischemic cardiomyopathy. *Circulation* (1992) 86:426–430. doi: 10.1161/01.CIR.86.2.426

32. Feric NT, and Radisic M. Maturing human pluripotent stem cell-derived cardiomyocytes in human engineered cardiac tissues. *Adv Drug Deliv Rev* (2016) 96:110–134. doi: 10.1016/j.addr.2015.04.019

33. Angst BD, Khan LU, Severs NJ, Whitely K, Rothery S, Thompson RP, Magee AI, Gourdie RG. Dissociated spatial patterning of gap junctions and cell adhesion junctions during postnatal differentiation of ventricular myocardium. *Circ Res* (1997) 80:88–94. doi: 10.1161/01.RES.80.1.88

34. Xu XQ, Soo SY, Sun W, Zweigerdt R. Global expression profile of highly enriched cardiomyocytes derived from human embryonic stem cells. *Stem Cells* (2009) 27:2163–2174. doi: 10.1002/stem.166

35. Bedada FB, Chan SSK, Metzger SK, Zhang L, Zhang J, Garry DJ, et al. Acquisition of a quantitative, stoichiometrically conserved ratiometric marker of maturation status in stem cell-derived cardiac myocytes. *Stem Cell Reports* (2014) 3(4):594–605. doi: 10.1016/j.stemcr.2014.07.012

36. Xu C, Police S, Rao N, Carpenter MK. Characterization and enrichment of cardiomyocytes derived from human embryonic stem cells. *Circ Res* (2002) 91(6):501–8.

37. Lundy SD, Zhu WZ, Regnier M, Laflamme M. Structural and functional maturation of cardiomyocytes derived from human pluripotent stem cells. *Stem Cells Dev* (2013) 22(14):1991–2002. doi: 10.1089/scd.2012.0490

38. Lopaschuk GD, Jaswal JS. Energy metabolic phenotype of the cardiomyocyte during development, differentiation, and postnatal maturation. *J Cardiovasc Pharmacol* (2010) 56(2):130–40. doi: 10.1097/FJC.0b013e3181e74a14

39. Ribeiro AJS, Ang YS, Fu JD, Rivas RN, Mohamed TMA, Higgs GC. et al. Contractility of single cardiomyocytes differentiated from pluripotent stem cells depends on physiological shape and substrate stiffness. *Proc Natl Acad Sci U S A* (2015) 112(41):12705–12710. doi: 10.1073/pnas.1508073112

40. Korte FS, Herron TJ, Rovetto MJ, McDonald KS. Power output is linearly related to MyHC content in rat skinned myocytes and isolated working hearts. *Am J Physiol Heart Circ Physiol* (2005) 289:H801–H812. doi: 10.1152/ajpheart.01227.2004

41. Pekkanen-Mattila M, Chapman H, Kerkela E, Suuronen R, Skottman H, Koivisto AP et al. Human embryonic stem cell-derived cardiomyocytes: demonstration of a portion of cardiac cells with fairly mature electrical phenotype. *Exp Biol Med* (2010) 235:522–530. doi: 10.1258/ebm.2010.009345

42. Lee P, Klos M, Bollensdorff C, Hou L, Ewart P, Kamp T J, et al. Simultaneous voltage and calcium mapping of genetically purified human induced pluripotent stem cell-derived cardiac myocyte monolayers. *Circ Res* (2012) 110:1556–1563. doi: 10.1161/circresaha.111.262535

43. Caspi O, Itzhaki I, Kehat I, Gepstein A, Arbel G, Huber I, et al. In vitro electrophysiological drug testing using human embryonic stem cell derived cardiomyocytes. *Stem Cells Dev* (2009) 18:161–172. doi: 10.1089/scd.2007.0280

44. Drouin E, Charpentier F, Gauthier C, Laurent K, and Le Marec H. Electrophysiologic characteristics of cells spanning the left ventricular wall of human heart: evidence for presence of M cells. *J Am Coll Cardiol* (1995) 26:185–192.

45. Lu P, Ceto S, Wang Y, Graham L, Wu D, Kumamaru H, et al. Prolonged human neural stem cell maturation supports recovery in injured rodent CNS. *J Clin Invest* (2017) 127(9):3287–3299. doi: 10.1172/JCI92955

46. Kroon E, Martinson LA, Kadoya K, Bang AG, Kelly OG, Eliazer S, et al. Pancreatic endoderm derived from human embryonic stem cells generates glucose-responsive insulin-secreting cells in vivo. *Nat Biotechnol* (2008) 26(4):443–452. doi: 10.1038/nbt1393

47. Rezania A, Bruin JE, Riedel MJ, Mojibian M, Asadi A, Xu J, et al. Maturation of human embryonic stem cell-derived pancreatic progenitors into functional islets capable of treating pre-existing diabetes in mice. *Diabetes* (2012) 61(8):2016–2029. doi: 10.2337/db11-1711

48. Kadota S, Minami I, Morone N, Heuser JE, Agladze K, Nakatsuji N. Development of a reentrant arrhythmia model in human pluripotent stem cell-derived cardiac cell sheets. *Eur Heart J* (2013) 34(15):1147–56. doi: 10.1093/eurheartj/ehs418

49. Funakoshi S, Miki K, Takaki T, Okubo C, Hatani T, Chonabayashi K, et al. Enhanced engraftment, proliferation, and therapeutic potential in heart using optimized human iPSC-derived cardiomyocytes. *Sci Rep* (2016) 6:19111. doi: 10.1038/srep19111

50. Wu J, Platero-Luengo A, Sakurai M, Sugawara A, Gil MA, Yamauchi T, et al. C. Interspecies Chimerism with Mammalian Pluripotent Stem Cells. *Cell* (2017) 168(3):473–486.e15. doi: 10.1016/j.cell.2016.12.036

51. Ivashchenko CY, Pipes GC, Lozinskaya IM, Lin Z, Xiaoping X, Needle S, et al. Human-induced pluripotent stem cell-derived cardiomyocytes exhibit temporal changes in phenotype. *Am J Physiol Heart Circ Physiol* (2013) 305(6):H913-22. doi: 10.1152/ajpheart.00819.2012

52. Luxán G, Casanova JC, Martínez-Poveda B, Prados B, D'Amato G, MacGrogan D, et al. Mutations in the NOTCH pathway regulator MIB1 cause left ventricular noncompaction cardiomyopathy. *Nat Med* (2013) 19(2):193–201. doi: 10.1038/nm.3046

53. Lavine KJ, Yu K, White AC, Zhang X, Smith C, Partanen J, Ornitz DM. Endocardial and epicardial derived FGF signals regulate myocardial proliferation and differentiation in vivo. *Dev Cell* (2005) 8(1):85–95. doi: 10.1016/j.devcel.2004.12.002

54. Kim C, Majdi M, Xia P, Wei K, Talantova M, Spiering S, et al. Non-cardiomyocytes influence the electrophysiological maturation of human embryonic stem cell-derived cardiomyocytes during differentiation. *Stem Cells Dev* (2010) 19(6):783–95. doi: 10.1089/scd.2009.0349

55. Souders CA, Bowers SLK, Baudino TA. Cardiac fibroblast: the renaissance cell. *Circ Res* (2009) 105(12):1164–76. doi: 10.1161/CIRCRESAHA.109.209809

56. Pedrotty DM, Klinger RY, Kirkton RD, Bursac N, Hall H. Cardiac fibroblast paracrine factors alter impulse conduction and ion channel expression of neonatal rat cardiomyocytes. *Cardiovasc Res* (2009) 83:688–697. doi: 10.1093/cvr/cvp164

57. Fan D, Takawale A, Lee J, Kassiri Z. Cardiac fibroblasts, fibrosis and extracellular matrix remodeling in heart disease. *Fibrogenesis Tissue Repair* (2012) 5(1):15. doi: 10.1186/1755-1536-5-15

58. Suhaeri M, Subbiah R, Kim SH, Kim CH, Oh SJ, Kim SH, Park K. Novel Platform of Cardiomyocyte Culture and Coculture via Fibroblast-Derived Matrix-Coupled Aligned Electrospun Nanofiber. *ACS Appl. Mater. Interfaces* (2017) 9(1):224–35. doi: 10.1021/acsami.6b14020

59. Marchionni, MA. Neu tack on neuregulin. *Nature* (1995) 378(6555):334–335. doi: 10.1038/378334a0

60. Iglesias-García O, Baumgartner S, Macrí-Pellizzeri L, Rodriguez-Madoz JR, Abizanda G, Guruceaga E, et al. Neuregulin-1β Induces Mature Ventricular Cardiac Differentiation from Induced Pluripotent Stem Cells Contributing to Cardiac Tissue Repair. *Stem Cells Dev* (2015) 24(4):484–496. doi: 10.1089/scd.2014.0211

61. Lee DS, Chen JH, Lundy DJ, Liu CH, Hwang SM, Pabon L, et al. Defined MicroRNAs Induce Aspects of Maturation in Mouse and Human Embryonic-Stem-Cell-Derived Cardiomyocytes. *Cell Rep* (2015) 12(12):1960–7. doi: 10.1016/j.celrep.2015.08.042

62. Pasquier J, Gupta R, Rioult D, Hoarau-Véchot J, Courjaret R, Machaca K, et al. Coculturing with endothelial cells promotes in vitro maturation and electrical coupling of human embryonic stem cell–derived cardiomyocytes. *J Heart Lung Transplant* (2017) 36(6):684–693. doi: 10.1016/j.healun.2017.01.001

63. Krüger M, Sachse C, Zimmermann WH, Eschenhagen T, Klede S, Linke WA. Thyroid hormone regulates developmental titin isoform transitions via the phosphatidylinositol-3-kinase/Akt pathway. *Circ Res* (2008) 102(4):439–447. doi: 10.1161/circresaha.107.162719

64. Kosmidis G, Bellin M, Ribeiro MC, Van Meer B, Ward-Van Oostwaard D, Passier R, et al. Altered calcium handling and increased contraction force in human embryonic stem cell derived cardiomyocytes following short term dexamethasone exposure. *Biochem Biophys Res Commun* (2015) 467(4):998–1005. doi: 10.1016/j.bbrc.2015.10.026

65. Parikh SS, Blackwell DJ, Gomez-Hurtado N, Frisk M, Wang L, Kim K, et al. Thyroid and Glucocorticoid Hormones Promote Functional T-Tubule Development in Human-Induced Pluripotent Stem Cell-Derived Cardiomyocytes. *Circ Res* (2017) 121(12):1323–1330. doi: 10.1161/CIRCRESAHA.117.311920

66. Bhute VJ, Bao X, Dunn KK, Knutson KR, McCurry EC, Jin G, et al. Metabolomics Identifies Metabolic Markers of Maturation in Human Pluripotent Stem Cell-Derived Cardiomyocytes. *Theranostics* (2017) 7(7):2078–2091. doi: 10.7150/thno.19390

67. Correia C, Koshkin A, Duarte P, Hu D, Tei A. Distinct carbon sources affect structural and functional maturation of cardiomyocytes derived from human pluripotent stem cells. *Sci Rep* (2017) 7(1):8590. doi: 10.1038/s41598-017-08713-4

68. Marquardt LM, Heilshorn SC. Design of Injectable Materials to Improve Stem Cell Transplantation. *Curr Stem Cell Rep* (2016) 2(3), 207–220. doi: 10.1007/s40778-016-0058-0

69. Park S, Koh YJ, Jeon J, Cho Y, Jang M, Kang Y, et al. Efficient differentiation of human pluripotent stem cells into functional CD34+ progenitor cells by combined modulation of the MEK / ERK and BMP4 signaling pathways. *Blood* (2010) 116(25):5762–5772. doi: 10.1182/blood-2010-04-280719

70. Bao X, Lian X, Dunn KK, Shi M, Han T, Qian T, et al. Chemically-defined albumin-free differentiation of human pluripotent stem cells to endothelial progenitor cells. *Stem Cell Res* (2015) 15(1):122–129. doi: 10.1016/j.scr.2015.05.004

71. Lui KO, Zangi L, Silva E, Bu L, Sahara M, Li R, et al. Driving vascular endothelial cell fate of human multipotent Isl1+ heart progenitors with VEGF modified mRNA. *Cell Res* (2013) 23(10):1172–86. doi: 10.1038/cr.2013.112

72. Iyer D, Gambardella L, Bernard WG, Serrano F, Mascetti VL, Pedersen RA, et al. Robust derivation of epicardium and its differentiated smooth muscle cell progeny from human pluripotent stem cells. *Development* (2016) 143(5):904–904. doi: 10.1242/dev.136143

73. Bao X, Lian X, Hacker TA, Schmuck EG, Qian T, Bhute VJ, et al. Long-term self-renewing human epicardial cells generated from pluripotent stem cells under defined xeno-free conditions. *Nat Biomed Eng* (2016) 1(December):3. doi: 10.1038/s41551-016-0003

74. Bao X, Bhute VJ, Han T, Qian T, Lian X, Palecek SP. Human pluripotent stem cell-derived epicardial progenitors can differentiate to endocardial-like endothelial cells. *Bioeng Transl Med* (2017) 2(2):191–201. doi: 10.1002/BTM2.10062

75. Stevens KR, Kreutziger KL, Dupras SK, Korte FS, Regnier M, Muskheli V, et al. Physiological function and transplantation of scaffold-free and vascularized human. *Proc Natl Acad Sci U S A* (2009) 106(39):16568–16573. doi: 10.1073/pnas.0908381106

76. Caspi O, Lesman A, Basevitch Y, Gepstein A, Arbel G, Habib IHM, et al. Tissue engineering of vascularized cardiac muscle from human embryonic stem cells. *Circ Res* (2007) 100(2):263–72. doi: 10.1161/01.RES.0000257776.05673.ff

77. Sekine H, Shimizu T, Hobo K, Sekiya S, Yang J, Yamato M, et al. Endothelial cell coculture within tissue-engineered cardiomyocyte sheets enhances neovascularization and improves cardiac function of ischemic hearts. *Circulation* (2008) 118(14 Suppl):S145-52. doi: 10.1161/circulationaha.107.757286

78. Vuorenpää H, Penttinen K, Heinonen T, Pekkanen-Mattila M, Sarkanen JR, et al. Maturation of human pluripotent stem cell derived cardiomyocytes is improved in cardiovascular construct. *Cytotechnology* (2017) 69:785–800. doi: 10.1007/s10616-017-0088-1

79. Ravenscroft SM, Pointon A, Williams AW, Cross MJ, Sidaway JE. Cardiac non-myocyte cells show enhanced pharmacological function suggestive of contractile maturity in stem cell derived cardiomyocyte microtissues. *Toxicol Sci* (2016) 152(1):99–112. doi: 10.1093/toxsci/kfw069

80. Matsuura K, Nagai T, Nishigaki N, Oyama T, Nishi J, Wada H, et al. Adult Cardiac Sca-1-positive Cells Differentiate into Beating Cardiomyocytes. *J Biol Chem* (2004) 279(12):11384–11391. doi: 10.1074/jbc.M310822200

81. Beltrami AP, Barlucchi L, Torella D, Baker M, Limana F, Chimenti S, et al. Adult Cardiac Stem Cells Are Multipotent and Support Myocardial Regeneration. *Cell* (2003) *114*:763–776. doi: 10.1016/S0092-8674(03)00687-1

82. Le T, Chong J. Cardiac progenitor cells for heart repair. *Cell Death Dis* (2016) *2*(May):16052. doi: 10.1038/cddiscovery.2016.52

83. Misfeldt AM, Boyle SC, Tompkins KL, Bautch VL, Labosky P, Baldwin HS. Endocardial cells are a distinct endothelial lineage derived from Flk1+ multipotent cardiovascular progenitors. *Dev Biol* (2009) 333(1):78–89. doi: 10.1016/j.ydbio.2009.06.033

84. Moretti A, Caron L, Nakano A, Lam JT, Bernshausen A, Chen Y, et al. Multipotent Embryonic Isl1+Progenitor Cells Lead to Cardiac, Smooth Muscle, and Endothelial Cell Diversification. *Cell* (2006) 127(6):1151–1165. doi: 10.1016/j.cell.2006.10.029

85. Narazaki G, Uosaki H, Teranishi M, Okita K, Kim B, Matsuoka S, et al. Directed and systematic differentiation of cardiovascular cells from mouse induced pluripotent stem cells. *Circulation* (2008) 118(5):498–506. doi: 10.1161/circulationaha.108.769562

86. Ruan JL, Tulloch N, Saiget M, Paige S, Razumova M, Regnier M, et al. Mechanical Stress Promotes Maturation of Human Myocardium from Pluripotent Stem Cell-Derived Progenitors. *Stem Cells* (2015) 33:2148–57. doi: 10.1002/stem.2036

87. Chen IY, Wu JC. Finding expandable induced cardiovascular progenitor cells. *Circ Res* (2016) 119:16–20. doi: 10.1161/circresaha.116.308679

88. Birket MJ, Ribeiro MC, Verkerk AO, Ward D, Leitoguinho AR, den Hartogh SC, et al. Expansion and patterning of cardiovascular progenitors derived from human pluripotent stem cells. *Nat Biotechnol* (2015) 33(July):1–12. doi: 10.1038/nbt.3271

89. Zhang Y, Cao N, Huang Y, Spencer CI, Fu JD, Yu C, et al. Expandable Cardiovascular Progenitor Cells Reprogrammed from Fibroblasts. *Cell Stem Cell* (2016) 18(3):368–381. doi: 10.1016/j.stem.2016.02.001

90. Wang H, Cao N, Spencer CI, Nie B, Ma T, Xu T, et al. Small molecules enable cardiac reprogramming of mouse fibroblasts with a single factor, oct4. *Cell Rep* (2014) 6(5):951–960. doi: 10.1016/j.celrep.2014.01.038

91. Giacomelli E, Bellin M, Sala L, van Meer BJ, Tertoolen LGJ, Orlova VV, Mummery CL. Three-dimensional cardiac microtissues composed of cardiomyocytes and endothelial cells co-differentiated from human pluripotent stem cells. *Development* (2017) 144:1008–17. doi: 10.1242/dev.143438

92. Tulloch NL, Muskheli V, Razumova MV, Steven F, Regnier M, Hauch KD, et al. Growth of Engineered Human Myocardium with Mechanical Loading and Vascular Coculture. *Circ Res* (2011) 109(1):47–59. doi: 10.1161/circresaha.110.237206

93. Mihic A, Li J, Miyagi Y, Gagliardi M, Li SH, Zu J, et al. The effect of cyclic stretch on maturation and 3D tissue formation of human embryonic stem cell-derived cardiomyocytes. *Biomaterials* (2014) 35(9):2798–808. doi: 10.1016/j.biomaterials.2013.12.052

94. Chan YC, Ting S, Lee YK, Ng KM, Zhang J, Chen Z, et al. Electrical stimulation promotes maturation of cardiomyocytes derived from human embryonic stem cells. *J Cardiovasc Transl Res* (2013) 6(6):989–99. doi: 10.1007/s12265-013-9510-z

95. Eng G, Lee BW, Protas L, Gagliardi M, Brown K, Kass RS, et al. Autonomous beating rate adaptation in human stem cell-derived cardiomyocytes. *Nature Commun* (2016) 7(10312):1–10. doi: 10.1038/ncomms10312

96. Scuderi GJ, Butcher J. Naturally Engineered Maturation of Cardiomyocytes. *Front Cell Dev Biol* (2017) 5:50. doi: 10.3389/fcell.2017.00050

97. Fong AH, Romero-López M, Heylman CM, Keating M, Tran D, Sobrino A, et al. Three-Dimensional Adult Cardiac Extracellular Matrix Promotes Maturation of Human Induced Pluripotent Stem Cell-Derived Cardiomyocytes. *Tissue Eng Part A* (2016) 22(15–16):1016–25. doi: 10.1089/ten.tea.2016.0027

98. Herron TJ, Da Rocha AM, Campbell KF, Ponce-Balbuena D, Willis BC, Guerrero-Serna G, et al. Extracellular matrix-mediated maturation of human pluripotent stem cell-derived cardiac monolayer structure and electrophysiological function. *Circ Arrhythm Electrophysiol* (2016) 9(4):e003638. doi: 10.1161/circep.113.003638

99. Li J, Minami I, Yu L, Tsuji K, Nakajima M, Qiao J, et al. Extracellular recordings of patterned human pluripotent stem cell-derived cardiomyocytes on aligned fibers. *Stem Cells Int* (2016) 2016:26340131–9. doi: 10.1155/2016/2634013

100. Tohyama S, Fujita J, Fujita C, Yamaguchi M, Kanaami S, Ohno R, et al. Efficient Large-Scale 2D Culture System for Human Induced Pluripotent Stem Cells and Differentiated Cardiomyocytes. *Stem Cell Rep* (2017) 9(5):1406–1414. doi: 10.1016/j.stemcr.2017.08.025

101. Ting S, Chen A, Reuveny S, Oh S. An intermittent rocking platform for integrated expansion and differentiation of human pluripotent stem cells to cardiomyocytes in suspended microcarrier cultures. *Stem Cell Res* (2014) 13(2):202–213. doi: 10.1016/j.scr.2014.06.002

102. Nguyen DC, Hookway TA, Wu Q, Jha R, Preininger MK, Chen X, et al. Microscale Generation of Cardiospheres Promotes Robust Enrichment of Cardiomyocytes Derived from Human Pluripotent Stem Cells. *Stem Cell Rep* (2014) 3(2):260–268. doi:10.1016/j.stemcr.2014.06.002

103. Chen VC, Ye J, Shukla P, Hu G, Chen D, Lin Z, et al. Development of a scalable suspension culture for cardiac differentiation from human pluripotent stem cells. *Stem Cell Res* (2016) 15(2):137–143. doi: 10.1016/j.scr.2015.08.002

104. Kempf H, Kropp C, Olmer R, Martin U, Zweigerdt R. Cardiac differentiation of human pluripotent stem cells in scalable suspension culture. *Nat Protoc* (2015) 10(9):1345–61. doi: 10.1038/nprot.2015.089

105. Shadrin IY, Allen BW, Qian Y, Jackman CP, Carlson AL, Juhas ME, Bursac N. Cardiopatch platform enables maturation and scale-up of human pluripotent stem cell-derived engineered heart tissues. *Nat Commun* (2017) 8(1):1825. doi: 10.1038/s41467-017-01946-x

106. Lux M, Andrée B, Horvath T, Nosko A, Manikowski D, Hilfiker-Kleiner D, et al. In vitro maturation of large-scale cardiac patches based on a perfusable starter matrix by cyclic mechanical stimulation. *Acta Biomater* (2016) 30:177–187. doi: 10.1016/j.actbio.2015.11.006

107. Tandon N, Taubman A, Cimetta E, Saccenti L, Vunjak G, Tandon N, et al. Portable bioreactor for perfusion and electrical stimulation of engineered cardiac tissue. *Conf Proc IEEE Eng Med Biol Soc* (2013) 2013:6219–6223. doi: 10.1109/EMBC.2013.6610974

108. Kempf H, Olmer R, Haase A, Franke A, Bolesani E, Dra G, et al. Bulk cell density and Wnt/TGFbeta signalling regulate mesendodermal patterning of human pluripotent stem cells. *Nat Commun* (2016) 7:13602 doi: 10.1038/ncomms13602

109. Tavakoli T, Xu X, Derby E, Serebryakova Y, Reid Y, Rao MS, et al. Self-renewal and differentiation capabilities are variable between human embryonic stem cell lines I3, I6 and BG01V. *BMC Cell Biol* (2009) 10:44. doi: 10.1186/1471-2121-10-44

110. Choo AB, Tan HL, Ang SN, Fong WJ, Chin A, Lo J, et al. Selection Against Undifferentiated Human Embryonic Stem Cells by a Cytotoxic Antibody Recognizing Podocalyxin-Like Protein-1. *Stem Cells* (2008) 26(6):1454–63. doi: 10.1634/stemcells.2007-0576

111. Dubois NC, Craft AM, Sharma P, Elliott Da, Stanley EG, Elefanty AG, et al. SIRPA is a specific cell-surface marker for isolating cardiomyocytes derived from human pluripotent stem cells. *Nature Biotechnol* (2011) 29(11):1011–8. doi: 10.1038/nbt.2005

112. Uosaki H, Fukushima H, Takeuchi A, Matsuoka S, Nakatsuji N, Yamanaka S, Yamashita JK. Efficient and scalable purification of cardiomyocytes from human embryonic and induced pluripotent stem cells by VCAM1 surface expression. *PLoS One* (2011) 6(8):e23657. doi: 10.1371/journal.pone.0023657

113. Hattori F, Chen H, Yamashita H, Tohyama S, Satoh YS, Yuasa S, et al. Nongenetic method for purifying stem cell-derived cardiomyocytes. *Nat Methods* (2010) 7(1):61–66. doi: 10.1038/nmeth.1403

114. Page E, McCallister LP. Quantitative electron microscopic description of heart muscle cells. Application to normal, hypertrophied and thyroxin-stimulated hearts. *Am J Cardiol* (1973) 31(2):172–81. doi: 10.1016/0002-9149(73)91030-8

115. Klug MG, Soonpaa MH, Koh GY, Field LJ. Genetically selected cardiomyocytes from differentiating embryonic stem cells form stable intracardiac grafts. *J Clin Invest* (1996) 98(1):216–224. doi: 10.1172/JCI118769

116. Huber I, Itzhaki I, Caspi O, Arbel G, Tzukerman M, Gepstein A, et al. Identification and selection of cardiomyocytes during human embryonic stem cell differentiation. *Faseb J* (2007) 21(10):2551–2563. doi: 10.1096/fj.05-5711com

117. Miki, K., Endo, K., Takahashi, S., Funakoshi, S., Takei, I., Katayama, S., et al. Efficient Detection and Purification of Cell Populations Using Synthetic MicroRNA Switches. *Cell Stem Cell* (2015) 16(6):699–711. doi: 10.1016/j.stem.2015.04.005

118. Tohyama S, Hattori F, Sano M, Hishiki T, Nagahata Y, Matsuura T, et al. Distinct metabolic flow enables large-scale purification of mouse and human pluripotent stem cell-derived cardiomyocytes. *Cell Stem Cell* (2013) 12:127–137. doi: 10.1016/j.stem.2012.09.013

119. Darkins CL, Mandenius CF. Design of large-scale manufacturing of induced pluripotent stem cell derived cardiomyocytes. *Chem Eng Res Des* (2014) 92(6):1142–52. doi: 10.1016/j.cherd.2013.08.021

120. Xu C, Police S, Hassanipour M, Li Y, Chen Y, Priest C, et al. Efficient generation and cryopreservation of cardiomyocytes derived from human embryonic stem cells. *Regen Med* (2011) 6(1):53–66. doi: 10.2217/rme.10.91

121. Hunt CJ. Cryopreservation of human stem cells for clinical application: A review. *Transfus Med Hemother* (2011) 38(2):107–123. doi: 10.1159/000326623

122. Correia C, Koshkin A, Carido M, Espinha N, Saric T, Lima PA, et al. Effective Hypothermic Storage of Human Pluripotent Stem Cell-Derived Cardiomyocytes Compatible With Global Distribution of Cells for Clinical Applications and Toxicology Testing. *Stem Cells Transl Med* (2016) 5:658–669. doi: 10.5966/sctm.2015-0238

123. Benjamin EJ, Virani SS, Callaway CW, Chamberlain AM, Chang AR, Cheng S, et al. Heart disease and stroke statistics - 2018 update: A report from the American Heart Association. *Circulation* (2018) 137(12):E67–E492. doi: 10.1161/CIR.0000000000000558

124. Senyo SE, Lee RT, Kühn B. Cardiac regeneration based on mechanisms of cardiomyocyte proliferation and differentiation. *Stem Cell Res* (2014) 13(3):532–541. doi: 10.1016/j.scr.2014.09.003

125. Dunn KK, Palecek SP. Engineering Scalable Manufacturing of High-Quality Stem Cell-Derived Cardiomyocytes for Cardiac Tissue Repair. *Front Med* (2018) 5(April). doi: 10.3389/fmed.2018.00110

126. Liu YW, Chen B, Yang X, Fugate JA, Kalucki FA, Futakuchi-Tsuchida A, et al. Human embryonic stem cell-derived cardiomyocytes restore function in infarcted hearts of non-human primates. *Nature Biotechnol* (2018) 36(7):597–605. doi: 10.1038/nbt.4162

127. Xiu QX, Set YS, Sun W, Zweigerdt R. Global expression profile of highly enriched cardiomyocytes derived from human embryonic stem cells. *Stem Cells* (2009) 27(9):2163–2174. doi: 10.1002/stem.166

128. Ronaldson-Bouchard K, Ma SP, Yeager K, Chen T, Song LJ, Sirabella D, et al. Advanced maturation of human cardiac tissue grown from pluripotent stem cells. *Nature* (2018) 556(7700):239–243. doi: 10.1038/s41586-018-0016-3

129. Salick MR, Napiwocki BN, Sha J, Knight GT, Chindhy SA, Kamp, TJ, et al. Micropattern width dependent sarcomere development in human ESC-derived cardiomyocytes. *Biomaterials* (2014) 35(15):4454–64. doi: 10.1016/j.biomaterials.2014.02.001

130. Tan Y, Richards D, Xu R, Stewart-Clark S, Mani SK, Borg TK, et al. Silicon nanowire-induced maturation of cardiomyocytes derived from human induced pluripotent stem cells. *Nano Letters* (2015) 15(5):2765–2772. doi: 10.1021/nl502227a

131. Spearman BS, Hodge AJ, Porter JL, Hardy JG, Davis ZD, Xu T, et al. Conductive interpenetrating networks of polypyrrole and polycaprolactone encourage electrophysiological development of cardiac cells. *Acta Biomater* (2015) 28:109–120. doi: 10.1016/j.actbio.2015.09.025

132. Yoshida S, Miyagawa S, Fukushima S, Kawamura T, Kashiyama N, Ohashi F, et al. Maturation of Human Induced Pluripotent Stem Cell-Derived Cardiomyocytes by Soluble Factors from Human Mesenchymal Stem Cells. *Mol Ther* (2018) 26(11):2681–2695. doi: 10.1016/j.ymthe.2018.08.012

133. Matsuda Y, Takahashi K, Kamioka H, Naruse K. Human gingival fibroblast feeder cells promote maturation of induced pluripotent stem cells into cardiomyocytes. *Biochem Biophys Res Commun* (2018) 503(3):1798–1804. doi: 10.1016/j.bbrc.2018.07.116

134. Hsieh PCH, Davis ME, Lisowski LK, Lee RT. Endothelial-Cardiomyocyte Interactions in Cardiac Development and Repair. *Annu Rev Physiol* (2006) 68:51–66. doi: 10.1146/annurev.physiol.68.040104.124629

135. Fishman M, Chien K. Fashioning the vertebrate heart: earliest embryonic decisions. *Development* (1997) 124(11):2099–2117. doi: 10.1007/s11064-008-9608-x

136. Thomson JA, Itskovitz-eldor J, Shapiro SS, Waknitz MA, Swiergiel JJ, et al.. Embryonic Stem Cell Lines Derived from Human Blastocysts. *Science* (1998) 282(5391):1145–1148. doi: 10.1126/science.282.5391.1145

137. Yu J, Hu K, Smuga-otto K, Tian S, Stewart R, et al. Human Induced Pluripotent Stem Cell Free of Vector Transgene Sequences. *Science* (2009) 324(5928):797–801. doi: 10.1126/science.1172482

138. Wrighton PJ, Klim JR, Hernandez BA, Koonce CH, Kamp TJ, et al. Signals from the surface modulate differentiation of human pluripotent stem cells through glycosaminoglycans and integrins. *Proc Natl Acad Sci U S A* (2014) 111(51):18126–18131. doi: 10.1073/pnas.1409525111

139. Zhang, M., & Shah, A. M. ROS signalling between endothelial cells and cardiac cells. *Cardiovasc Res* (2014) 102(2):249–57. doi: 10.1093/cvr/cvu050

140. Saggin L, Gorza L, Ausoni S, Schiaffino S. Troponin I switching in the developing heart. *J of Biol Chem* (1989) 264(27):16299–16302. doi: 10.1680/jgere.15.00010

141. Yang X, Pabon L, Murry CE. Engineering adolescence: maturation of human pluripotent stem cell-derived cardiomyocytes. *Circ Res* (2014) 114(3):511–23. doi: 10.1161/circresaha.114.300558

142. Yu T, Miyagawa S, Miki K, Saito A, Fukushima S, Higuchi T, et al. In Vivo Differentiation of Induced Pluripotent Stem Cell-Derived Cardiomyocytes. *Circulation* (2013) 77(5):1297–1306. doi: 10.1253/circj.CJ-12-0977

143. Zhang J, Wilson GF, Soerens AG, Koonce CH, Yu J, Palecek SP, et al. Functional Cardiomyocytes Derived from Human Induced Pluripotent Stem Cells. *Circ Res* (2009) 104(4):e30–e41. doi: 10.1161/circresaha.108.192237

144. Smolich JJ. Ultrastructural and functional features of the developing mammalian heart: A brief overview. *Reprod Fertil Dev* (1995) 7(3):451–461. doi: 10.1071/RD9950451

145. Bird SD, Doevendans PA, Van Rooijen MA, Brutel De La Riviere A, Hassink RJ, et al. The human adult cardiomyocyte phenotype. *Cardiovasc Res* (2003) 58(2):423–434. doi: 10.1016/S0008-6363(03)00253-0

146. He JQ, Conklin MW, Foell JD, Wolff MR, Haworth RA, Coronado R, et al. Reduction in density of transverse tubules and L-type Ca2+ channels in canine tachycardia-induced heart failure. *Cardiovasc Res* (2001) 49(2):298–307. doi: 10.1016/S0008-6363(00)00256-X

147. Mahdavi V, Lompre AM, Chambers AP, Nadal-Ginard B. Cardiac myosin heavy chain isozymic transitions during development and under pathological conditions are regulated at the level of mRNA availability. *Eur Heart J* (1984) 5 Suppl F:181–191.

148. Van Den Heuvel NHL, Van Veen TAB, Lim B, Jonsson MKB. Lessons from the heart: Mirroring electrophysiological characteristics during cardiac development to in vitro differentiation of stem cell derived cardiomyocytes. *J Mol and Cell Cardiol* (2014) 67:12–25. doi: 10.1016/j.yjmcc.2013.12.011

149. Jung G, Fajardo G, Ribeiro AJS, Kooiker KB, Coronado M, Zhao M, et al. Time-dependent evolution of functional vs. remodeling signaling in induced pluripotent stem cell-derived cardiomyocytes and induced maturation with biomechanical stimulation. *FASEB Journal* (2016) 30(4):1464–1479. doi: 10.1096/fj.15-280982

150. Harding SE, Vescovo G, Kirby M, Jones SM, Gurden J, et al. Contractile responses of isolated adult rat and rabbit cardiac myocytes to isoproterenol and calcium. *J Mol Cell Cardiol* (1988) 20(7):635-47.

151. Brito-Martins M, Harding SE, Ali NN. B 1 - and B 2 -Adrenoceptor Responses in Cardiomyocytes Derived From Human Embryonic Stem Cells: Comparison With Failing and Non-Failing Adult Human Heart. *British Journal of Pharmacology* (2008) 153:751–759. doi: 10.1038/sj.bjp.0707619

152. Nolan DJ, Ginsberg M, Israely E, Palikuqi B, Poulos MG, James D, et al. Molecular Signatures of Tissue-Specific Microvascular Endothelial Cell Heterogeneity in Organ Maintenance and Regeneration. *Dev Cell* (2014) 26(2):204–19. doi: 10.1016/j.devcel.2013.06.017

153. Lee SJ, Kim KH, Yoon Y. Generation of Human Pluripotent Stem Cell-derived Endothelial Cells and Their Therapeutic Utility. *Curr Cardiol Rep* (2018) 20(45):1–12. doi: 10.1007/s10995-015-1800-4

154. Li G, Xu A, Sim S, Priest JR, Tian X, Khan T, et al. Transcriptomic Profiling Maps Anatomically Patterned Subpopulations among Single Embryonic Cardiac Cells. *Dev Cell* (2016) 39(4):491–507. doi: 10.1016/j.devcel.2016.10.014

155. Friedman CE, Nguyen Q, Lukowski SW, Helfer A, Chiu HS, Miklas J, et al. Single-Cell Transcriptomic Analysis of Cardiac Differentiation from Human PSCs Reveals HOPX-Dependent Cardiomyocyte Maturation. *Cell Stem Cell* (2018) 23(4):586–598. doi: 10.1016/j.stem.2018.09.009

156. Churko JM, Garg P, Treutlein B, Venkatasubramanian M, Wu H, Lee J, et al. Defining human cardiac transcription factor hierarchies using integrated single-cell heterogeneity analysis. *Nat Commun* (2018) 9(1):4906. doi: 10.1038/s41467-018-07333-4

157. de Groot ACG, Winter EM, Poelmann RE. Epicardium-derived cells (EPDCs) in development, cardiac disease and repair of ischemia. *J Cell Mol Med* (2010) 14(5):1056–1060. doi: 10.1111/j.1582-4934.2010.01077.x

158. Wessels A, van den Hoff MJB, Adamo RF, Phelps AL, Lockhart MM, et al. Epicardially derived fibroblasts preferentially contribute to the parietal leaflets of the atrioventricular valves in the murine heart. *Dev Biol* (2012) 366(2):111–124. doi: 10.1016/j.ydbio.2012.04.020

159. Goumans MJ, Gittenberger-de Groot AC, Smits AM, Jongbloed MRM, Végh AMD, Kruithof BPT, et al. The epicardium as modulator of the cardiac autonomic response during early development. *J Mol Cell Cardiol* (2015) 89(2015):251–259. doi: 10.1016/j.yjmcc.2015.10.025

160. Weeke-Klimp A, Bax NAM, Bellu AR, Winter EM, Vrolijk J, et al. Epicardium-derived cells enhance proliferation, cellular maturation and alignment of cardiomyocytes. *J Mol Cell Cardiol* (2010) 49(4):606-616. doi: 10.1016/j.yjmcc.2010.07.007

161. Smits AM, Dronkers E, Goumans MJ. The epicardium as a source of multipotent adult cardiac progenitor cells: Their origin, role and fate. *Pharmacol Res* (2018) 127:129–140. doi: 10.1016/j.phrs.2017.07.020

162. Lavine KJ, Yu K, White AC, Zhang X, Smith C, et al. Endocardial and epicardial derived FGF signals regulate myocardial proliferation and differentiation in vivo. *Dev Cell* (2005) 8(1):85–95. doi: 10.1016/j.devcel.2004.12.002

163. Merki E, Zamora M, Raya A, Kawakami Y, Wang J, et al. Epicardial retinoid X receptor is required for myocardial growth and coronary artery formation. *Proc Natl Acad Sci U S A* (2005) 102(51):18455–18460. doi: 10.1073/pnas.0504343102

164. Bian W, Badie N, Himel HD, Bursac N. Robust T-tubulation and maturation of cardiomyocytes using tissue-engineered epicardial mimetics. *Biomaterials* (2014) 35(12):3819–28. doi: 10.1016/j.biomaterials.2014.01.045

165. Lin SC, Dollé P, Ryckebüsch L, Noseda M, Zaffran S, et al. Endogenous retinoic acid regulates cardiac progenitor differentiation. *Proc Natl Acad Sci U S A* (2010) 107(20):9234–9239. doi: 10.1073/pnas.0910430107

166. Wu KC, Jin JP. Calponin in non-muscle cells. *Cell Biochem Biophys* (2008) 52(3):139–148. doi: 10.1007/s12013-008-9031-6

167. Olivey HE, Svensson EC. Epicardial-Myocardial Signaling Directing Coronary Vasculogenesis. *Circ Res* (2010) 106(5):818–832. doi: 10.1161/circresaha.109.209197

168. Mou Y, Duval K, Chen Z, Pegoraro AF, Han LH, et al. Modeling Physiological Events in 2D vs. 3D Cell Culture. *Physiology* (2017) 32(4):266–277. doi: 10.1152/physiol.00036.2016

169. Correia C, Koshkin A, Duarte P, Hu D, Carido M, et al. 3D aggregate culture improves metabolic maturation of human pluripotent stem cell derived cardiomyocytes. *Biotechnol Bioeng* (2018) 115(3):630–644. doi: 10.1002/bit.26504